



National Library  
of Canada

Bibliothèque nationale  
du Canada

0-315-00452-5

Canadian Theses Division / Division des thèses canadiennes

Ottawa, Canada  
K1A 0N4

48149

**PERMISSION TO MICROFILM — AUTORISATION DE MICROFILMER**

• Please print or type — Écrire en lettres moulées ou dactylographier.

Full Name of Author — Nom complet de l'auteur

Colin Calnan

Date of Birth — Date de naissance  
July 17, 1953

Country of Birth — Lieu de naissance  
Canada

Permanent Address — Résidence fixe

500 Stout Court  
Bathurst, N.B.

Title of Thesis — Titre de la thèse

Core Radii Determinations for Four Clusters of Galaxies

University — Université

Saint Mary's University

Degree for which thesis was presented — Grade pour lequel cette thèse fut présentée

Master of Science in Astronomy

Year this degree conferred — Année d'obtention de ce grade

1979

Name of Supervisor — Nom du directeur de thèse

Dr. Gary A. Welch

Permission is hereby granted to the NATIONAL LIBRARY OF CANADA to microfilm this thesis and to lend or sell copies of the film.

The author reserves other publication rights, and neither the thesis nor extensive extracts from it may be printed or otherwise reproduced without the author's written permission.

L'autorisation est, par la présente, accordée à la BIBLIOTHÈQUE NATIONALE DU CANADA de microfilmer cette thèse et de prêter ou de vendre des exemplaires du film.

L'auteur se réserve les autres droits de publication; ni la thèse ni de longs extraits de celle-ci ne doivent être imprimés ou autrement reproduits sans l'autorisation écrite de l'auteur.

Date

July 7, 1979

Signature

*Colin Calnan*



National Library of Canada  
Collections Development Branch

Canadian Theses on  
Microfiche Service

Bibliothèque nationale du Canada  
Direction du développement des collections

Service des thèses canadiennes  
sur microfiche

## NOTICE

## AVIS

The quality of this microfiche is heavily dependent upon the quality of the original thesis submitted for microfilming. Every effort has been made to ensure the highest quality of reproduction possible.

If pages are missing, contact the university which granted the degree.

Some pages may have indistinct print especially if the original pages were typed with a poor typewriter ribbon or if the university sent us a poor photocopy.

Previously copyrighted materials (journal articles, published tests, etc.) are not filmed.

Reproduction in full or in part of this film is governed by the Canadian Copyright Act, R.S.C. 1970, c. C-30. Please read the authorization forms which accompany this thesis.

**THIS DISSERTATION  
HAS BEEN MICROFILMED  
EXACTLY AS RECEIVED**

La qualité de cette microfiche dépend grandement de la qualité de la thèse soumise au microfilmage. Nous avons tout fait pour assurer une qualité supérieure de reproduction.

S'il manque des pages, veuillez communiquer avec l'université qui a conféré le grade.

La qualité d'impression de certaines pages peut laisser à désirer, surtout si les pages originales ont été dactylographiées à l'aide d'un ruban usé ou si l'université nous a fait parvenir une photocopie de mauvaise qualité.

Les documents qui font déjà l'objet d'un droit d'auteur (articles de revue, examens publiés, etc.) ne sont pas microfilmés.

La reproduction, même partielle, de ce microfilm est soumise à la Loi canadienne sur le droit d'auteur, SRC 1970, c. C-30. Veuillez prendre connaissance des formules d'autorisation qui accompagnent cette thèse.

**LA THÈSE A ÉTÉ  
MICROFILMÉE TELLE QUE  
NOUS L'AVONS REÇUE**

CORE RADII DETERMINATIONS FOR  
FOUR CLUSTERS OF GALAXIES

Colin Calnan

A thesis submitted as partial  
requirement for the degree of  
Master of Science

from the

Department of Astronomy

at

Saint Mary's University

Saint Mary's University

1979



Colin Calnan 1979

My thesis now is all complete,

My obligations I did meet.

A new degree

Awarded me,

'Twas not a trifling feat.

## Table of Contents

Acknowledgements	1
Abstract	11
I. Introduction	1
II. Computer Program Development	6
III. Program Testing	
i) Fits to model isothermal gas sphere	17
ii) Comparison with results published by Taff) for the Perseus cluster and A2199	21
iii) Comparison with results published by Bahcall for twelve clusters	31
IV. Observational Material	
i) Program input file	36
ii) Photographic enlargements	37
iii) Limiting magnitudes	39
iv) Cluster centres from strip counts	41
v) Ring counts	43
V. Results	
i) Results tabulated	48
ii) Comparison of $\sigma_{bg}$ and $\sigma_{bg}^*$	52
iii) Comparison of 10 ring core radii and 20 ring core radii	53
iv) Comparison of $R_c$ and $R_c^*$	54
v) Individual cluster abnormalities	57

vi) The mass segregation question	61
vii) Comparison with published core radii	64
viii) Combination of present core radii with those of Bahcall	66
ix) Conclusions	68
References	71
Appendix A - Program listing	72
Appendix B - Auxiliary listings	90
Appendix C - Detailed program explanations	99
Appendix D - Plate and cluster information	132
Appendix E - Strip counts	134
Appendix F - Ring counts	143
Appendix G - Background counts	148
Appendix H - Complete results	151
Appendix I - Density profiles	157
Appendix J - Sample output	164

## Acknowledgements

Many many thanks go to Dr. Gary Welch for a multitude of reasons, some of which are:

- suggesting this topic
- providing the plates used
- giving a seemingly endless supply of hints, suggestions, and near-orders
- going over all the many versions of this thesis and supplying even more of the above
- providing encouragement when days were dark and computer programs seemed to be proving their complete non-operability.

Thanks also goes to the thesis defense committee consisting of Drs. Chia, Dupuy, Reynolds, and Welch for further suggestions when I thought I was almost finished and to the computer centre staff at St. Mary's for a lot of help before, after, and especially during the aforementioned dark days.

## Abstract

Bahcall (1975) has found that the average core radius for a group of 15 clusters of galaxies is  $0.25 \pm 0.05$  Mpc. At the suggestion of Dr. G. Welch it was decided to study four nearby clusters of galaxies (A2052, A2593, A2626, and A154) in order to determine their core radii. If it turned out that the dispersion of core radii at low redshifts is small, then these core radii could be said to be effectively constant. Any variation of the core radius at large redshifts would then be due to the geometry of the universe.

Accordingly, a computer program was written that would find a core radius by fitting ring counts data from the chosen clusters to an Emden isothermal gas sphere. The ring counts were made to three magnitude limits, one of which approximated that of Bahcall. Also, each magnitude limit was used to find four core radii: one using all the ring count data and a counted background density; one using half the ring count data (only the core region) and a counted background density; one using all the data but solving for a background density (among other parameters); and one using half the data and solving for the background density. These four results were compared in various ways in order to determine which method produced the "best" core radius. Then the "best" core radius for each cluster at the magnitude

limit used by Bahcall was added to her results to obtain a new average and standard deviation.

Several conclusions were drawn from the overall results.

1. In the course of testing the program it was found that different results were found between this and other programs using the same data. This indicates the need of a unique program to be used exclusively.

2. Better results seem to be found when the background density is counted.

3. Better results seem to be found when all data (about out to the Abell radius) is used as opposed to only the core data.

4. Two clusters show evidence of mass segregation (A2052 and A2593).

5. The spread of core radii from the four clusters of this thesis at (or more precisely, "near") Bahcall's magnitude limit is large enough to cast doubt on the idea of using core radii as universal geometry indicators ( $R_c(\text{average}) = 0.20 \pm 0.13$  Mpc for the four clusters of this thesis).

I  
Introduction

One of the fundamental questions about the universe concerns its geometry; more specifically, whether it is open or closed. An indicator of this property is the deceleration parameter  $q_0$ , which is the measure of the deceleration rate of the expanding universe.

For values of  $q_0 < \frac{1}{2}$ , the universe is expanding too fast to ever stop and will continue forever; the universe is open. For  $q_0 = \frac{1}{2}$ , the expansion will stop, but only at an infinite time in the future. If  $q_0 > \frac{1}{2}$ , the universe will stop expanding to begin contracting at a definite time in the future, and the greater the value of  $q_0$  the nearer is this time. With  $q_0 > \frac{1}{2}$  the universe is said to be closed.

If there were a standard metrestick that could be placed in space at different distances (as indicated by recessional speed, or redshift), then the manner in which its apparent size changed with redshift would depend on  $q_0$ . Therefore a plot of apparent size versus redshift would enable a user to determine the value of  $q_0$ .

As it happens, a standard metrestick may be available. Studies of clusters of galaxies, principally by Bahcall (Bahcall 1975, and references therein) have shown that rich galaxy clusters of low redshift ( $z < 0.14$ , where  $z = \text{radial velocity} / \text{speed of light}$ ) have a linear core radius

$R_C$  (to be explained later) which is approximately constant. For fifteen clusters in the redshift range  $0.0181 \leq z \leq 0.134$ , the average of  $R_C$  is  $0.25 \pm 0.05$  Mpc ( $H_0 = 50 \text{ km s}^{-1} \text{ Mpc}^{-1}$ , Bahcall, 1975). If this value is characteristic of clusters of galaxies to within sufficiently narrow limits then  $R_C$  may serve as a standard metrestick.

For quite some time it has been known that the radial number density distribution of the members of rich clusters could be closely matched to the radial density distribution of a bounded Emden isothermal gas sphere projected to two dimensions (Zwicky, 1957). To fit observations, the usual model, which is constructed with dimensionless variables, must be scaled in density and size. The core radius is the radius at which the density is about half the central value (see Figure 1).

Actually, by definition  $r_C = 3\alpha$ , where  $r_C$  is the observed core radius in arcmin and  $\alpha$  is the structural length (or scale factor) of the cluster in arcmin, a value found during the computer fitting process. (In Figure 1  $\xi = r/\alpha$ , and at  $r = r_C$ , i.e.  $\xi = 3$ , the actual value of the density is about 0.43.)

Knowing  $r_C$ , the redshift of the cluster, and a value for Hubble's constant, the physical core radius  $R_C$  in Mpc can be determined. Then a plot of  $R_C$  versus  $z$  for a large number of clusters can be used to find  $q_0$ .

Despite the fact that the physical data are fitted

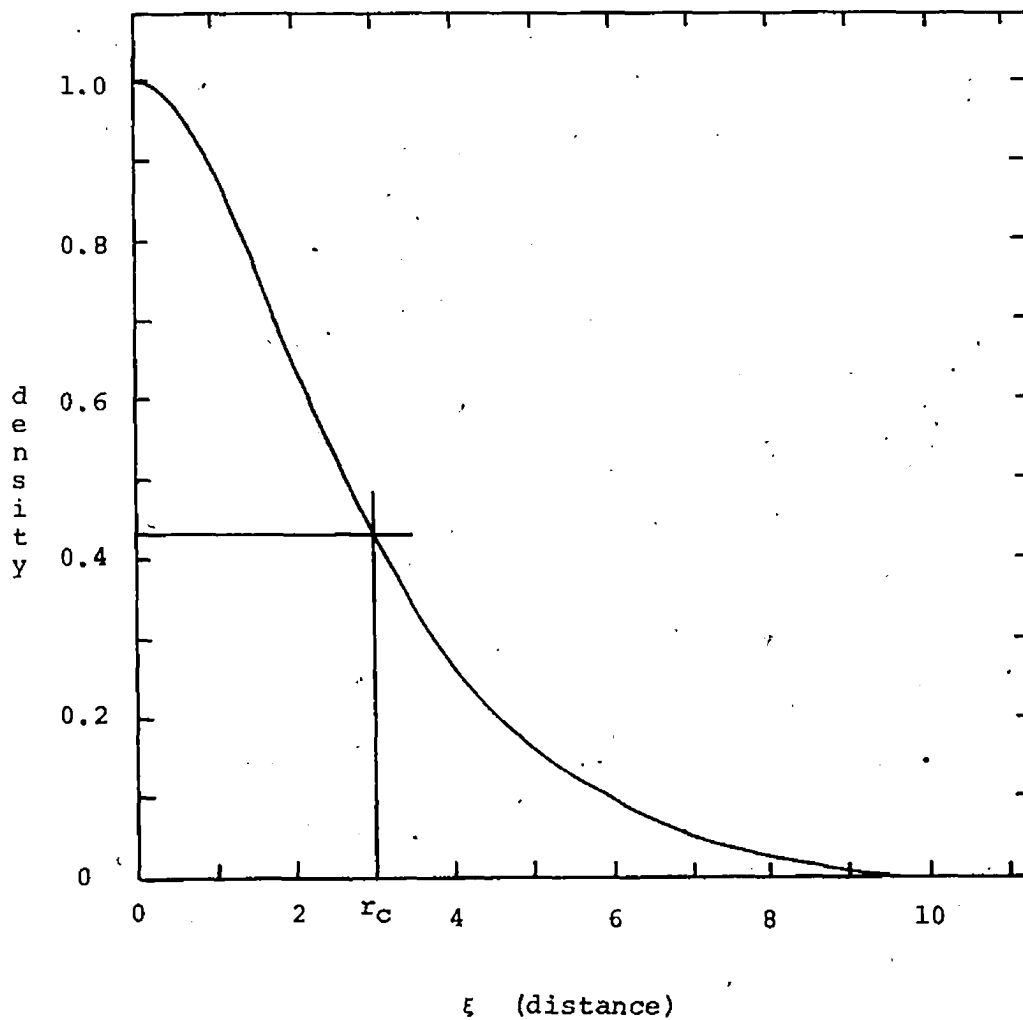


Figure 1 Emden isothermal gas sphere density profile projected to two dimensions and bounded at 10

to an isothermal gas sphere, it is not necessarily true that the particles (galaxies) behave as the particles in a perfect isothermal gas sphere. The only justifications for using this model are that it fits well to the observed data and enables definition of a useful parameter,  $r_c$  (and so  $R_c$ ). Undoubtedly other mathematical relations would do just as well, and could also (or alternatively) be used. (Two other relations that also fit well are given by King 1966 and de Vaucouleurs 1960.) The major criteria in choosing a mathematical relation are its ability to give a good mathematical fit and a structural size parameter.

The major purpose of this thesis is to obtain core radii for four rich galaxy clusters at low redshift (A2052,  $z=0.0351$ ; A2593,  $z=0.044$ ; A2626,  $z=0.055$ ; and A154,  $z=0.056$ ). When combined with Bahcall's results these radii will possibly provide an improved average value and standard deviation for  $R_c$ . If it turns out that the standard deviation in  $R_c$  is small for low redshift clusters then the assumption can be made that  $R_c$  is nearly constant. In that case, deviations in  $R_c$  at high redshifts from this constant value (assuming the deviations occur in a systematic manner) can be assumed to be due to the value of  $q_0$ , which may then be determined. Another possibility to explain a changing  $R_c$  with  $z$  is that clusters evolve dynamically, and that the more distant clusters have a different radial distribution. However, since dynamical cluster evolution is poorly under-

stood it is necessary to neglect it. Since the clusters being studied in this thesis are all nearby and within a narrow range of redshifts, then dynamical evolution is not expected to be of any importance in comparing with the results of Bahcall.

## Computer Program Development

A major task was the writing of a computer program that uses the data (in the form of the numbers of galaxies in rings centred on the cluster centre and the corresponding ring sizes) to find the parameters leading to a best fit with a projected isothermal gas sphere. The basis for most of what follows is a technique suggested by Taff (1975).

Since the isothermal gas sphere model is expressed in terms of particle number density, it is necessary to change the observed counts to number densities:

$$\sigma_{\text{obs}}(i) = \frac{N_{\text{obs}}(i)}{\pi (r_{i+1}^2 - r_i^2)} \quad (1)$$

where  $\sigma_{\text{obs}}(i)$  is the observed number density of galaxies in the  $i$ th ring;  $N_{\text{obs}}(i)$  is the observed number of galaxies in the  $i$ th ring; and  $r_i$  and  $r_{i+1}$  are the inner and outer radii of the  $i$ th ring. Note that for the first ring (actually a circle) the inner radius,  $r_1$ , is equal to zero. The values  $N_{\text{obs}}(i)$  and  $r_i$  are the input data.

Also needed for the construction of a model are the distance from the centre at which these densities occur. These values,  $r_{\text{av}}(i)$ , are taken to be the radii that divide ring ( $i$ ) into two rings of equal area. So

$$r_{\text{av}}(i) = \left\{ (r_{i+1}^2 + r_i^2) / 2 \right\}^{1/2} \quad (2)$$

The expression for an isothermal gas sphere in terms of the observable quantities is

$$\sigma_{\text{calc}}(i) = \sigma_c \sigma_{\text{iso}}(r_{\text{av}}(i)/\alpha) + \sigma_{\text{bg}} \quad (3)$$

where  $\sigma_{\text{calc}}(i)$  is the calculated projected number density corresponding to  $r_{\text{av}}(i)$ ;  $\sigma_c$  is the projected central number density; and  $\sigma_{\text{bg}}$  is the background number density added to the model cluster. The function  $\sigma_{\text{iso}}(r_{\text{av}}(i)/\alpha)$  gives the projected normalized density of the isothermal gas sphere alone at the unitless distance  $r_{\text{av}}(i)/\alpha$ .

If we let

$$x_i = r_{\text{av}}(i)/\alpha$$

then the expression for  $\sigma_{\text{iso}}$  is given by

$$\sigma_{\text{iso}}(x_i) = \frac{\int_{x_i}^{x_0} \sqrt{\xi^2 - x_i^2} e^{-\psi} \psi' d\xi}{\int_0^{x_0} \xi e^{-\psi} \psi' d\xi} \quad (4)$$

(see Chandrasekhar, 1942). Here  $\psi' = d\psi/d\xi$  and the quantity  $e^{-\psi}$  is the solution to the equilibrium equation for the three dimensional isothermal sphere, as in:

$$e^{-\psi} = \xi^{-2} d/d\xi (\xi^2 d\psi/d\xi) \quad (5)$$

The upper boundary limit  $x_0$  in equation (4) is a

convenient cutoff to integration. For globular clusters, the stellar distribution ceases to approximate an isothermal gas sphere at about  $\xi=10$ , and so for these clusters the limit is set at about  $x_0=10$  (Chandrasekhar, 1942). For galaxy clusters  $x_0$  will be allowed to vary to see which value best fits the cluster.

Equation (4) produces a radial density curve of the type shown in Figure 1, where the projected density becomes zero at  $x_0$ .

Numerical values for  $e^{-\psi}$ ,  $\psi'$ , and  $\xi$  can be obtained from various sources. The ones for this thesis were generated by a BASIC program (see Appendix B for a listing) which calculated values at increments of  $\xi$  by using the Runge-Kutta method on equation (5). Then  $\sigma_{iso}(x_i)$  can be found by numerical integration.

The above equations leave four parameters to be determined for a best fit with the isothermal gas sphere; namely:  $\sigma_c$ , the central density;  $\sigma_{bg}$ , the background density;  $\alpha$ , the scale factor; and  $x_0$ , the upper limit of integration.

The method of obtaining these is, to some extent, dependant on the procedure used to test the goodness of fit of the model. A common procedure, and the one used here, is the  $\chi^2$  test. Besides the fact that the minimum of  $\chi^2$  is a well defined indicator of the best fit, there is the advantage that the value of  $\chi^2$  can be used to estimate the probability of this specific  $\chi^2$  occurring randomly.

The usual way of expressing  $\chi^2$  is

$$\chi^2 = \sum (o_i - t_i)^2 / t_i$$

where  $t_i$  is the  $i^{th}$  theoretical value and  $o_i$  is the  $i^{th}$  observed value. In the present case we get

$$\chi^2 = \sum \{N_{obs}(i) - N_{calc}(i)\}^2 / N_{calc}(i) \tag{6}$$

where  $N_{calc}(i)$  is the number of galaxies predicted for the  $i^{th}$  ring from the equation

$$N_{calc}(i) = \sigma_{calc}(i) \pi (r_{i+1}^2 - r_i^2) \tag{7}$$

From equations (1) and (3) the equation for  $\chi^2$  becomes

$$\chi^2 = \sum \pi (r_{i+1}^2 - r_i^2) \frac{\{\sigma_{obs}(i) - \sigma_c \sigma_{iso}(x_i) - \sigma_{bg}\}^2}{\sigma_c \sigma_{iso}(x_i) + \sigma_{bg}} \tag{8}$$

This form possesses only three unknown factors:  $\sigma_{iso}(x_i)$ ,  $\sigma_c$ , and  $\sigma_{bg}$ . If the assumption is made, for the moment, that the set of values  $\sigma_{iso}$  is known, then the equation becomes one with two unknown constants, whose values can be found through the minimization of  $\chi^2$  with respect to each of them. Since equations of the form of (8) cannot be solved analytically, a numerical method must be used. The method chosen is the Newton-Raphson method, which states

$$\begin{pmatrix} x_{i+1} \\ y_{i+1} \end{pmatrix} = \begin{pmatrix} x_i \\ y_i \end{pmatrix} - \begin{pmatrix} f_x & f_y \\ g_x & g_y \end{pmatrix}^{-1} \begin{pmatrix} f \\ g \end{pmatrix} \quad (9)$$

when  $f(x,y)=0$  and  $g(x,y)=0$ . In equation (9):  $f_x=\partial f/\partial x$ ;  $f_y=\partial f/\partial y$ ;  $g_x=\partial g/\partial x$ ;  $g_y=\partial g/\partial y$ ;  $f=f(x,y)$ ; and  $g=g(x,y)$ . All expressions involving  $f$  and  $g$  and their partial derivatives are evaluated at  $x_i$  and  $y_i$ .

This method is an iterative one which, given sufficiently accurate initial estimates for the quantities to be found, will quickly converge to the correct value. Since the initial equation (8) has sums of squares over a number of rings, the number of solutions is greater than one. However, if the initial estimates are close to the physically correct solutions, then these solutions will be found.

In this case, to satisfy the conditions for equation (9), and due to the fact that solutions will be found by minimization of  $\chi^2$  as expressed in equation (8), the following relations are used. Defining

$$\sigma_c \equiv x_i \text{ (successively)}$$

$$\sigma_{bg} \equiv y_i \text{ (successively)}$$

$$\beta_i \equiv r_{i+1}^2 - r_i^2$$

$$\epsilon_i \equiv \frac{\sigma_{\text{obs}}(i) - \sigma_c \sigma_{\text{iso}}(x_i) - \sigma_{bg}}{\sigma_c \sigma_{\text{iso}}(x_i) + \sigma_{bg}}$$

and

$$\mu_i = \frac{1}{\sigma_c \sigma_{iso}(x_i) + \sigma_{bg}} + \frac{2\{\sigma_{obs}(i) - \sigma_c \sigma_{iso}(x_i) - \sigma_{bg}\}}{\{\sigma_c \sigma_{iso}(x_i) + \sigma_{bg}\}^2} + \frac{\{\sigma_{obs}(i) - \sigma_c \sigma_{iso}(x_i) - \sigma_{bg}\}^2}{\{\sigma_c \sigma_{iso}(x_i) + \sigma_{bg}\}^3}$$

We can further define the terms of equation (9) as:

$$\begin{aligned} f &\equiv \partial \chi^2 / \partial \sigma_c \\ g &\equiv \partial \chi^2 / \partial \sigma_{bg} \\ f_x &\equiv \partial^2 \chi^2 / \partial \sigma_c^2 \\ f_y = g_x &\equiv \partial^2 \chi^2 / \partial \sigma_c \partial \sigma_{bg} \\ g_y &\equiv \partial^2 \chi^2 / \partial \sigma_{bg}^2 \end{aligned}$$

The terms of equation (9) can now be written in terms related to the isothermal gas sphere:

$$f = \sum \beta_i \sigma_{iso}(x_i) (2\epsilon_i + \epsilon_i^2) = 0$$

$$g = \sum \beta_i (2\epsilon_i + \epsilon_i^2) = 0$$

$$f_x = 2 \sum \beta_i \sigma_{iso}^2(x_i) \mu_i$$

$$f_y = g_x = 2 \sum \beta_i \sigma_{iso}(x_i) \mu_i$$

$$g_y = 2 \sum \beta_i \mu_i$$

Furthermore, solving equation (9) gives

$$x_{i+1} = x_i - \frac{gf_y - fg_y}{f_x g_y - f_y^2}$$

and

$$y_{i+1} = y_i + \frac{ff_x - gf_x}{f_x g_y - f_y^2}$$

However, to get this far the assumption was made that in equation (8) the set of values  $\sigma_{iso}$  was known, which means that  $x_0$  and  $\alpha$  must first be chosen.

Initially  $x_0$  is set to 10 and  $\alpha$  to  $0.999r_{av}(1)/x_0$ , which allows the calculation of  $\sigma_{iso}$ , and so allows  $\sigma_c$ ,  $\sigma_{bg}$ , and  $\chi^2$  to be found. Then  $\alpha$  is incremented by increasing  $\log \alpha$  in steps of 0.08. This is continued until either  $\log \alpha = \log \alpha_{initial} + 4$  or until the results for  $\sigma_c$  and  $\sigma_{bg}$  arising from the  $\alpha$ - $x_0$  combination become physically unreasonable. During the process of incrementing  $\alpha$  the  $\chi^2$  values drop to a minimum and then rise again. The values for  $\alpha$ ,  $\sigma_c$ , and  $\sigma_{bg}$  that produce the minimum  $\chi^2$  are the ones producing the best fitting isothermal gas sphere model for the  $x_0$  used.

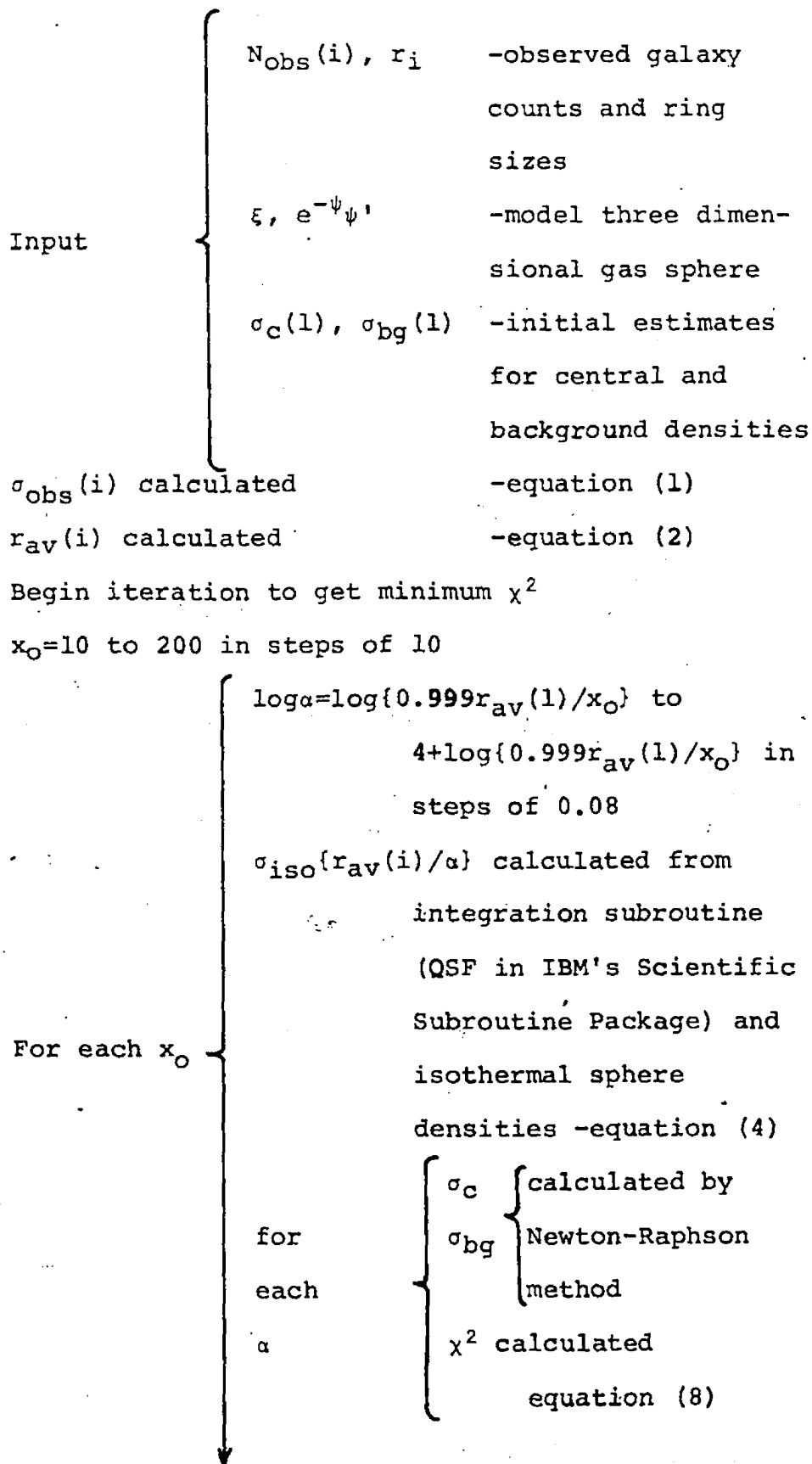
A new  $x_0$  is obtained by adding 10 to the previous value, a new  $\alpha$  is calculated and incremented as for  $x_0=10$ , and new  $\sigma_c$ ,  $\sigma_{bg}$ , and  $\chi^2$  values are found for each  $\alpha$ ; the usual maximum for  $x_0$  is 200.

What is produced is a set of values of  $x_0$ , for each of which exists a set of "chosen" values of  $\alpha$  and the

values of  $\sigma_c$ ,  $\sigma_{bg}$ , and  $\chi^2$  resulting from the Newton-Raphson method. From the set of  $\chi_{\min}^2$  (minimum  $\chi^2$  for a specific  $x_0$ ) the  $x_0$  which produces  $\chi_{\text{absmin}}^2$  (the minimum  $\chi_{\min}^2$ ) is found.  $\chi_{\text{absmin}}^2$ , therefore, determines the four parameters which produce the best fitting isothermal gas sphere model.

Since values of  $\alpha$  are chosen in discrete steps it is probable that the minimum  $\chi^2$  for a given  $x_0$  will occur somewhere between two  $\alpha$  values. However, since  $\chi^2$  decreases monotonically to a minimum and then rises again in a similar fashion, a simple approach to look for a "better"  $\alpha$  is adopted. The two consecutive values of  $\alpha$  giving the lowest  $\chi^2$  values are averaged and this average is used to get new  $\sigma_c$ ,  $\sigma_{bg}$ , and  $\chi^2$ . The  $\chi^2$  found for the new  $\alpha$  is always lower than at least one of the two original  $\chi^2$  values. The new  $\alpha$  is then averaged with the  $\alpha$  giving the smallest of the two original  $\chi^2$  values to get another  $\alpha$ . This new  $\alpha$  value is used to get an even smaller  $\chi^2$  value. The procedure of averaging the  $\alpha$ s that produce the two smallest  $\chi^2$  values is repeated twenty times, at which point successive differences in all other parameters occur only in the fifth or higher significant digit.

A general schematic of what the computer program must be designed to do can be drawn up:



From two smallest  $\chi^2$  values, iterative averaging of associated  $\alpha$  values gives a smaller  $\chi^2$  and "better" associated values for  $\alpha$ ,  $\sigma_c$ , and  $\sigma_{bg}$

The computer program is written in Fortran IV and a listing is provided in Appendix A, with detailed notes in Appendix C.

Another way to approach the problem is to obtain a value for  $\sigma_{bg}$  by counting galaxies on an area of the photographic plate removed from the cluster. In this case only  $x_0$ ,  $\alpha$ , and  $\sigma_c$  are left to be found as free parameters. If the assumption is again made that  $\sigma_{iso}$  is known (see equation 8) then only  $\sigma_c$  is left to be found. The Newton-Raphson method can again be used to find  $\sigma_c$  iteratively, the form for one unknown is

$$x_{i+1} = x_i - f/f_x$$

when  $f(x)=0$ . In this equation  $x_i = \sigma_c$  (successively);  $f = d\chi^2/d\sigma_c$ ;  $f_x = d^2\chi^2/d\sigma_c^2$ ;  $f = f(x)$ ; and  $f$  and  $f_x$  are evaluated for  $x_i$ .

The only changes this would make in the schematic is that instead of  $\sigma_c$  and  $\sigma_{bg}$  being calculated, only  $\sigma_c$  is found, and  $\sigma_{bg}$  is entered as part of the input. A program was written for each method, total results from both are

presented in Appendix H, partial results (including core radii in Mpc) are presented in Chapter V. Modifications to the original program to get one for the second method are listed in Appendix B and explanations of these changes are in Appendix C.

## Program Testing

## i) Fits to model isothermal gas sphere

For initial testing of the computer program a data set was fabricated which described a projected isothermal gas sphere with known values of  $x_0$ ,  $\alpha$ ,  $\sigma_c$ , and  $\sigma_{bg}$ . It was expected that if the program was working properly the Newton-Raphson method would cause convergence to the correct  $\sigma_c$  and  $\sigma_{bg}$  values and that the iterative dividing method for  $\alpha$  would provide a minimum  $\chi^2$  for the correct  $\alpha$ .

The values chosen to produce the data for this test were:  $x_0=10$ ;  $\alpha=2.40$  arcmin;  $\sigma_c=0.50$  galaxies/arcmin<sup>2</sup>; and  $\sigma_{bg}=0.05$  galaxies/arcmin<sup>2</sup>.

Figure 2 displays part of the results. The three curves are constructed from the  $\sigma_c$  and  $\sigma_{bg}$  values to which the program converges at the stated  $\alpha$  values. These are only three representative cases; many more  $\alpha$  values were produced than are displayed in Figure 2 but the trend with changing  $\alpha$  is as shown.

As can be seen from this **diagram** a small value of  $\alpha$  tends to produce a compressed gas sphere model and increasingly larger values give increasingly extended models. At large  $\alpha$  values,  $\sigma_{bg}$  values are eventually produced which are large and negative and are obviously physically unreasonable.

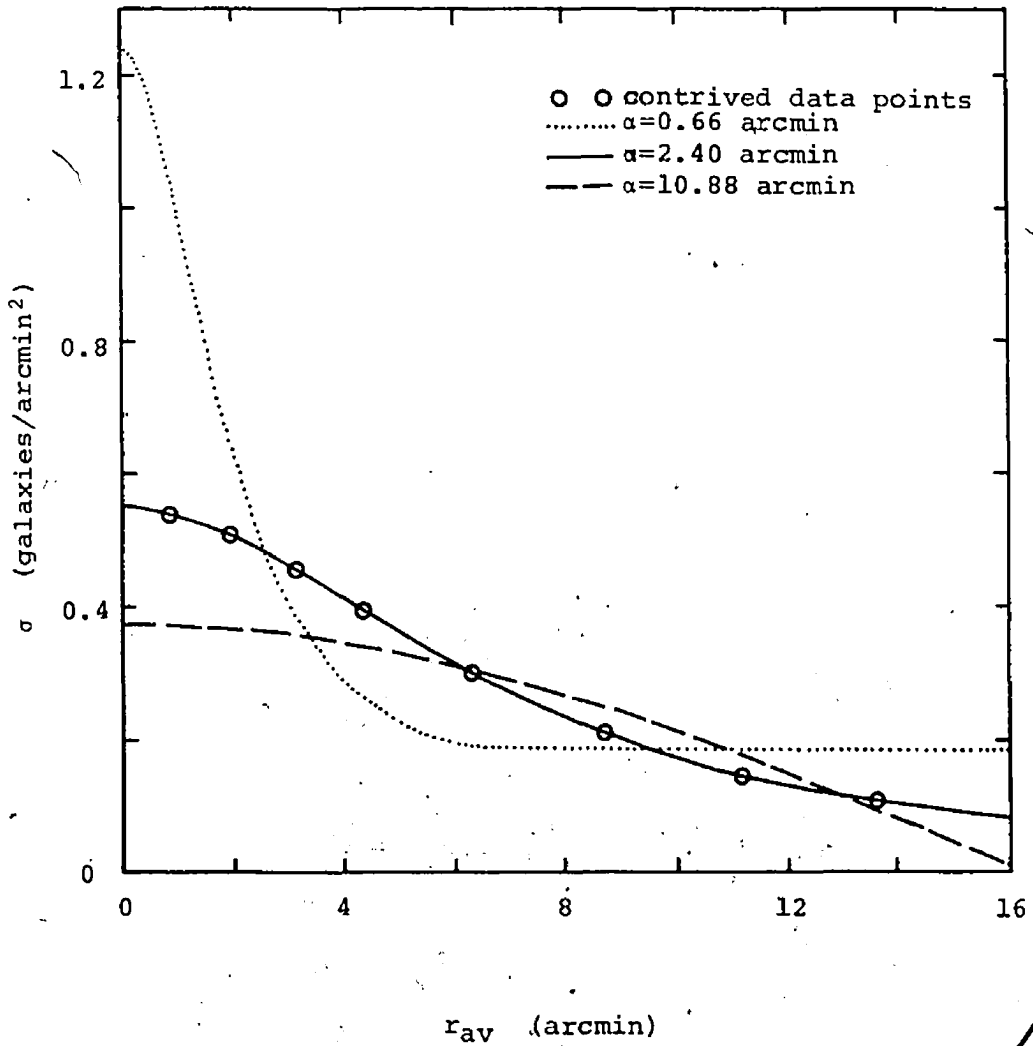


Figure 2 Fits to isothermal gas sphere data

Table 1

Results of fits to isothermal gas sphere data

 $(x_0=10)$ 

$\alpha$	$\sigma_c$	$\sigma_{bg}$	$\chi^2$
.1048	17.55	.2241	35.30
.6610	1.055	.1887	19.26
1.149	.7635	.1463	5.772
1.660	.5840	.1067	1.001
2.400	.5000	.05000	3.944(-8)*
4.171	.5398	-.1031	1.356
10.48	1.514	-1.139	4.251

\* 3.944(-8) =  $3.944 \times 10^{-8}$  This notation is used elsewhere in this thesis

Units:  $\alpha$ -arcmin  
 $\sigma_c$ -galaxies/arcmin<sup>2</sup>  
 $\sigma_{bg}$ -galaxies/arcmin<sup>2</sup>

Table 2

 $\chi_{min}^2$  results for various  $x_0$ 

$x_0$	$\alpha$	$\sigma_c$	$\sigma_{bg}$	$\chi_{min}^2$
10	2.400	.5000	.5000(-1)	3.944(-8)
40	2.358	.5572	-.5711(-2)	2.160(-4)
70	2.358	.5637	-.1226(-1)	2.218(-4)
100	2.358	.5664	-.1493(-1)	2.203(-4)
130	2.357	.5681	-.1642(-1)	2.278(-4)
160	2.357	.5689	-.1774(-1)	2.202(-4)
190	2.358	.5696	-.1814(-1)	2.209(-4)

Units: as in Table 1

Columns 2 to 4 of Table 1 show the  $\sigma_C$ ,  $\sigma_{bg}$ , and  $\chi^2$  values that result from the  $\alpha$  values in column 1. These particular results are all calculated with  $x_0=10$  and are only a small sample of the total but are typical of the values for other integration cutoff limits. Rows 2, 5, and 7 of this table correspond to the three curves of Figure 2. It must be pointed out that to get  $\sigma(r_{av}=0)$  the values of  $\sigma_C$  and  $\sigma_{bg}$  must be added.

One of the first things obvious from Table 1 is that the program did converge to the correct values, producing the extremely good fit for the  $\alpha=2.400$  case. Also as  $\alpha$  increases  $\sigma_C$  decreases to a minimum in the neighbourhood of the correct  $\alpha$ . A more comprehensive version of Table 1 shows that the minimum  $\sigma_C$  is not reached exactly at  $\alpha=2.400$  but at  $\alpha=2.886$ , the next incremental value of  $\alpha$ . For other  $x_0$  values the  $\sigma_C$  also reaches a minimum just after the minimum  $\chi^2$ , and rises again as  $\alpha$  continues to increase. The background density, however, decreases monotonically with increasing  $\alpha$  and eventually becomes negative, a physically unreasonable possibility. The  $\chi^2$  is found to decrease monotonically to a minimum at the correct  $\alpha$ ,  $\sigma_C$ , and  $\sigma_{bg}$  combination, and then rise again monotonically with the rate of increase being less than that of decrease.

Table 2 shows the  $\alpha$ ,  $\sigma_C$ , and  $\sigma_{bg}$  values producing the  $\chi_{min}^2$  for the given  $x_0$  values. It can be seen that  $\alpha$  changes to 2.358 and remains roughly constant as soon as

$x_0$  exceeds 10, and  $\sigma_c$  slowly increases as  $\sigma_{bg}$  slowly decreases at about the same rate. In fact, the sum of  $\sigma_c$  and  $\sigma_{bg}$  produces a minimum of 0.5500 for  $x_0=10$  and averages about 0.5515 for the other integration limits, with the sum of 0.5523 for  $x_0=100$  being an extreme case. Aside from the absolute minimum for  $x_0=10$ ,  $\chi_{min}^2$  maintains a fairly constant value as  $x_0$  increases. The product  $\alpha\sigma_c$ , which Bahcall (1972) finds to remain fairly constant for various  $\chi_{min}^2$ , has a minimum of 1.200 for  $x_0=10$  and rises slowly to 1.343 for  $x_0=190$ , a change of only 12%.

Table 2 indicates that the  $\chi_{min}^2$  values of  $\alpha$  and  $\sigma_c$  arrived at by the fitting process are fairly insensitive to the choice of  $x_0$ , even if the choice is far from the one producing  $\chi_{absmin}^2$ .

Initial testing described above showed that the program successfully converged to the correct parameters when given an artificial data set generated from a projected, bounded isothermal gas sphere.

- ii) Comparison with results published by Taff for the Perseus cluster and A2199

Secondary testing involved running the program using published data and comparing the results to those

published for these data. Since the program was written following the technique suggested by Taff (1975) it is presumably similar to the one used by him, and since the program and Taff used the same data his results form the basis for comparison.

Results for the Perseus cluster are found in Table 3, the data used is from Bahcall (1974). Case (a) uses counts with galaxies brighter than  $16^m0$  and case (b) uses counts with galaxies brighter than  $17^m5$ ; in both cases the number and size of the rings used for counting were the same. For each case there are three lines of values: the top line gives Taff's results with the value in parentheses to the right of the  $\chi^2$  column being the  $\chi^2$  found by this program when forced to fit the data to the model made with Taff's values for  $x_0$ ,  $\alpha$ ,  $\sigma_C$ , and  $\sigma_{bg}$ ; the second line gives the  $\chi^2_{absmin}$  parameters produced by this program; and the third line consists of the  $\chi^2_{min}$  parameters produced by this program using the minimizing value of  $x_0$  found by Taff.

The large discrepancy between Taff's  $\chi^2$  and the one calculated by this program from his parameters may be due to differences in the fitting procedures. However, if the value of  $x_0$  is set equal to the best fit value found by Taff, the values of the three other independent variables (i.e.,  $\alpha$ ,  $\sigma_C$ , and  $\sigma_{bg}$ ) are close to those of Taff, as seen in row three of each case.

A plot of  $x_0$  versus  $\chi^2_{min}$  is shown in Figure 3 to

Table 3  
Perseus cluster results

	$x_0$	$\alpha$	$\sigma_c$	$\sigma_{bg}$	$\chi^2$	
(a)	10	2.89	7.28(-2)	4.24(-3)	1.28	(22.14)
	160	1.95	1.03(-1)	3.19(-3)	6.49	
	10	2.98	7.82(-2)	6.37(-3)	6.78	
(b)	10	3.47	1.33(-1)	1.12(-2)	3.35	(12.55)
	20	2.92	1.65(-1)	1.07(-2)	3.07	
	10	4.28	1.22(-1)	1.14(-2)	4.36	

Units:  $\alpha$ -arcmin  
 $\sigma_c$ -galaxies/arcmin<sup>2</sup>  
 $\sigma_{bg}$ -galaxies/arcmin<sup>2</sup>

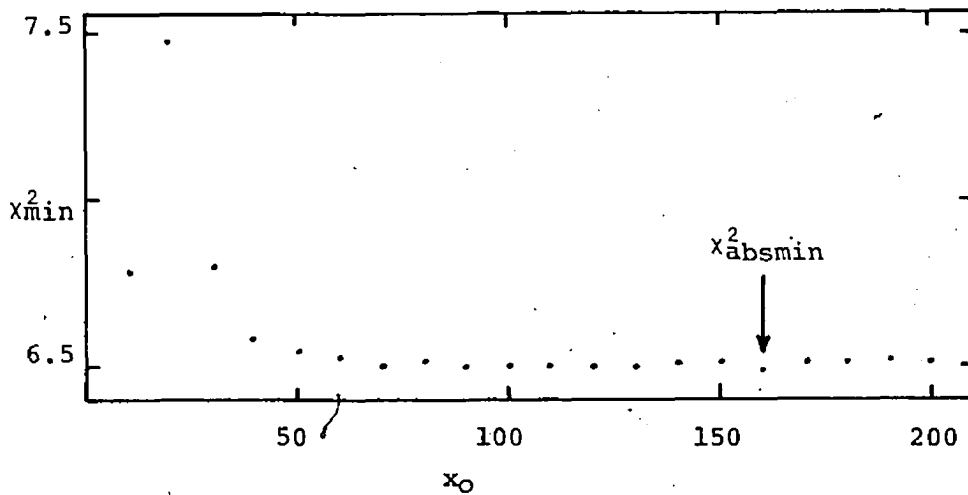


Figure 3  
Plot of  $\chi^2_{min}$  to  $x_0$  for case (a) of the Perseus cluster

illustrate the fact that fits can be rather insensitive to the value of  $x_0$ . This was also found in the initial testing. Beyond a certain value of  $x_0$  (about 40 in this case), the  $\chi_{\min}^2$  values appear to fluctuate randomly, here about a value of -6.5. The fact that  $\chi_{\text{absmin}}^2$  occurs at  $x_0=160$  is not considered significant, that is, the minimizing value of  $x_0$  does not seem to be well determined. This raises the question of how well determined  $\chi_{\text{absmin}}^2$  and  $x_0$  are, a question that will be discussed later.

A graph similar to Figure 3 for case (b) shows the largest  $\chi_{\min}^2$  for  $x_0=10$ , the smallest for  $x_0=20$ , and increasingly larger  $\chi_{\min}^2$  values up to  $x_0=80$ , beyond which it fluctuates about  $\chi_{\min}^2=3.85$ .

Another indication that differences exist between the program described in this thesis and the one used by Taff is that this program did not find, for the Perseus cluster, minimum  $\chi^2$  values using Taff's best fit parameters  $\alpha$ ,  $\sigma_C$ , and  $\sigma_{bg}$  at the values of  $x_0$  cited by Taff. In case (a) use of Taff's parameters produced  $\chi_{\text{absmin}}^2$  of 7.91 at  $x_0=40$  (as opposed to  $\chi^2=22.14$  at  $x_0=10$ ) and case (b)  $\chi_{\text{absmin}}^2=6.26$  at  $x_0=20$  (as opposed to  $\chi^2=12.55$  at  $x_0=10$ ).

It should be pointed out that although this program produces a  $\chi_{\min}^2$  that fluctuates about a certain value for large  $x_0$  values (as in Figure 3), the variations of  $\chi^2$  on  $x_0$  found when the program uses Taff's  $\alpha$ ,  $\sigma_C$ , and  $\sigma_{bg}$  shows a pronounced minimum, as illustrated in Figure 4.

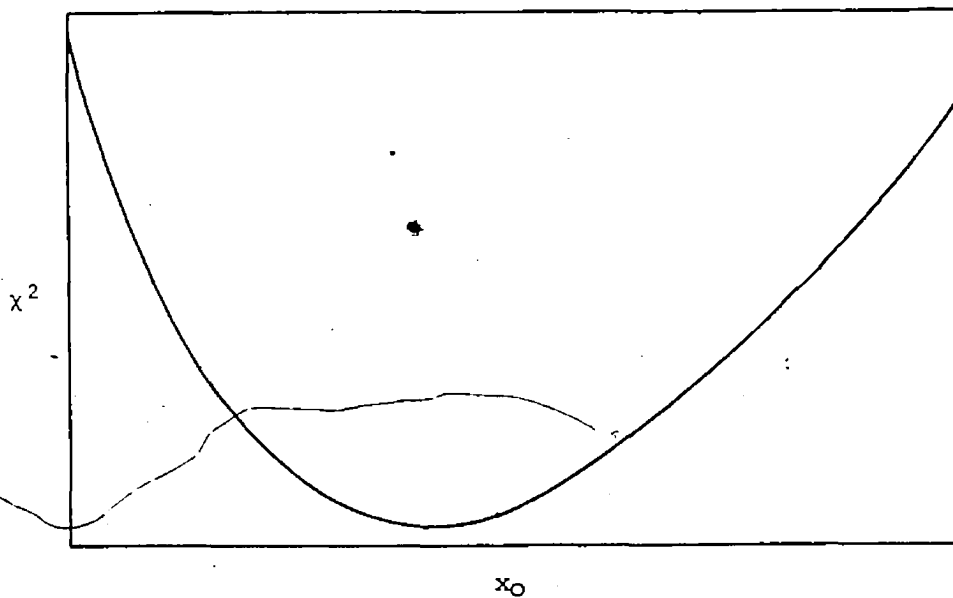


Figure 4  $\chi^2$  versus  $x_0$  for fixed values of  $\alpha$ ,  $\sigma_C$ , and  $\sigma_{bg}$ .

Table 4

Comparison of  $\alpha$  values (in arcmin) for the Perseus cluster

case	mag. limit	Taff	Bahcall	this program
(a)	16 <sup>m</sup> 0	2.89	2.9	1.95
(b)	17.5	3.47	2.7	2.92

This difference in behaviour arises from the fact that in the latter case  $x_0$  is the only remaining variable, whereas normally the parameters  $\alpha$ ,  $\sigma_C$ , and  $\sigma_{bg}$  are all varied for each  $x_0$ .

Table 4 compares the best fit  $\alpha$  values found by Taff, Bahcall, and this program. The  $\alpha$  values for Taff and this program have been given in Table 3, and Bahcall's results are published with her data (Bahcall, 1974). The case (a) result from this program is significantly different from the other two, but this  $\alpha$  value occurred when  $x_0=160$  (see Table 3). For  $x_0=10$ , Taff's best fit value, this program finds  $\alpha=2.98$ . The case (b) result for this program lies between Taff's and Bahcall's values, and so is not significantly different.

Table 5 compares the best fitting models of the cluster A2199. Data for the calculations were obtained from Bahcall (1973). Again, the top line in each case gives Taff's results, the second line those of this program, and the third line this program's results at Taff's best fit  $x_0$ . A third line is omitted when this program and Taff agree on the best fit  $x_0$ . Cases (a) and (d) use galaxy counts down to  $17^m.5$ ; (b) and (e) use galaxy counts down to  $18^m.5$ ; and (c) and (f) use galaxy counts down to  $19^m.0$ . Also, cases (a), (b), and (c) use 15 rings out to  $30'$  on a 103a-D plate while cases (d), (e), and (f) use 26 rings out to  $58:24$  from the cluster centre on a IIIa-J plate.

Table 5  
A2199 results

	$x_0$	$\alpha$	$\sigma_c$	$\sigma_{bg}$	$\chi^2$	$D$
(a)	30	.897	.525	1.31(-2)	7.22	(18.07)
	20	1.236	.393	2.11(-2)	7.40	
	30	.971	.507	2.01(-2)	7.41	
(b)	20	.931	.721	8.65(-2)	3.29	(6.93)
	30	1.073	.633	8.45(-2)	4.10	
	20	1.233	.558	8.78(-2)	4.15	
(c)	200	.135	9.84	3.63(-1)	50.2	(10.27)
	150	1.261	.768	3.51(-1)	6.33	
	200	1.261	.770	3.50(-1)	6.33	
(d)	200	.262	1.85	6.27(-3)	18.0	(68.53)
	200	.455	1.12	8.35(-3)	24.11	
(e)	200	.262	3.38	1.36(-2)	19.5	(66.48)
	200	.386	2.61	1.58(-2)	24.17	
(f)	200	.262	4.20	2.86(-2)	14.5	(45.39)
	200	.315	4.19	3.25(-2)	19.46	

Table 6  
Case (e) extended from Table 5

$x_0$	$\alpha$	$\sigma_c$	$\sigma_{bg}$	$\chi^2$
500	.1730	5.994	1.242(-2)	20.47
700	.1564	6.567	9.293(-3)	19.90
1000	.1520	6.722	5.922(-3)	19.71

Units for Tables 5 and 6:  $\alpha$  - arcmin  
 $\sigma_c$  - galaxies/arcmin<sup>2</sup>  
 $\sigma_{bg}$  - galaxies/arcmin<sup>2</sup>

For cases (a), (b), and (c) the  $x_{\min}^2$  values begin fluctuating at  $x_0$  equal to about 20, 20, and 80 respectively. When constrained to Taff's results this program produced  $x_{\text{absmin}}^2$  at  $x_0=70$  for case (a) and at  $x_0=30$  for case (b). Case (c) has  $x_{\text{absmin}}^2$  for Taff's parameters at 200, where it was still decreasing. The last three cases show  $x_{\min}^2$  for Taff's parameters and for this program's results still decreasing at  $x_0=200$ , which implies that  $x_{\text{absmin}}^2$  actually occurs beyond this limit. In fact, case (e) was extended out to  $x_0=1000$  and was still decreasing, but very slowly. From  $x_0=700$  to  $x_0=1000$   $x_{\min}^2$  decreased from 19.90 to 19.71, a decline of less than 1%. Table 6 gives the  $x_{\min}^2$  parameters for the cases  $x_0=500$ , 700, and 1000. For these large  $x_0$  values the parameters are changing very slowly. Although it is possible to extend the program beyond  $x_0=1000$ , for the testing it was not deemed necessary.

Case (c) in Table 5 is anomalous in that Taff's results differ by almost an order of magnitude from his results for the first two cases. However, the parameters for the last three cases found by Taff and this program change in more or less the same manner from case to case, as do this program's results for the first three cases. It appears that Taff's results may be in error for case (c).

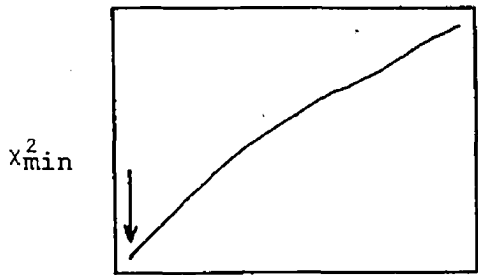
For the Perseus cluster the  $\alpha$  values found by this program appear to be somewhat smaller than those of Taff, but for A2199 Taff's values are consistently smaller. It

was hoped that a study of Taff's computer program could be made to determine the reason for these differences.

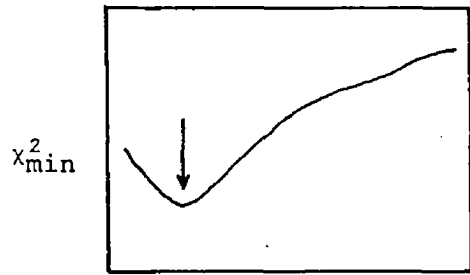
However it was not possible to obtain a copy of his program.

In general, fairly good agreement is found between results from this program and those published by Taff and Bahcall. However, a possible problem arises because of the fluctuations of  $x_{\min}^2$  with changing  $x_0$ . Figure 5 illustrates ways in which  $x_{\min}^2$  is found to vary with  $x_0$  in the tests described above.

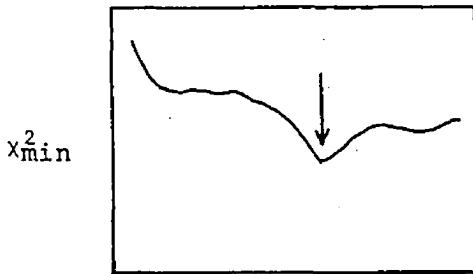
In Figure 5 the ordinate represents a possible range of  $x_{\min}^2$  values for the range of  $x_0$  along the abscissa. In cases 5(a) to 5(d) the choice of  $x_{\text{absmin}}^2$  is obvious, but in case 5(e) there are several choices since more than one  $x_{\min}^2$  have the same minimum value (within truncation limits). It was decided to take as  $x_{\text{absmin}}^2$  the first value arrived at (i.e. that with the lowest  $x_0$  value) because i) there may be an indefinite series of  $x_{\text{absmin}}^2$  as  $x_0$  increases, and since an arbitrary choice must be made, the first will be chosen; and ii) the  $\alpha$  values for similar values of  $x_{\min}^2$  are nearly identical, as will be seen later.



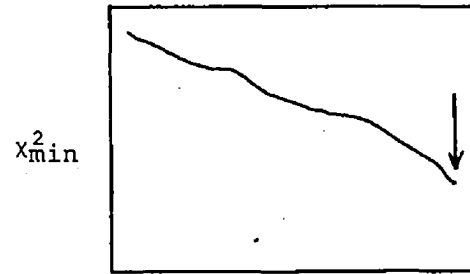
(a)

 $x_0$ 

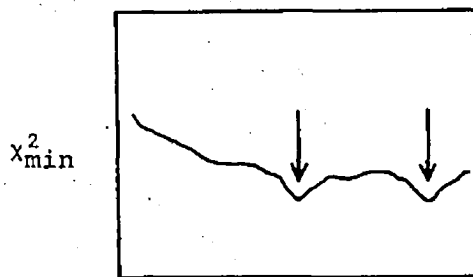
(b)

 $x_0$ 

(c)

 $x_0$ 

(d)

 $x_0$ 

(e)

 $x_0$ 

Figure 5 Possible variations of  $x_{\min}^2$  with respect to  $x_0$ . All arrows point to  $x_{\text{absmin}}^2$ .

iii) Comparison with results published by Bahcall for twelve clusters

A third test of the program was made by comparing results of Bahcall with those of this program using her data. In one of her papers, Bahcall (1975) lists ring counts and ring sizes as well as core radii for twelve clusters. A tabulation of results is shown in Table 7. For this table all  $\alpha$  values were converted to core radii in Mpc through the equation

$$R_c \text{ (Mpc)} = 5.25\alpha z(1+z)^{-2}.$$

In Table 7 (B) identifies Bahcall's results and (C) identifies the results of this program.

If the two columns of  $R_c$  values are compared no systematic differences can be seen. However this program's values are occasionally quite different from those of Bahcall. Two notable examples are A2052 and A2319. These clusters also happen to have, probably not coincidentally,  $\chi_{\min}^2 - x_0$  relations different from the others, which tend to resemble one of the relations shown in Figure 5. The two anomalous relations are shown in Figure 6.

For A2052 the first  $\chi_{\min}^2$  (for  $x_0=10$ ) is much smaller than the rest. The corresponding  $R_c$  is 0.43 Mpc. For  $x_0=20$  through  $x_0=200$   $R_c=0.35$  or  $0.36$  Mpc, much nearer Bahcall's value. But although the core radius is almost

Table 7  
Results of fits to Bahcall's data

Cluster	z	$R_C$ (B)	$R_C$ (C)	$\chi^2_{\text{absmin}}$ (B)	$\chi^2_{\text{absmin}}$ (C)
A194	.0181	.23	.13	1.9	0.50
A1367	.0205	.34	.35	1.9	1.84
A2052	.0351	.28	.43	3.2	1.38
A2319	.0549	.22	.02	2.4	1.43
A2256	.06	.20	.17	7.5	5.84
A401	.075	.24	.19	2.3	1.43
A1775	.0718	.26	.18	1.3	0.15
A1904	.0719	.24	.24	0.3	0.18
A2065	.0722	.29	.33	11.6	8.63
A2029	.0777	.27	.28	1.3	1.27
A1795	.063	.25	.22	0.5	0.12
A1132	.134	.20	.23	2.3	1.81

Both  $R_C$  (B) and  $R_C$  (C) are in Mpc

$$\langle R_C \text{ (B)} \rangle = 0.25 \pm 0.04 \text{ Mpc}$$

$$\langle R_C \text{ (C)} \rangle = 0.23 \pm 0.11 \text{ Mpc}$$

constant for all  $x_0$  values greater than 10, it is this first value that is used since it produces  $\chi_{\text{absmin}}^2$ .

The  $\chi_{\text{min}}^2$  values for A2319 decrease out to  $x_0=60$ , are nearly constant out to  $x_0=160$ , and decrease again at least as far as  $x_0=200$ , where  $\chi_{\text{absmin}}^2$  occurs. For  $x_0=60$  and 160,  $R_c=0.11$  Mpc, as well as for most cases in between. However, for the  $\chi_{\text{absmin}}^2$  at  $x_0=200$ ,  $R_c=0.02$  Mpc. From Figure 6(b) it is expected that  $\chi_{\text{absmin}}^2$ , and possibly  $R_c$ , will decrease even further if  $x_0$  is increased beyond 200, but this expectation has not been tested.

It is also seen in Table 7 that the  $\chi_{\text{absmin}}^2$  values as found by this program are either lower than or equal to those cited by Bahcall, at least to the accuracy quoted by her. This means that the parameters found by this program produce isothermal gas sphere models that fit the published data better than the parameters found by Bahcall. However it must be remembered that different procedures for fitting were used: where this program fit by changing  $\alpha$ ,  $\sigma_c$ , and  $\sigma_{bg}$ , the background densities were fixed as part of the input to Bahcall's program. It is possible that the background densities found by this program are vastly different from the actual (counted) values used by Bahcall, but since she did not publish her background counts comparison is not possible.

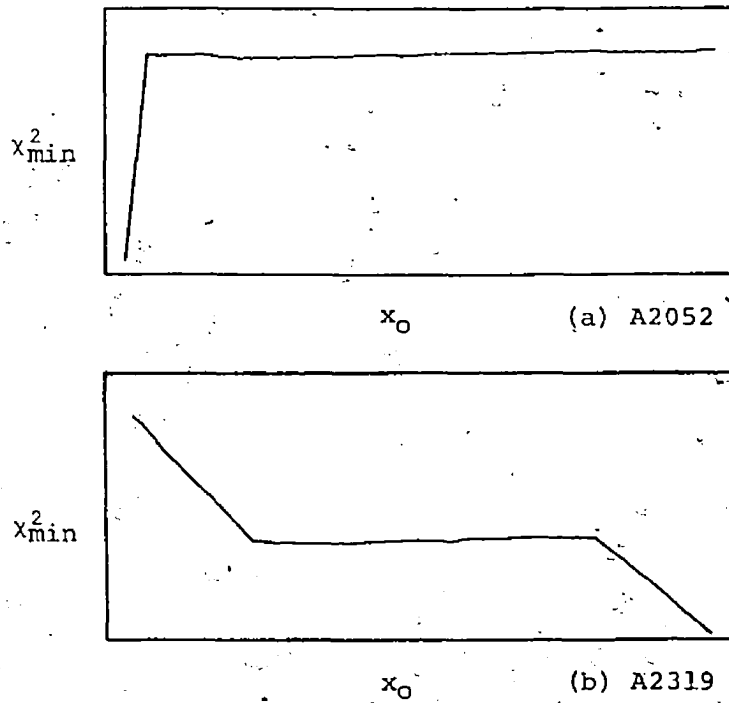


Figure 6  $x_{\min}^2 - x_0$  relations for two clusters

Table 8.

$\alpha$  variations with  $x_0$  for like values of  $x_{\text{absmin}}^2$

Cluster	A1367		A2029	
$x_{\text{absmin}}^2$	1.835		1.270	
	$x_0$	$\alpha$	$x_0$	$\alpha$
	60	3.359	110	.8014
	70	3.358	130	.8011
	100	3.357	140	.8007
	150	3.358	150	.8012
	160	3.358	170	.8013
	180	3.357		

Units:

$\alpha$  - arcmin

Two of the clusters of Table 7 showed variations of  $\chi^2_{\min}$  with  $x_0$  which corresponded to the case shown in Figure 5(e). For these two clusters more than one  $x_0$  was found to produce the same value for  $\chi^2_{\text{absmin}}$ . Table 8 below shows how  $\alpha$  varies with  $x_0$  for the same values of  $\chi^2_{\text{absmin}}$ .

In each case the  $R_c$  values were the same to three decimal places for each value of  $x_0$  shown. This indicates that in cases such as Figure 5(e) the decision to use results from the lowest  $x_0$  producing  $\chi^2_{\text{absmin}}$  will probably not greatly affect the core radius obtained for the cluster.

In summary, although individual values for the core radius may differ from Bahcall's values, the average  $R_c$  values are within a standard deviation of each other. It can also be seen that the results of this program show a standard deviation over twice that of Bahcall, even though the models of this program are found in all but one case to yield lower  $\chi^2$ . This result is of interest because it is the standard deviation of the core radius which measures its usefulness as a cosmological metrestick. Further work should be done to determine whether this difference is produced by the different methods of treating the background or whether it originates within the programs themselves.

## Observational Material

## i) Program input file

To be used by the program a data file must consist of:

- 1) a line of 80 characters. This line is reproduced by the program as entered and is placed in the data file to ensure that the computer terminal is set at the proper line width and is operating correctly;
- 2) the isothermal gas sphere data. These values, entered in E8.5 format, correspond to the values of  $e^{\psi}$  in equation (4) and are obtained for the  $\xi$  values 0.0, 0.1, 0.2, 0.3, ..., 9.8, 9.9, 10.0, 11, 12, 13, ..., 98, 99, 100, 110, 120, 130, ..., 980, 990, 1000. These 281 values were produced by a BASIC program reproduced in Appendix B;
- 3) another line of characters which describes the format of the next three items. This line is skipped by the program;
- 4) the number of rings to be used, entered in I2 format;
- 5) the number of galaxies in each ring, from the centre outwards, in F4.0 format;
- 6) the outer radius of each ring in arcmin, from the centre outwards, in F4.2 format;
- 7) the initial estimates of central and background

densities in galaxies/arcmin<sup>2</sup>, entered respectively in E5.2, 2X, E5.2 format; and

8), a line of characters describing the format of item 7). Since this line and anything following it are ignored by the program it may be omitted.

N.B. If the program version TAFCHEC is being used a line is inserted between items 7) and 8). This contains Taff's values for  $\alpha$ ,  $\sigma_c$ , and  $\sigma_{bg}$  for the cluster under study. These values are entered respectively in the format E5.2, 2(2X, E5.2).

The necessary data for each cluster are the number of rings; number of galaxies per ring, ring sizes, and initial estimates of  $\sigma_c$  and  $\sigma_{bg}$ . Furthermore, each cluster was studied to three magnitude limits, two on a IIIa-J plate and one on a 103a-D plate, all plates were taken by Dr. G. Welch on the Hale Observatory's 48 inch Schmidt telescope.

## ii) Photographic enlargements

The galaxies were identified on the original plates and their images marked on an enlarged photographic print of the cluster. All further work was performed using the print.

To obtain the prints, contact copies were made of the IIIa-J plates of each of the four clusters studied. The Abell radius of each cluster on the copy was calculated through the equation given by Abell (1958)

$$R(\text{Abell}) = 4.6 \times 10^5 / cz \text{ mm} = 1.53 / z \text{ mm}.$$

The contact copies were used to make prints enlarged so that the Abell diameter was just inside the border of the prints, which were 14 by 14 inches. Two identical prints were made for each cluster, one for marking the location of galaxies identified on the IIIa-J plate and another for the 103a-D plate.

The 10X stereo microscope to be used for identifying galaxies on the original plates was found to have a comfortable viewing area of about 10' by 10', so the prints were divided into areas of approximately this angular size. These areas were numbered and a BASIC random number generator was used to determine the order in which they would be examined. It was felt that this process would minimize the systematic effect of any time-dependant errors in identifying galaxies. During the course of examining different areas of the print, some of the first areas checked were re-examined to ensure the consistent use of the chosen limiting magnitude.

iii) Limiting magnitudes

For each of the eight plates the objects identified as galaxies were marked on the prints. In all cases identification was made to the plate limit, where the plate limit is defined as the faintest magnitude at which it is possible to distinguish with certainty stellar from galaxian images.

Since this thesis is attempting to augment the work of Bahcall (1975) who counted galaxies within  $3^m$  of the brightest galaxy of each cluster, and since photometry is unavailable for the clusters being studied here, an approximation to Bahcall's  $3^m$  difference must be made.

From the relation

$$\Delta M = 6.00 \log(x)$$

(from Holmberg, 1975) where  $\Delta M$  is the magnitude difference between two galaxies whose absolute major axes differ by a factor of  $x$ , it is found that an axial ratio of 3 corresponds to a magnitude difference of almost 3. The use of such a relation to approximate a magnitude difference is possible in the present case because the galaxies are assumed to be at the same distance. It must be remembered that Holmberg bases his results on an examination of normal galaxies, whereas the brightest members of A2052, A2593, A2626, and A154 have extended halos characteristic of supergiant

galaxies. It is therefore clear that applying the Holmberg relation will allow a derived magnitude difference to be only roughly approximated.

The prints used for IIIa-J counts were examined under a 4X eyepiece with a graduated reticle and the size of the major axis of the cluster's brightest galaxy was estimated. All galaxies on this print that had major axes greater than or equal to  $1/3$  this size were identified. Since the galaxies do not have well defined edges, a cutoff was chosen arbitrarily where the image density lessened perceptibly from that of its centre. The use of the print for this identification was necessary because no means were available to measure the image size on the original plates with sufficient accuracy.

Visual examination of the prints showed no evidence of background density variations which could have arisen during the production of the prints and might introduce systematic position-dependent variations in the cutoff density. Also, as will be seen in the next chapter, the background number densities computed by the program for this bright limit agrees well with the background densities counted at the print corners, which suggests that such errors are not significant.

This process identifies three magnitude limits: the faintest being that of the IIIa-J plate; the next being that of the 103a-D plate; and the brightest corresponding to the

size ratio of 1:3 on the IIIa-J plate. No bright limit was found for the 103a-D plates because the image resolution was noticeably poorer than on the IIIa-J plates, making the establishment of a uniform density cutoff more difficult.

iv) Cluster centres from strip counts

The location of the cluster centre corresponding to each magnitude limit now had to be obtained. Since previous work has shown that if a cluster possesses a dominant galaxy it is usually at or near the cluster centre, it was assumed that such was the case for the clusters being studied here. Of the four, three have a dominant, probably cD, galaxy and the other (A154) has a dominant binary galaxy.

A square grid of strips 1.5 cm by 18 cm was centred over the dominant galaxy (or between the pair of A154) and strip counts were taken of all galaxies to the limit being studied. Counts were made on the print in four orientations: N-S; E-W; NE-SW; and SE-NW. The estimated cluster centre for each orientation was the point having equal numbers of galaxies on either side. The cluster centre for each magnitude limit was found by averaging the estimates of each orientation.

Table 9 is a partial result of strip counting. In it is presented the maximum difference between the cluster centres determined from the three limits, both in arcmin and as a fraction of the width of the rings used to tabulate the radial density distribution.

Table 9  
Separation of magnitude limit centres

cluster	A2052	A2593	A2626	A154
distance (arcmin)	0.79	0.88	2.08	0.84
dist/(ring width)	0.35	0.42	1.28	0.54

Three of the clusters show all three estimates to lie much closer together than the resolution of the ring counts, but the IIIa-J bright limit estimate for A2626 differs significantly from the other two (the IIIa-J faint and the 103a-D limits for A2626 are 0.31 ring widths apart). The difference is assumed to be real and so the centres for each limit will be taken as those found from the strip counts. The small differences among centre positions is not considered likely to introduce significant differences

in the ring counts and eventually core radii. Complete results of strip counting are presented in Appendix E.

v) Ring counts

After the centre was chosen for each magnitude limit a grid of 20 concentric rings, having radii differing by 7.9 mm, was laid over the centre and ring counts were made. These counts were performed on one quadrant at a time to check for major azimuthal density variations that might suggest a mislocation of the cluster's centre. No such variations were found. The ring count results are presented in Appendix F.

Table 10 gives, in arcmin, strip widths and lengths, the width of each ring, the overall ring radius (i.e. the radius of the 20<sup>th</sup> ring), and the Abell radius for each cluster studied.

The ring sizes and number of galaxies per ring for each magnitude limit were converted into densities and average radii ( $r_{av}$ , see equation 2), and a plot of density versus  $r_{av}$  was made. A smoothed curve was drawn by eye to obtain an initial estimate for  $\sigma_C$ .

The initial estimate for  $\sigma_{bg}$  was obtained in a different manner. Since the actual background density is

Table 10

Strip width and length, ring size, and total and Abell radii

cluster	A2052	A2593	A2626	A154
strip width	4.28	4.04	3.12	2.97
strip length	51.36	48.48	37.44	35.64
ring width	2.24	2.12	1.63	1.55
outer ring radius	44.80	42.40	32.66	31.09
Abell radius	48.96	38.95	31.16	30.60

Units: all values are in arcmin

Table 11

Areas involved in background counts

(see Figure 7)

cluster	A2052	A2593	A2626	A154
one corner area	620.0	587.0	350.4	317.6

Units: all values are in arcmin<sup>2</sup>

needed for the program BGIN, which more closely approximates Bahcall's program, it was decided that the estimate should be the background density as obtained from counts.

An area about 9 cm by 9 cm was marked off at each corner of each print (NE, NW, SE, and SW, the prints being so aligned) and the galaxies in each corner were counted to the limits previously discussed. This provided the estimate for  $\sigma_{bg}$ , the counts for these are in Appendix G.

The diagram on the next page (Figure 7) is a scale drawing of the "working features" of the prints used. The concentric circles indicate the 10 and 20 ring sizes and the four corner squares represent the areas used for background counting. It can be seen that the background areas overlap rings out to about fifteen. This is not considered a matter of concern since the density profiles usually reach background levels by the 10<sup>th</sup> and almost always by the 14<sup>th</sup> ring.

Of the original list of required data all values are fixed but the number of rings. Since the background was usually just reached by the 10<sup>th</sup> ring and because data were obtained for all 20 rings, it was decided to run the programs twice for each set of data, once with all 20 rings and once with only the inner 10. The 20 ring case gives higher weight to the background and the 10 ring case emphasizes the cluster but loses information regarding background. It is

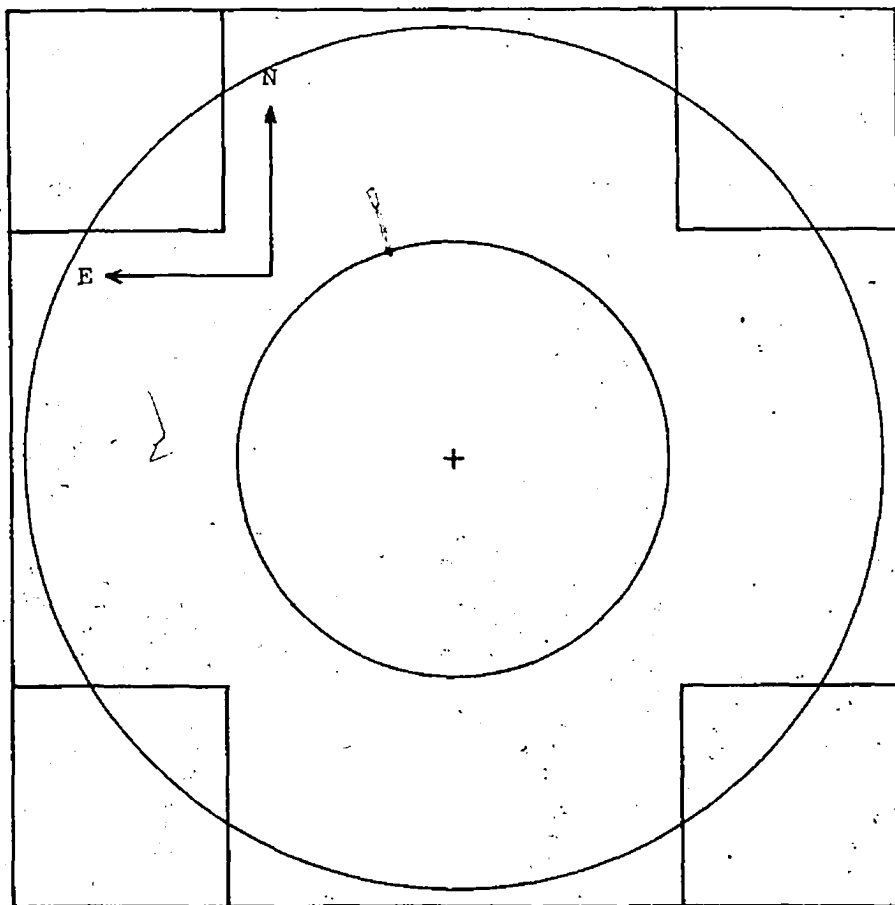


Figure 7. Diagram of the major "working features"  
of the photographic prints drawn to scale

expected that if the program produces realistic fits and the background is uniform throughout the cluster then results from both runs should be similar. For the purpose of this thesis nothing was done with the rings but use either all 20 or just the inner 10. At no time were rings combined in any fashion (e.g. as done by Bahcall, 1975).

## Results

## i) Results tabulated

A table containing core radii and background densities is presented on the next page, Appendix H contains the complete results. The computer programs used to produce the values for the tables in this chapter do not output linear core radii but give structural lengths,  $\alpha$ , in arcminutes. Conversion to linear core radii is done through the relation

$$R_c = 5.25\alpha z(1+z)^{-2} \text{ Mpc.}$$

In Table 12, for each cluster there are three double rows of numbers. The top pair corresponds to the IIIa-J bright magnitude limit (the brightest limit), the second pair to the 103a-D limit, and the third to the IIIa-J faint limit (the faintest limit). Henceforth these limits are to be referred to as the "b", "D", and "f" limits respectively. The top line of each pair presents results obtained when the counts from all 20 rings are used and the bottom line gives the results when the counts from the inner 10 rings are used.

The columns show, from left to right: the emulsion; ML - the magnitude limit;  $\Delta M$  - the approximate magnitude difference between the b limit and the D and f limits;

Table 12  
Final results

Cluster/ Emulsion	ML	$\Delta M$	NR	NG	$R_C$	$R_C^*$	$\sigma_{bg}$	$\sigma_{bg}^*$
<u>A2052:</u>								
IIIa-J	b	-	20 10	58 40	.037 .023	.031 .030	2.42(-3) 8.52(-3)	4.44(-3) "
103a-D	D	1.6	20 10	341 140	.495 .499	.508 .458	4.31(-2) 8.20(-3)	4.15(-2) "
IIIa-J	f	2.3	20 10	848 315	.467 .413	.477 .467	1.13(-1) 1.28(-1)	1.12(-1) "
<u>A2593:</u>								
IIIa-J	b	-	20 10	78 36	.303 .311	.253 .318	1.19(-2) 3.15(-3)	6.39(-3) "
103a-D	D	1.8	20 10	678 312	.554 .656	.481 .672	4.52(-2) 5.74(-3)	7.75(-2) "
IIIa-J	f	2.1	20 10	882 359	.829 .794	.847 .780	6.34(-2) 4.55(-2)	1.13(-1) "
<u>A2626:</u>								
IIIa-J	b	-	20 10	91 40	.336 .365	.330 .334	1.19(-2) 9.67(-3)	1.85(-2) "
103a-D	D	1.8	20 10	697 228	.408 .268	.299 .251	1.67(-1) 2.02(-1)	2.14(-1) "
IIIa-J	f	2.3	20 10	1528 498	.378 .280	.313 .250	3.79(-1) 5.36(-1)	4.44(-1) "
<u>A154 :</u>								
IIIa-J	b	-	20 10	95 40	.167 .014	.178 .178	1.79(-2) 3.77(-2)	1.65(-2) "
103a-D	D	1.3	20 10	498 187	.133 .016	.144 .146	1.05(-1) 1.70(-1)	1.06(-1) "
IIIa-J	f	1.5	20 10	634 232	.051 .027	.070 .038	1.51(-1) 1.71(-1)	1.37(-1) "

Units:

$\Delta M$  - magnitudes  
 $R_C$  and  $R_C^*$  - Mpc  
 $\sigma_{bg}$  and  $\sigma_{bg}^*$  - galaxies/arcmin<sup>2</sup>

NR - the number of rings used; NG - the number of galaxies included;  $R_c$  - the core radius in Mpc obtained when  $\sigma_{bg}$  is treated as a free parameter;  $R_c^*$  - the core radius in Mpc obtained using the observed background density as a fixed value;  $\sigma_{bg}$  - the background density in galaxies/arcmin<sup>2</sup> obtained by treating this density as a free parameter; and  $\sigma_{bg}^*$  - the observed background density in galaxies/arcmin<sup>2</sup>, a value that is the same for the 20 and 10 ring cases for a given magnitude limit. In addition, the cluster to which each set of figures pertains is listed at the upper left. The values of  $\Delta M$  are obtained from the relation

$$\Delta M = 1.6667 \log(N_2/N_1)$$

where  $N_2$  is either the D or f background count and  $N_1$  is the b background count. The only major assumption incorporated into this relation is that the galaxies counted are uniformly distributed in space. For a derivation of this relation see Mihalas (1968).

Table 12 shows that in cases where the same number of rings are used the greatest number of galaxies is included in the f limit and the smallest number in the b limit. This reflects the different magnitude limits to which galaxies are counted.

The core radii alone, in Mpc, are presented in Table 13 in the same format as in Table 12.

Table 13  
Core radii only

Emulsion	ML NR	A2052		A2593		A2626		A154	
		$R_C$	$R_C^*$	$R_C$	$R_C^*$	$R_C$	$R_C^*$	$R_C$	$R_C^*$
IIIa-J	b 20	.037	.031	.303	.253	.336	.330	.167	.178
	10	.023	.030	.311	.318	.365	.334	.014	.178
103a-D	D 20	.495	.508	.584	.481	.408	.299	.133	.144
	10	.499	.458	.656	.672	.268	.251	.016	.146
IIIa-J	f 20	.467	.477	.829	.847	.378	.313	.051	.070
	10	.413	.467	.794	.780	.280	.250	.027	.038

Units for  $R_C$  and  $R_C^*$  are Mpc

ii) Comparison of  $\sigma_{bg}$  and  $\sigma_{bg}^*$ 

When the computer generated  $\sigma_{bg}$  values are compared to the corresponding observed  $\sigma_{bg}^*$  values, it is found that the computer program generally produces a realistic background density. Only a few computed values are significantly different from the observed ones. However, whenever the relative difference is greatest for each cluster (A2052-D, A2593-D, A2626-b, and A154-b) the computed value is obtained for the 10 ring case. This is probably because the counts reach background by about the 10<sup>th</sup> ring, allowing a more accurate background fit to the 20 ring counts. The 10 ring counts, therefore, refer mainly to cluster galaxies and the background is given little weight. As Table 10 shows, the diameter of the 20<sup>th</sup> ring is almost coincident with the Abell diameter.

These facts suggest that if a computer program similar to the one used here is to consistently obtain a realistic background density as part of the fitting process, galaxy counts should be made out to the Abell radius. This further suggests that core radii obtained from 10 ring counts with  $\sigma_{bg}$  treated as a free parameter may also be unrealistic, a possibility that will be checked in the next section.

iii) Comparison of 10 ring core radii and 20 ring core radii

If core radii obtained from 10 ring counts when the background density is calculated ( $R_C(10)$ ) are occasionally unrealistic because of poorly determined background densities, then these radii should be significantly different from those obtained using 10 ring counts with the observed, fixed, background densities ( $R_C^*(10)$ ). These differences would be expected to be larger than the differences between  $R_C(20)$  and  $R_C^*(20)$ , because using 20 rings presumably allows a more realistic background density to be determined. The results of Table 13 were used to compute the percent difference between the 10 ring and 20 ring core radii using the expressions

$$\frac{|R_C(10) - R_C^*(10)| \times 100}{0.5 \times \{R_C(10) + R_C^*(10)\}} \quad \text{and} \quad \frac{|R_C(20) - R_C^*(20)| \times 100}{0.5 \times \{R_C(20) + R_C^*(20)\}}$$

These values were calculated for each magnitude limit and each cluster. Then the  $b(10)$ ,  $D(10)$ , and  $f(10)$  differences and the  $b(20)$ ,  $D(20)$ , and  $f(20)$  differences were averaged for each cluster to see if there was a significant discrepancy between the 10 and 20 ring cases.

For two clusters the 20 ring cases produced smaller differences than the 10 ring cases by factors of 2 and 10. However, for the other two clusters the 10 ring cases produced differences smaller by factors of 5 and 2.

The 20 ring and 10 ring average differences for all four clusters were respectively  $12\% \pm 11\%$  and  $37\% \pm 61\%$ . The large standard deviation in the 10 ring difference is due mainly to the A154 results, which have large internal inconsistencies. If A154 is omitted the 20 and 10 ring averages become  $12\% \pm 10\%$  and  $9\% \pm 8\%$  respectively.

For individual clusters the percentage differences show that one or the other of the 10 or 20 ring core radii are probably better representatives for the cluster. The overall averages, however, do not suggest that either 10 or 20 ring counts consistently give better results. If A154 is omitted, these results indicate that the occasional inability of the program to produce realistic background densities using 10 ring counts does not significantly affect the value of the core radii.

#### iv) Comparison of $R_C$ and $R_C^*$

Since core radii depend to some extent on background densities it is appropriate to consider the effects of differences in background densities on these radii. Specifically, consider for each magnitude limit the  $R_C(10)$  and  $R_C(20)$  percentage differences (where each value has a characteristic background density) to the  $R_C^*(10)$  and

$R_C^*(20)$  percentage differences (where each value has the same background density). If the observed background provides a better base for calculating core radii then the percentage differences between  $R_C^*(10)$  and  $R_C^*(20)$  should be smaller on the average than those between  $R_C(10)$  and  $R_C(20)$ .

For each magnitude limit and each cluster the percentage differences were found through

$$\frac{|R_C(10) - R_C(20)| \times 100}{0.5 \times \{R_C(10) + R_C(20)\}} \quad \text{and} \quad \frac{|R_C^*(10) - R_C^*(20)| \times 100}{0.5 \times \{R_C^*(10) + R_C^*(20)\}}$$

The  $b(R_C)$ ,  $D(R_C)$ , and  $f(R_C)$  differences and the  $b(R_C^*)$ ,  $D(R_C^*)$ , and  $f(R_C^*)$  differences were averaged for each cluster and compared.

For three clusters the differences between the  $R_C^*$  values were less than the  $R_C$  differences by factors of 2, 4, and 6. In the other case the differences between  $R_C$  values were smaller by a factor of 3.

The overall average of all four clusters including the three magnitude limits showed that  $R_C^*$  differences were  $15\% \pm 17\%$  while the  $R_C$  differences were  $46\% \pm 58\%$ . Most of the spread in the  $R_C$  difference is again due to A154, which has a wide range of core radii. Without A154, the  $R_C^*$  percentage difference is still smaller ( $13\% \pm 11\%$  compared to  $18\% \pm 17\%$  for  $R_C$ ), but the discrepancy between the two has shrunk considerably. These percentage differences suggest that  $R_C^*$  values may be slightly more consistent than  $R_C$  values (in

that there is closer agreement, generally, between  $R_C^*(10)$  and  $R_C^*(20)$  than between  $R_C(10)$  and  $R_C(20)$ ). It appears that, again neglecting A154, only marginal differences in core radii result when the background density is either left constant or calculated with the other parameters, a result consistent with the findings of the previous section.

There are seven cases where the differences are greater than 30% of the average: the  $R_C$ -b case of A2052 (47%); the  $R_C^*$ -D case of A2593 (33%); the  $R_C$ -D case of A2626 (41%); the three  $R_C$  cases of A154 (b-169%, D-159%, and f-62%); and the  $R_C^*$ -f case of A154 (59%). Five of these seven have density profiles with a first ring density significantly higher than the rest of the ring densities, the A2593 and A2626 cases are the exceptions. If the high first ring densities are the cause of the discrepancies, it is probably because of the higher weight these points have in the 10 ring case. The effect on the model is to produce a higher central density and a correspondingly smaller core radius, particularly in the cases where the background density is found as part of the fitting procedure. Table 13 supports this conclusion, showing that for the cases where the discrepancy is in the  $R_C$  columns, it is indeed the 10 ring core radius that is smaller.

To see how significant the central data point is, the data for A2052-b were run with the inner ring omitted. The core radius obtained for the outer 19 rings was  $R_C^* = 0.602$

Mpc, as opposed to 0.031 Mpc with all 20 rings. (For comparison, this core radius occurs at 10.5 on the first graph of Appendix I.)

v) Individual cluster abnormalities

The Rood-Sastry (1971) classification for each cluster is listed below.

Table 14  
Rood-Sastry classifications

cluster	R-S class
A2052	cD
A2593	--
A2626	cDp
A154	Bb

The R-S type for A2626 indicates that the supergiant galaxy is a multiple or has some other sort of peculiarity. What this may be is not discussed by Rood and Sastry, but visual inspection through a 10X stereo

microscope shows that the densest part of the image is not located at the centre of symmetry. It is not known if this is the peculiarity referred to, or even if this observed oddity is inherent in the galaxy or due to a superimposed stellar or galaxian image.

The type assigned A154 indicates a cluster with a central binary galaxy whose components are connected by a luminous bridge. It is not known whether binary clusters are basically different in structure, which might explain the anomalous (i.e. very small)  $f$  radii of this cluster.

A2593 is not classified by Rood and Sastry since they feel it to be either an I cluster superimposed on a CD cluster or a single peculiar I cluster. The possibility that we view two superimposed clusters is supported both by inspecting the prints with galaxies identified to D and  $f$  limits and by strip count histograms. These suggest the presence of a small group of relatively faint galaxies about  $15''$  south of the dominant elliptical. If this is the case, then the strip count centre would possibly be chosen further south than otherwise, resulting in a larger core radius.

To test this possibility ring counts were made of only the north half of this cluster, with rings centred on the brightest galaxy. These numbers were doubled to simulate a cluster with north-south symmetry and treated as a cluster by the program. The resulting core radii are presented in Table 15 with a format and notations identical

to those of Table 13.

These results show that the smallest changes in core radius are those of the b limit. This is consistent with the existence of a background cluster which would not have been included in these counts.

The D limit core radii have changed drastically. This is mainly because 10 of the 13 galaxies in the first ring are located in the northern half of the cluster. The assumption of north-south symmetry about the brightest galaxy thus leads to a central ring containing 20 galaxies, an increase of 54%.

The f limit values also decreased, as would be expected if a background cluster were present to the south. However, an inspection of ring counts indicates that this may be due more to an increase of galaxies in the first ring than to a decrease in numbers in the outer rings, a supposition supported by the new f core radii.

The evidence is that the background cluster, if it exists, becomes apparent between the b and D magnitude limits, and affects the corresponding core radii. But it is also apparent that asymmetries in the distribution of fainter galaxies within the foreground cluster itself can significantly change the core radius, depending upon the choice of centre for the ring counts. Fortunately, neither this asymmetry nor the possible background cluster affect the b limit core radii.

Table 15  
Core radii for A2593

Emulsion	ML	NR	From Table 13		N only	
			$R_C$	$R_C^*$	$R_C$	$R_C^*$
IIIa-J	b	20	.303	.253	.212	.250
		10	.311	.318	.318	.349
103a-D	D	20	.554	.481	.044	.043
		10	.656	.672	.032	.044
IIIa-J	f	20	.829	.847	.659	.459
		10	.794	.780	.381	.381

Units for  $R_C$  and  $R_C^*$  are Mpc

## vi) The mass segregation question

It has been decided to use the  $R_C^*(20)$  values hereafter as the values representing the core radii for the magnitude limits. These were chosen because the  $R_C^*$  values have been found to be possibly more consistent than the  $R_C$  values and because 10 ring counts generally do not extend appreciably into the background and so possibly give unrealistic radii at times (the results of section iii notwithstanding). These core radii are displayed in Table 16.

Table 16  
Adopted core radii in Mpc

ML	A2052	A2593	A2626	A154
b	.031	.253	.330	.178
D	.508	.481	.299	.144
f	.477	.847	.313	.070

As clusters of galaxies evolve the tendency towards equipartition of energy results in the more massive galaxies losing kinetic energy to the less massive ones. As a result the less massive galaxies will move farther out

in the cluster and the more massive ones will fall to the centre. Equipartition of energy will therefore result in a radial segregation of mass. The more massive galaxies, as a group, would thus define a smaller core radius than a group of less massive galaxies, with a mixed group having an intermediate core radius.

Oemler (1974) has found evidence of mass segregation in all six cD clusters he studied (of a total of 15). Quintana (1979) has recently found evidence for mass segregation by fitting isothermal gas sphere models to galaxy counts of the Coma and CA0340-538 clusters. Dressler (1978), on the other hand, has studied 15 rich clusters, including five cD clusters, and has found evidence of mass segregation in only three cases, only one of which is a cD cluster. The other four cD clusters display somewhat larger core radii for the brighter (more massive) galaxies than for fainter ones. This phenomenon is attributed to a further stage of cluster evolution in which bright galaxies near the cluster centre are accreted by the central cD galaxy. The resulting lower central number density is reflected in a larger core radius.

From the values in Table 16, only A2052 and A2593 give evidence of mass segregation. Both of these clusters have possible anomalies, however. The extremely low core radius for A2052-b seems unlikely (as do other core radii near this size) despite the goodness of fit, especially when

the core radius obtained through omission of the inner ring is considered (see section iv of this chapter). Also the A2593-D and f core radii may be too large because of the presence of a superimposed cluster.

A2626 shows no evidence for mass segregation and the A154 values suggest that the fainter galaxies are more centrally concentrated than the brighter ones, a situation which is consistent with the accretion process described by Dressler. The A154-f result is probably due mainly to a grouping of faint galaxies observed around the central binary, a phenomenon not believed to be associated with accretion but merely a chance positioning on galaxies.

If the four values for each magnitude limit are averaged, the ratio  $R_C^*(b):R_C^*(D):R_C^*(f)$  is .20:.36:.43, which taken at face value implies an overall tendency towards mass segregation. However the scatter is so large that these averages are probably not significant. Although a general trend can not be cited, two of the clusters studied do show signs of mass segregation.

vii) Comparison with published core radii

Core radii have been published by Bahcall (1975) for A2052 and by Dressler (1978) for A154, allowing comparisons with the values found here.

Bahcall's data for A2052 indicate that her counts covered 12 of the 20 rings used here. Furthermore, instead of using rings of uniform width, Bahcall used four central rings 2.24 wide and four outer rings 4.48 wide while this investigation used rings 2.24 wide. Therefore, the data found here were combined to simulate wider rings in order to determine if results similar to those of Bahcall would be obtained.

Table 17 shows in column 1 the data source of the ring counts. Column 2 indicates the magnitude limit of the present data, the b limit was chosen because it is closest to Bahcall's magnitude limit. Column 3 gives the number of rings used, either the inner 10, the inner 12 (B), or all 20. The last two columns give, respectively, the number of galaxies used in the calculations and the core radii obtained in Mpc.

The top three rows present results using the data from this thesis. The bottom rows give results produced by Bahcall and by this program using Bahcall's data.

The results show that analysing the present data using rings having the same width as those used by Bahcall

Table 17  
Core radii for A2052

	ML	NR	NG	$R_c$
Thesis data:	b	10	40	.023
		B	46	.025
		20	58	.037
Bahcall's data: her results	-	B	73	.28
	-	B	73	.430

produces no appreciable difference in the core radius compared to others found with this study's data. The bottom lines show that using Bahcall's data this program produces a much larger core radius than that found by Bahcall, a result which has been discussed in Chapter III. Comparison with Table 13 shows that this core radius is similar to the value found with the f limit data for this cluster. This result is probably at least partly due to mass segregation. This possibility presents itself because Bahcall counts 60% more galaxies and so presumably reaches a fainter magnitude limit than the b limit used here. Mass segregation in this cluster is strongly suggested by the values in Table 16. The possibility exists that the disparate results are due to the two sets of data (Bahcall's and those of this study) being centred differently. This

seems unlikely to give the large differences, however, as the centres are the same to within  $0^m.1$  and  $1'$ .

Dressler used a method similar to that of Bahcall to obtain the core radius of A154. He found a core radius of 0.19 Mpc with counts out to about the eighth ring used here. This area was apparently divided into 11 rings of the same width. Unfortunately, neither ring counts nor limiting magnitudes are given by Dressler so a detailed comparison is precluded. However, his result is close to the A154 core radius obtained from the b counts (see Table 16).

viii) Combination of present core radii with those of Bahcall

Bahcall (1975) has published core radii of 15 Abell clusters and has obtained an average value of  $0.25 \pm 0.05$  Mpc (the 0.05 value is the standard deviation of scatter, and has no bearing on errors inherent in the individual core radii). The b limit core radii of Table 16 will be combined with Bahcall's results to obtain a new average and standard deviation. Bahcall's results may have been influenced by the fact that she only once counted out to near the Abell radius; on the average the distance to which she counted from the cluster centre is only 53% of the Abell radius, as opposed to an average of 102% for this

thesis.

Using the core radii specified above from Table 16 and Bahcall's results, the combined average is

$$\langle R_C \rangle = 0.24 \pm 0.07 \text{ Mpc} \quad (H_0 = 50 \text{ km s}^{-1} \text{ Mpc}^{-1})$$

Bahcall's value is not changed much, mainly because of her larger sample. For comparison, the average of the four core radii from this thesis is  $0.20 \pm 0.13 \text{ Mpc}$ . (If the core radius of A2052 is neglected the average core radius for the remaining three clusters is  $0.25 \pm 0.08 \text{ Mpc}$ .)

To see if the number of core radii averaged is a significant factor, four random groups of four core radii were taken from Bahcall's results and averaged. The averages found were  $0.28 \pm 0.07 \text{ Mpc}$ ,  $0.23 \pm 0.02 \text{ Mpc}$ ,  $0.24 \pm 0.07 \text{ Mpc}$ , and  $0.24 \pm 0.06 \text{ Mpc}$ . This implies that the large standard deviation for the average of the four core radii of this thesis has little to do with the number of values averaged.

The fact that the clusters studied here tend to be cD clusters as opposed to spiral rich or spiral poor clusters is not an influential factor. An inspection of the clusters used in Bahcall's paper show six cD, four B, two L, one F, one C, and an unclassified cluster. No type shows a significantly larger or smaller mean core radius.

If the spread of core radii is as large as Table 16 (or worse yet, Table 13) implies then the validity of using this radius as a cosmological metrestick may be

questioned. Calculations can be made to determine how far away in  $z$  clusters would have to be before the spread of standard deviation is overcome by the changes in radius caused by the value of  $q_0$ . For example, in universes with deceleration parameters 0 and +1, a 0.25 Mpc object would differ in size by 0.05 Mpc (Bahcall's standard deviation) at  $z=0.43$ , and the same object would differ in size by 0.13 Mpc (the standard deviation for all four clusters from this thesis) at  $z=1.17$ . It is obvious that if the value of the standard deviation is near the value found for the four clusters of this thesis the probability of determining  $q_0$  from core radii is low.

Also, if there is mass segregation present in some clusters of galaxies further problems arise, namely that the core radius will be a function of the limiting magnitude.

## ix) Conclusions

1.) Results in the bottom two rows of Table 17, as well as those in Chapter III, indicate that the same data can produce widely differing results depending on their treatment. Even when the general method of analysing the data is supposedly the same (see Chapter III, section iii)

different results are obtained by different programs for individual clusters.

This suggests that a study should be made of all programs used by researchers to determine which is best, however that may turn out to be defined, for a given method of finding core radii. This program should then be used by everyone in this line of study to ensure consistent results. Or, if it happens that no one program is any better than another, to maintain consistency one program should be chosen to be used exclusively. Then the comparison of results would acquire a greater significance. (This obviously does not exclude further work at attempts to devise an improved program for core radius determination.)

2.) More consistent results seem to be found in the present investigation when the background density is counted, rather than calculated as a free parameter in the fitting process.

3.) Care should be taken to include a large background sample in the data by counting out sufficiently far from the cluster centre. The Abell radius seems to contain a large enough area for this purpose. This procedure seems to be of greater importance when the background density is to be calculated rather than counted directly.

4.) Two clusters show evidence of mass segregation but a general trend is not evident in the small sample studied here. In at least one of these clusters,

A2593, this effect may be caused by the presence of a second cluster in the field.

5.) The spread of core radii appears to be larger than that in the sample studied by Bahcall. This raises new questions concerning the use of these radii as standard metresticks in attempts to determine the value of the deceleration parameter.

If the spread of core radii is as great as is suggested by this thesis, then only very large  $z$  (greater than about 1) clusters will be usable in determinations of  $q_0$ . The lack of rich clusters at these distances could prevent the determination of the deceleration parameter.

Part of this spread may be due to mass segregation. If this is so, then establishment of a sufficiently accurate magnitude limit would be required before a large sample of such clusters could be used for this purpose.

## References

- Abell, G. 1958, Ap.J.Suppl., 3, 211.
- Bahcall, N.A. 1972, A.J., 77, 550.
- 1973, Ap.J., 186, 1179.
- 1974, Ap.J., 187, 439.
- 1975, Ap.J., 198, 249.
- Chandrasekhar, S. 1942, Principles of Stellar Dynamics,  
(Chicago: University of Chicago Press).
- Dressler, A. 1978, Ap.J., 226, 55.
- Holmberg, E. 1975, Galaxies and the Universe, ed. A. Sandage,  
M. Sandage, and J. Kristian, (Chicago: University  
of Chicago Press), Chap. 4.
- Mihalas, D. 1968, Galactic Astronomy, (W.H. Freeman and  
Company).
- Oemler, A. 1974, Ap.J., 194, 1.
- Quintana, H. 1979, A.J., 84, 15.
- Rood, H.J. and Sastry, G.N. 1971, P.A.S.P., 83, 313.
- Taff, L.G. 1975, Ast. & Ap., 77, 550.
- Zwicky, F. 1957, Morphological Astronomy, (Berlin: Springer-  
Verlag).

Appendix A  
Program listing

A listing is provided of the program version (named YAHOO) that finds the best fit values for  $x_0$ ,  $\alpha$ ,  $\sigma_C$ , and  $\sigma_{bg}$ . The listing should contain enough comment cards to enable a user to follow proceedings; if these are insufficient an extensive explanation is presented in Appendix C. These, combined with the description of the type and format of required input data provided at the beginning of Chapter IV, fully explain the workings of this program. The first page of a typical output run of YAHOO is presented in Appendix J with sample outputs of two other programs.

```

C
C
C      INPUT
C      DATID(I)  PRINTER CHECK
C      EPSI(I)  THE SERIES OF VALUES (EXP(-PSI)*PSI4)
C      J        TOTAL NUMBER OF RINGS (NOT NECESSARILY ALL OF SAME WIDTH)
C      NOBS(I)  NUMBER OF OBSERVED GALAXIES IN RING I
C      ROUT(I)  OUTER RADIUS OF RING I
C      SC1      INITIAL ESTIMATE OF CENTRAL DENSITY
C      SBG1     INITIAL ESTIMATE OF BACKGROUND DENSITY
C
C      MAJOR ARRAYS AND VARIABLES
C      XI(I)    THE SERIES OF XI VALUES CORRESPONDING TO EPSI(I)
C      SIGOB(I) GALAXY DENSITY IN RING I
C      SIGISO(I) CALCULATED GALAXY DENSITY AT SAME DISTANCE FROM CLUSTER
C               CENTRE AS SIGOB(I)
C      NCALC(I) THEORETICAL VALUE FOR NOBS(I), CALCULATED FROM SIGISO(I)
C      INTDI(I) STORAGE PLACE OF INTEGRATION RESULTS, REQUIRED BY
C               INTEGRATION SUBROUTINE
C      RAV(I)   AVERAGE (I;E: EQUAL AREA) RADIUS BETWEEN ROUT(I) AND
C               ROUT(I+1)
C      AXXA(I)  STORAGE SPACE FOR ALPHA, SIGC, SIGBG, AND CHISQ BEFORE
C               PRINTING
C      XIEPS(I) ARRAYS TO BE INTEGRATED; FED INTO SUBROUTINES
C      SC(I)    SERIES OF CENTRAL DENSITIES FOUND ITERATIVELY BY THE
C               NEWTON-RAPHSON METHOD
C      SBG(I)   BACKGROUND DENSITY ANALOGUE TO SC(I)
C      XO      UPPER LIMIT TO ISOTHERMAL GAS SPHERE INTEGRATION
C      LOGA1   MAXIMUM ALPHA FOR A GIVEN XO
C      LOGA1   LOG(MAXIMUM ALPHA FOR A GIVEN ALPHA)
C      LOGAL   INCREMENTAL BASE FOR LOG(ALPHA)
C      DIVN    ISOTHERMAL GAS SPHERE VALUE; TOTAL INTEGRAL FROM 0 TO XO
C      SIGC    NEWTON-RAPHSON VALUE FOR CENTRAL DENSITY FOR A SPECIFIC
C               XO-ALPHA COMBINATION
C      SIGBG   BACKGROUND DENSITY ANALOGUE TO SIGC
C      CHISQ   CHI-SQUARE VALUE FROM COMPARING CURRENT MODEL TO DATA
C      IAM     ERROR MESSAGE MARKER
C      G, F, FC, FBG, GBG
C      C2      SUMS USED BY NEWTON-RAPHSON METHOD TO GET SIGC AND SIGBG
C      A2, S2, SB2
C      IND     ALPHA, SIGC, AND SIGBG ASSOCIATED WITH C2
C               MARKER; IND=5 ALPHA BEING INCREMENTED; IND=70 LOWEST
C               CHISQ ALPHAS BEING AVERAGED
C      IDD     COUNTER; NO. OF TIMES ALPHA AVERAGING HAS OCCURRED
C
C      SUBROUTINES
C      SIGI    CALCULATES AN INTEGRAL FROM X TO XO FOR AN ISOTHERMAL
C               DENSITY AT RADIAL DISTANCE X
C      DIVIN   CALCULATES AN INTEGRAL FROM 0 TO XO FOR ISOTHERMAL DENSITIES
C               USING THAT SPECIFIC XO
C      IOSF    CALCULATES INTEGRALS OVER RANGES WITH EQUALLY SPACED
C               FUNCTION VALUES

```

```

C
C
0001 REAL NOBS(40),ROUT(41),RAV(40)
0002 DOUBLE PRECISION BI(40),SIGISO(40),NCALC(40),SIGOB(40)
0003 REAL EPSI(281),XI(281),LOGAL,LOGA1,AXXA(12)
0004 DOUBLE PRECISION INTDI(281),XIEPS(281),CHISO,DIWH,SIGC,SIGBG,
      SSC(20),SBG(20),XX1,XX2,G,F,FC,FBG,GBG,DNON,Z1,Z2,E1,E2
0005 INTEGER XO,DATID(40)
C
C DATA READ IN; SC1, SBG1, AND J PRINTED
C
0006 READ(1,888)(DATID(I),I=1,40)
0007 888 FORMAT(40A2)
0008 WRITE(6,889)(DATID(I),I=1,40)
0009 889 FORMAT(5X,40A2)
0010 READ(1,225)(EPSI(I),I=1,281)
0011 225 FORMAT(10(E8,5))
0012 READ(1,222)J
0013 222 FORMAT(/,I2)
0014 READ(1,223)(NOBS(I),I=1,J)
0015 223 FORMAT(20(F4.0))
0016 IJK=J+1
0017 READ(1,224)(ROUT(I),I=2,IJK)
0018 224 FORMAT(20(F4.2))
0019 READ(1,230)SC1,SBG1
0020 SC2=2,*SC1
0021 SBG2=2,*SBG1
0022 WRITE(6,880)SC1,SBG1
0023 880 FORMAT(/,5X,'INITIAL GENT DENS=',1PE11,2,/,5X,'INITIAL BG DENS',
      S'=',1PE11,2)
0024 230 FORMAT(E5,2,2X,E5,2)
0025 IF(J.LE.40)GO TO 15
0027 WRITE(6,803)J
0028 803 FORMAT(/,10X,'CHANGE LINE 1 AND 2 ARRAY SIZES FROM 40 TO',I4,/)
0029 GO TO 999
0030 15 IJK=0
0031 WRITE(6,883)J
0032 883 FORMAT(/,5X,'THERE-ARE',I3,' RINGS',/)
C
C VALUES OF XI CALCULATED IN THREE RANGES: BY 0.1 FROM 0 TO 10,
C BY 1 FROM 10 TO 100, AND BY 10 FROM 100 TO 1000
C
0033 DO 50 I=1,100
0034 X=I-1
0035 X=X/10.
0036 50 XI(I)=X
0037 JX=10
0038 DO 51 I=101,190
0039 XI(I)=JX
0040 51 JX=JX+1
0041 JX=100
0042 DO 52 I=191,281
0043 XI(I)=JX
0044 52 JX=JX+10

```



0087 WRITE(6,35)X,M,XI(M)  
 0088 35 FORMAT(//,12X,'X=',F7.2,' AND XI(',F7.2,')=',F7.2//,12X,'SEE SIGIGO',  
 & ' LOOP')

0089 GO TO 999  
 0090 34 DO 36 K=M,R81  
 0091 XYZ=XI(K)\*XI(K)-XS0  
 0092 36 XIEPS(K)=EPSI(K)\*SORT(XYZ)  
 0093 M=M-1

0094 DO 37 K=1,M  
 0095 XIEPS(K)=0.0  
 0096 CABL-SIGI(XIEPS, X0, X1, INTDI,IUK)  
 0097 IF(IJK.EQ.0)GO TO 8  
 0099 WRITE(6,42)  
 0100 42 FORMAT(//,'\*\*\*\*\* TROUBLES AT SIGI \*\*\*\*\*')

0101 GO TO 100  
 0102 8 SIGISO(I)=INTDI(1)/DIVN  
 0103 GO TO 9

0104 12 IF(I.EQ.1)GO TO 29  
 0106 DO 13 I=1,J  
 0107 13 SIGISO(I)=0.0

C  
 C C END OF SIGISO LOOP/ LOOP TO CALCULATE SIGC AND SIGBG BY NEWTON-  
 C RAPHSON METHOD-STARTED--- ITERATION IS DONE 20-TIMES  
 C C II IS THE NUMBER OF TIMES THE LOOP RUNS, MAX IIM4  
 C

0108 9 IIM=1  
 0109 IXI=0  
 0110 211 DO 202 IP=II,19  
 0111 K=0.0  
 0112 G=0.0  
 0113 FC=0.0  
 0114 FBG=0.0  
 0115 GBG=0.0  
 0116 DO 203 L=1,J  
 0117 21=86(IP)\*SIGISO(L)+86G(IP)  
 0118 IF(ZI.NE.0.0)GO TO 804  
 0120 IAM=1  
 0121 GO TO 444  
 0122 804 22=SIGOB(L)-Z1  
 0123 E1=22/Z1  
 0124 E1=2-S1+E1\*E1  
 0125 F2=(1./Z1)+(2.\*Z2/Z1)/Z1+((22/Z1)\*Z2/Z1)/Z1  
 0126 F=F-BI(L)\*SIGISO(L)\*E1  
 0127 G=G-BI(L)\*F1  
 0128 FC=FC+2.\*BI(L)\*SIGISO(L)\*SIGISO(L)\*E2  
 0129 FBG=FBG+2.\*BI(L)\*SIGISO(L)\*E2  
 0130 303 GRG=GRG+\*BI(L)\*E2  
 0131 ONOM=FC+GBG-FBG\*FBC  
 0132 IF(ABS(ONOM).GT.1.0E-12)GO TO 204  
 0134 SC(IP+1)=6C(IP)  
 0135 SRG(IP+1)=SBC(IP)  
 0136 IXI=IXI+1  
 0137 IF(IXI.NE.5)AND.(IP.LF.19)GO TO 202  
 0139 IAM=2

```

0140 GO TO 444
0141 IX=0
0142 SC(IP+1)=SG(IP)+(C*FBC-F*GBC)/DNOM
0143 SBG(IP+1)=SBG(IP)+(F*FBG-FC*G)/DNOM
0144 202 GDMRINUM

```

```

C
C END OF SIGC-SIGBG LOOP; LOOP TO CHECK FOR CONVERGENCE OVER THE
C LAST SIX VALUES OF SC AND SBG---NO CONVERGENCE MESSAGE
C AND GOES TO END OF XO LOOP
C

```

```

0145 DO 207 I=1,6,19
0146 XI=ABS(SC(L)-SC(L-1))+ABS(SG(L))*0.005
0147 XI2=ABS(SC(L+1)-SC(L))
0148 IF(XI2.LE.XI)GO TO 807
0150 IAME3
0151 GO TO 444
0152 807 XI=ABS(SBGL+1)-SBGL+1)+ABS(SBGL+1)+0.005
0153 XI2=ABS(SBGL+1)-SBGL+1)
0154 IF(XI2.LE.XI)GO TO 207
0156 IAME4
0157 GO TO 444
0158 207 CONPRINUM

```

```

C
C END OF CONVERGENCE LOOP; CHECK TO SEE IF LAST TWO VALUES OF BC
C AND SBG ARE WITHIN 0.01% OF EACH OTHER. IF NOT, THE LAST SC AND
C SBG VALUES ARE TAKEN TO BE THE INITIAL ESTIMATES AND NEWTON-
C RAPHSON CONVERGENCE IS AGAIN USED, TO A MAXIMUM OF FOUR TIMES.
C INSUFFICIENT AGREEMENT PRINTS A MESSAGE AND GOES TO END OF XO LOOP
C

```

```

0159 XI=ABS(SC(20)-SC(19))/ABS(SC(20))
0160 XI2=ABS(SBG(20)-SBG(19))/ABS(SBG(20))
0161 IF((XI,LE,0.0001)AND,(XI2,LE,0.0001))GO TO 209
0163 IF((I,LE,4)GO TO 810
0165 IAME5
0166 GO TO 444
0167 810 II=II+1
0168 SC(II)=SC(20)
0169 SBG(II)=SBG(20)
0170 GO TO 211

```

```

C
C IF CONVERGENCE AND AGREEMENT TESTS ARE PASSED SC(20) AND SBG(20)
C ARE ACCEPTED AS SIGC AND SIGBG. IF THESE ARE LESS THAN TWICE
C INITIAL ESTIMATES THESE ARE THE INITIAL ESTIMATES FOR THE
C NEXT ALPHA,
C

```

```

0171 209 SIGC=SC(20)
0172 SIGBG=SBG(20)
0173 IF(SIGC.GT,SC2)GO TO 700
0175 SC(1)=SC(20)
0176 GO TO 701
0177 700 SC(1)=SC1
0178 701 IF(SIGBG.GT,SBG2)GO TO 702
0180 SBG(1)=SBG(20)
0181 GO TO 703

```

0182 702 SBG(I)=SBG1  
 C  
 C SC AND SBG 2-20 SET TO 0 AS A SAFETY PRECAUTION

0183 DO 310 IR=2,20  
 0184 SC(IR)=0.0  
 0185 310 SBG(IR)=0.0

C  
 C CHISO CALCULATED

0186 CHISO=0.0  
 0187 DO 200 I=1,J  
 0188 NCALC(I)=3.141593881(I)\*(SIC\*SIGISO(I)+SIGBG)  
 0189 200 CHISO=CHISO+(NOBS(I)-NCALC(I))\*2)/NCALC(I)

C IF ALPHA IS BEING AVERAGED OPERATIONS ARE PASSED ON  
 C IF CHISO<0 IT IS NOT COMPARED TO C2 BECAUSE SIGBG<<0  
 C IF THE PREVIOUS CHISO IS C2 (KK=1) THEN CHISO AND ALPHA ARE SAVED

0190 IF (IND=0) GO TO 316  
 0192 IF (CHISO.LT.0.0) GO TO 317  
 0194 IF (CHISO.NE.C2) GO TO 315  
 0196 KK=KK+1  
 0197 IF (KK.GT.1) GO TO 317  
 0199 C3=CHISO  
 0200 A3=ALPHA  
 0201 GO TO 317

C  
 C IF CHISO IS THE SMALLEST SO FAR IT AND ALPHA ARE SAVED, AND THE  
 C PREVIOUS C2 AND A2 ARE RENAMED

0202 315 C1=C2  
 0203 C2=CHISO  
 0204 A1=A2  
 0205 A2=ALPHA  
 0206 S2=SIGC  
 0207 SB2=SIGBG  
 0208 KK=0

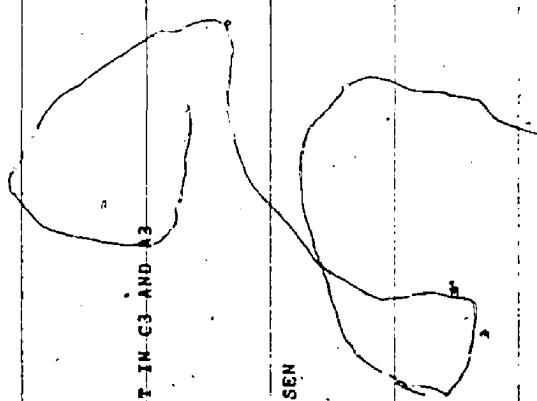
C  
 C RESULTS ARE STORED AS GROUPS OF FOUR. IF AXA IS FULL THE 12  
 C VALUES ARE PRINTED AND AXA-5 INDEX IS RESET

0209 317 AXA(I2)=ALPHA  
 0210 AXA(I2+1)=6IGC  
 0211 AXA(I2+2)=SIGBG  
 0212 AXA(I2+3)=CHISO  
 0213 I2=I2+4  
 0214 IF (I2.LE.9) GO TO 29  
 0216 I2=I2-1  
 0217 WRITE(6,28)(AXA(IX),IX=1,I2)  
 0218 28 FORMAT(12(1PE11.3))  
 0219 I2=1

C  
 C ALPHA IS INCREMENTED, IF IT IS SUFFICIENTLY SMALL GO

```

C      BACK TO START OF SIGISO LOOP
C
0220 LOCAL=LOGAL+.08
0221 ALPHA=10.**LOGAL
0222 IF(CHOGH<BT.DOGH)GO TO 10
0224 GO TO 445
0225 444 IF(IND.LT.20)GO TO 445
C
C      VARIOUS ERROR MESSAGES PRINTED (CONVERGENCE, ETC.)
C
0227 IF(IAM.EQ.1)WRITE(6,91)SG(IP),SIGISO(L),SBSG(IP),IP,L
0229 91 FORMAT(10X,'SC(IP)=',1PE11.3,4X,'SIGISO(L)=' ,1PE11.3,' SB',
    *'G(IP)=' ,1PE11.3,' IP=' ,43,' L=' ,13,/,10X,'PROBLEMS',
    *' IN THE 203 LOOP')
0230 IF(IAM.EQ.2)WRITE(6,806)DNOM,SC(IP),SBSG(IP)
0232 806 FORMAT(10X,'DNOM=' ,1PE11.3, ' AND NON-ITERATION OCCURRED TOO O',
    *' IF I=EN 65',1PE11.3, ' SBSG=' ,1PE11.3)
0233 IF(IAM.EQ.3)WRITE(6,808)L,SC(L-1),SC(L),SC(L+1)
0235 808 FORMAT(10X,'L=' ,13, ' SC(L-1,L,L+1)=' ,3(1PE12.3),5X,'NOT ',
    *' CONVERGING')
0236 IF(IAM.EQ.4)WRITE(6,809)L,SBSG(L-1),SBSG(L),SBSG(L+1)
0238 809 FORMAT(10X,'L=' ,13, ' SBSG(L-1,L,L+1)=' ,3(1PE12.3),5X,
    *' NOT CONVERGING')
0239 IF(IAM.EQ.5)WRITE(6,811)
0241 811 FORMAT(10X,'NO CONVERGENCE WITHIN 0.0001 AFTER 80 ITERATIONS')
0242 WRITE(6,324)X1-X2,X3-X4,IDD
0243 324 FORMAT(32X,'BOMB OUT! ',4(1PE11.3),10X,'IDDS',I4,
    *',10X,' INITIAL SIGC AND/DR SIGBG PROBABLY BAD')
0244 GO TO 100
C
C      IF A NEW XO IS TO BE USED AND AXXA VALUES REMAIN UNPRINTED
C      THESE VALUES AND THE MINIMUM CHISO PARAMETERS ARE PRINTED
C
0245 IF(IZ.LT.2)GO TO 318
0247 IZ=IZ+1
0248 WRITE(6,28)(AXXA(IX),IX=1,IZ)
0249 IZ=1
0250 318 WRITE(6,322)A2,62,882,C2
0251 322 FORMAT(24X,'MIN FROM PROGRAM: ',4(1PE11.3))
C
C      THE SECOND-SMALLEST-CHISO-AND-ITS-ALPHA-ARE-PUT-IN-C3-AND-A3
C
0252 IF(C1.GT.C3)GO TO 320
0254 A3=A1
0255 C3=C1
C
C      IND IS RESET, ALPHA-AVERAGING STARTS
C      ALPHA AVERAGING IS DONE BEFORE A NEW XO IS CHOSEN
C
0256 320 IND=70
0257 SC(1)=S2
0258 SRG(1)=SB2
0259 ALPHA=0.5*(A3+A2)
0260 IDD=1
    
```



```
0261      GO TO 10
C
C      AFTER CHISO IS FOUND AND IF IND=70 OPERATIONS ARE SENT HERE
C      IF NEW CHISO<C2 APPROPRIATE VALUES ARE RESET
C
```

```
0262      316 IF(CHISO.GE.C2)GO TO 340
0264      C3=C2
0265      A3=A2
0266      C2=CHISO
0267      A2=ALPHA
0268      SB2=SIGC
0269      SB2=SIGBG
0270      GO TO 341
```

```
C
C      IF NEW CHISO>C2 BUT <C3 APPROPRIATE VALUES ARE RESET
C
```

```
0271      340 IF(C3.LT.CHISO)GO TO 341
0273      C3=CHISO
0274      A3=ALPHA
```

```
C
C      IF AVERAGING HAS NOT OCCURRED 20 TIMES IT CONTINUES AND
C      PROGRAM RETURNS TO START OF SIGISO LOOP
C
```

```
0275      341 IF(IDD.GT.20)GO TO 342
0277      ALPHA=0.5*(A3+A2)
0278      IDD=IDD+1
0279      GO TO 10
```

```
C
C      IF 20 AVERAGES FOUND, MINIMUM CHISO PARAMETERS (C2, A2, ETC.) PRINTED
C
```

```
0280      342 WRITE(6,343)A2,SB2,SB2,C2
0281      343 FORMAT(25X,'MINIMUM METHOD--',4(1PE11.3))
0282      100 CONTINUE
```

```
C
C      END OF XO LOOP
C
```

```
0283      999 WRITE(6,555)
0284      555 FORMAT(///)
0285      CALL EXIT
0286      END
```

```

0001      SUBROUTINE SIGI(EPSI,IXO,X,XI,INTDI,IJK)
C
C      CALCULATES INTEGRAL FROM X TO IXO
C      EPSI  THE RANGE OF VALUES TO BE INTEGRATED OVER
C      IXO   UPPER LIMIT OF INTEGRATION
C      X     LOWER LIMIT OF INTEGRATION
C      XI    SET OF HORIZONTAL AXIS VALUES CORRESPONDING TO EPSI
C      INTDI STORAGE SPACE OF INTEGRATION RESULTS
C      IJK   ERROR MARKER
C
0002      DOUBLE PRECISION EPSI(1),INTDI(1),SUM
0003      DIMENSION XI(1)
0004      IJK=0
0005      IKK=0
C
C      X IS CHECKED TO ENSURE IT IS BETWEEN 0 AND IXO
C
0006      IF(X.LT.0.0)GO TO 100
0008      IF(X.LT.IXO)GO TO 101
0010      WRITE(6,200)X,IXO
0011      200 FORMAT(//,5X,'TROUBLES... X=',F7.2,' AND IXO=',I6)
0012      GO TO 198
C
C      STORAGE SPACE FOR INTEGRATION RESULTS SET TO 0
C      POSITION OF XI VALUE EQUAL TO OR GREATER THAN X FOUND
C      IF .XXXI(281) ERROR MESSAGE PRINTED
C
0013      101 SUM=0.0
0014      DO 102 I=1,281
0015      IF(XI(I)-X)102,103,104
0016      102 CONTINUE
0017      100 WRITE(6,201)X
0018      201 FORMAT(//,5X,'X IS ODD, IT IS',F7.2)
0019      GO TO 198
C
C      IF NO XI VALUE=X MARKER SET; POSITION OF XI VALUE EQUAL TO OR
C      GREATER THAN IXO FOUND; IF IXO>XI(281) ERROR MESSAGE OUTPUT
C
0020      104 IJK=25
0021      103 DO 105 K=1,281
0022      IF(XI(K)-IXO)105,106,107
0023      105 CONTINUE
0024      WRITE(6,202)IXO
0025      202 FORMAT(//,5X,'IXO IS ODD, IT IS',I6)
0026      GO TO 198
C
C      IF NO VALUE OF XI=IXO, MARKER SET
C
0027      107 IKK=30
0028      GO TO 106
C
C      IF IKK=30 TRAPEZOIDAL AREA BETWEEN IXO, EPSI(IXO), THE
C      CLOSEST XI, AND ITS EPSI IS FOUND AND ADDED TO SUM. EPSI(IXO)
C      IS FOUND BY LINEAR INTERPOLATION

```

```

C
0029 147 XAV=(XI(K)+XI(K-1))*0.5
0030 IF(XAV.LT.IXO)GO TO 108
0032 XFRAC=(IXO-XI(K-1))/(XI(K)-XI(K-1))
0033 XX=XFRAC*(EPSI(K)-EPSI(K-1))
0034 XX=EPSI(K-1)+XX*0.5
0035 SUM=SUM+(XX*(IXO-XI(K-1)))
0036 K=K-1
0037 GO TO 106
0038 108 XFRAC=(XI(K)-IXO)/(XI(K)-XI(K-1))
0039 XX=XFRAC*(EPSI(K)-EPSI(K-1))
0040 XX=EPSI(K)-XX*0.5
0041 SUM=SUM-(XX*(XI(K)-IXO))
0042 GO TO 141
C
C THE NUMBER OF XI VALUES BETWEEN X AND IXO IS FOUND. IF IT IS
C ZERO, SUM IS FOUND USING A TRIANGULAR AREA
C
0043 106 NDIM=K-1+1
0044 IF(NDIM-1)109,140,111
0045 109 XX=(IXO-X)/(XI(I)-X)
0046 SUM=0.5*XX*EPSI(I)*(IXO-X)
0047 GO TO 110
C
C IF NDIM=0, SUM IS FOUND USING A TRIANGULAR AREA
C
0048 140 IF(SUM.LT.0.0)SUM=0.5*(((IXO-X)/(XI(I)-X))*EPSI(I))*(IXO-X)
0050 IF(SUM.GT.0.0)SUM=SUM+0.5*(XI(I)-X)*EPSI(I)
0052 GO TO 110
C
C IF NO XI=X, AREA FROM X TO NEAREST LARGER XI IS FOUND TRIANGULARLY
C IF NO XI=IXO, AREA FROM IXO TO NEAREST XI IS FOUND (SEE 29-42 ABOVE)
C
0053 111 IF(IJK.EQ.25)SUM=0.5*(XI(I)-X)*EPSI(I)
0055 IF(IKK.EQ.30)GO TO 147
C
C CHECK TO SEE WHICH RANGES OF XI HOLD X AND XI, IF NOTHING
C MATCHES, ERROR MESSAGE PRINTED
C
0057 141 IF((I.LE.101).AND.(K.LE.101))GO TO 112
0059 IF(I.LE.100)GO TO 113
0061 IF((I.LE.191).AND.(K.LE.191))GO TO 114
0063 IF(I.LE.190)GO TO 115
0065 IF(I.LE.291)GO TO 116
0067 WRITE(6,205)
0068 205 FORMAT(//,5X,'TROUBLE IN THE 'IF' SECTION')
0069 GO TO 197
C
C IF X AND IXO ARE IN THE FIRST RANGE SUM INCREMENT AND TOTAL
C ARE FOUND. IF NDIM=2 INTEGRATION SUBROUTINE WON'T WORK SO
C SUM INCREMENT CALCULATED AS A TRAPEZOIDAL AREA.
C IF INTDI=2 OR THE DISTANCE FROM X OR IXO TO THE END OF A RANGE
C IS LESS THAN 3 STEPS ANYWHERE IN THIS SUBROUTINE OR THE NEXT
C ONE, THE SUM INCREMENT IS FOUND TRAPEZOIDALLY (FOR IXO) OR

```

C TRIANGULARLY (FOR X), FOR NDIM>2 OR MORE THAN THREE STEPS  
 C ARE AVAILABLE, THE SUM INCREMENT IS FOUND BY THE  
 C SUBROUTINE IQSF,  
 C

0070 112 IF(NDIM.GT.2)GO TO 117

0072 SUM=SUM+0.1\*(EPSI(I)+EPSI(K))\*0.5

0073 GO TO 110

0074 117 IJ=1

0075 DO 118 J=I,281

0076 EPSI(IJ)=EPSI(J)

0077 118 IJ=IJ+1

0078 CALL IQSF(0.1,EPSI,INTDI,NDIM)

0079 SUM=SUM+INTDI(NDIM)

0080 GO TO 110

C IF X IS IN THE FIRST XI RANGE AND IXO ISN'T, THE AREA (INTEGRAL)  
 C FROM X TO THE RANGE'S END IS FOUND  
 C

0081 113 IF(I.LT.100)GO TO 119

0083 SUM=SUM+0.1\*(EPSI(100)+EPSI(101))\*0.5

0084 NDIM=101

0085 GO TO 120

0086 119 NDIM=102-I

0087 IJ=1

0088 DO 121 J=I,281

0089 EPSI(IJ)=EPSI(J)

0090 121 IJ=IJ+1

0091 CALL IQSF(0.1,EPSI,INTDI,NDIM)

0092 SUM=SUM+INTDI(NDIM)

0093 120 IF(K.GE.191)GO TO 122

C IF X IS IN THE FIRST RANGE AND IXO IN THE SECOND, THE AREA FROM  
 C THE SECOND RANGE'S START TO IXO IS FOUND AND THE TOTAL INTEGRAL  
 C FOUND  
 C

0095 IF(K.GT.102)GO TO 123

0097 SUM=SUM+0.5\*(EPSI(NDIM)+EPSI(NDIM+1))

0098 GO TO 110

0099 123 IJ=1

0100 DO 124 J=NDIM,281

0101 EPSI(IJ)=EPSI(J)

0102 124 IJ=IJ+1

0103 NDIM=K-100

0104 CALL IQSF(1.0,EPSI,INTDI,NDIM)

0105 SUM=SUM+INTDI(NDIM)

0106 GO TO 110

C IF X IS IN THE FIRST RANGE AND IXO IN THE THIRD THE SUM INCREMENT  
 C OF THE INTEGRAL OVER THE SECOND RANGE IS FOUND  
 C

0107 122 IJ=1

0108 DO 125 J=NDIM,281

0109 EPSI(IJ)=EPSI(J)

0110 125 IJ=IJ+1

0111 MDIM=91  
 0112 CALL IOSF(1.0,EPSI,INTDI,NDIM)  
 0113 SUM=SUM+INTDI(NDIM)  
 0114 IF(K-192)110,126,127

C  
 C IF X IS IN THE FIRST RANGE AND IXO IN THE THIRD, THE LAST SUM  
 C INCREMENT, FROM THE THIRD'S START TO THE XI NEAREST IXO, IS  
 C FOUND AND THE FINAL INTEGRAL TOTALLED.

0115 126 SUM=SUM+(EPSI(NDIM)+EPSI(NDIM+1))\*5.0  
 0116 GO TO 110  
 0117 127 IJ=I  
 0118 DO 128 J=91,281  
 0119 EPSI(IJ)=EPSI(J)  
 0120 128 IJ=IJ+1  
 0121 NDIM=K-190  
 0122 CALL IOSF(10.0,EPSI,INTDI,NDIM)  
 0123 SUM=SUM+INTDI(NDIM)  
 0124 GO TO 110

C  
 C IF X AND IXO ARE IN THE SECOND RANGE THE TOTAL INTEGRAL IS FOUND

0125 114 IF(NDIM.GT.2)GO TO 129  
 0127 SUM=SUM+0.5\*(EPSI(1)+EPSI(K))  
 0128 GO TO 110  
 0129 129 IJ=I  
 0130 DO 130 J=I,281  
 0131 EPSI(IJ)=EPSI(J)  
 0132 130 IJ=IJ+1  
 0133 CALL IOSF(1.0,EPSI,INTDI,NDIM)  
 0134 SUM=SUM+INTDI(NDIM)  
 0135 GO TO 110

C  
 C IF X IS IN THE SECOND RANGE AND IXO IN THE THIRD THE INTEGRAL  
 C INCREMENTS FROM X TO THE END OF THE SECOND RANGE AND FROM THE  
 C END OF THE SECOND TO THE XI VALUE NEAREST IXO ARE FOUND  
 C AND THE TOTAL INTEGRAL IS ADDED UP

0136 115 IF(1.7.190)GO TO 131  
 0138 SUM=SUM+0.5\*(EPSI(190)+EPSI(191))  
 0139 MDIM=191  
 0140 GO TO 132  
 0141 131 NDIM=192-I  
 0142 IJ=I  
 0143 DO 133 J=I,281  
 0144 EPSI(IJ)=EPSI(J)  
 0145 133 IJ=IJ+1  
 0146 CALL IOSF(1.0,EPSI,INTDI,NDIM)  
 0147 SUM=SUM+INTDI(NDIM)  
 0148 132 IF(K.GT.192)GO TO 134  
 0150 SUM=SUM+5.0\*(EPSI(NDIM)+EPSI(NDIM+1))  
 0151 GO TO 110  
 0152 134 IJ=I  
 0153 DO 135 J=MDIM,281

```

0154 EPSI(IJ)=EPSI(J)
0155 135 IJ=IJ+1
0156 NDIM=K-190
0157 CALL IOSF(10.0,EPSI,INTDI,NDIM)
0158 SUM=SUM+INTDI(NDIM)
0159 GO TO 110

```

```

C
C IF X AND IXO ARE IN THE THIRD RANGE THE REMAINING INTEGRAL
C INCREMENT (FROM X TO THE XI VALUE NEAREST IXO) IS
C OBTAINED AND THE INTEGRAL TOTAL CALCULATED
C

```

```

0160 116 IF(NDIM.GT.2)GO TO 136
0162 SUM=SUM+5.0*(EPSI(I)+EPSI(K))
0163 GO TO 110
0164 136 IJ=1
0165 DO 137 J=I,281
0166 EPSI(IJ)=EPSI(J)
0167 137 IJ=IJ+1
0168 CALL IOSF(10.0,EPSI,INTDI,NDIM)
0169 SUM=SUM+INTDI(NDIM)

```

```

C
C INTEGRAL TOTAL IS REASSIGNED, ERROR MARKER IS RESET, AND IF
C INTEGRAL<0 ERROR MARKER IS RESET AND ERROR MESSAGE PRINTED
C RETURN TO MAIN PROGRAM WITH INTEGRAL
C

```

```

0170 110 INTDI(1)=SUM
0171 IJK=0
0172 IF(SUM.GE.0.0)GO TO 199
0174 197 WRITE(6,204)I,K,X,IXO,XI(I),XI(K),EPSI(I),EPSI(K),SUM
&,NDIM,EPSI(K-1)
0175 204 FORMAT(///,' CONFUSION IN SIGI AT 110: I=',I6,/,29X,
&'K=',I6,/,29X,'X=',IPE15.6,/,27X,'IXO=',I7,/,25X,'XI(I)='/,
&'IPE15.6,/,25X,'XI(K)='/,IPE15.6,/,23X,'EPSI(I)='/,IPE15.6,/,
&'23X,'EPSI(K)='/,IPE15.6,/,27X,'SUM='/,IPE15.6,/,
&'26X,'NDIM=',I6,/,21X,'EPSI(K-1)='/,IPE15.6,/)
0176 198 IJK=111
0177 199 RETURN
0178 END

```

```

0001      SUBROUTINE DIVIN(XIEPS,IXO,INTDI,XI,IJK)
C
C      CALCULATES INTEGRAL FROM 0 TO IXO, INTEGRATIONS IN THIS SUBROUTINE
C      ARE SUBJECT TO THE SAME LIMITATIONS AS IN THE PREVIOUS SUBROUTINE
C      AND ARE CIRCUMVENTED IN THE SAME WAY
C
C      XIEPS  THE RANGE OF VALUES TO BE INTEGRATED OVER
C      IXO    UPPER LIMIT OF INTEGRATION
C      INTDI  STORAGE SPACE OF INTEGRATION RESULTS
C      XI     SET OF HORIZONTAL AXIS VALUES CORRESPONDING TO XIEPS
C      IJK    ERROR MARKER
C
0002      REAL XI(1)
0003      DOUBLE PRECISION INTDI(1),SUM,XIEPS(1)
C
C      INTEGRAL STORAGE SPACE SET TO 0 AND POSITION OF XI VALUE
C      NEAREST BUT NOT SMALLER THAN IXO FOUND
C
0004      SUM=0.0
0005      DO 60 I=1,281
0006      IF(XI(I)-IXO)60,61,62
0007      60  CONTINUE
C
C      IF IXO<XI(281) ERROR MESSAGE PRINTED
C
0008      WRITE(6,65)IXO
0009      65  FORMAT(///,' IN DIVIN 60 LOOP IXO=',I7)
0010      IJK=111
0011      GO TO 999
C
C      IF IXO DOES NOT EQUAL A VALUE OF XI THE AREA BETWEEN IXO AND
C      THE NEAREST XI VALUE IS FOUND TRAPEZOIDALLY AND ADDED TO SUM
C
0012      62  XAV=(XI(I)+XI(I-1))/2.0
0013      IF((XAV.GT.IXO).AND.(I.GT.2))GO TO 64
0015      XFRAC=(XI(I)-IXO)/(XI(I)-XI(I-1))
0016      XX=(XIEPS(I)-XIEPS(I-1))*XFRAC
0017      XX=(XIEPS(I)+XIEPS(I)-XX)/2.0
0018      SUM=SUM-(XX*(XI(I)-IXO))
0019      GO TO 61
0020      64  XFRAC=(IXO-XI(I-1))/(XI(I)-XI(I-1))
0021      XX=(XIEPS(I)-XIEPS(I-1))*XFRAC
0022      XX=(XIEPS(I-1)+XIEPS(I-1)+XX)/2.0
0023      SUM=SUM+((IXO-XI(I-1))*XX)
0024      I=I-1
C
C      IF IXO IS IN THE FIRST XI RANGE THE TOTAL INTEGRAL IS FOUND,
C      IF IT IS NOT THE INTEGRAL PART FROM 0 TO THE END OF THE FIRST
C      RANGE IS FOUND AND ADDED TO SUM
C
0025      61  IF(I.GE.101)GO TO 3
0027      NDIM=I
0028      IF(NDIM.GT.2)GO TO 5
0030      SUM=SUM+(0.1*(XIEPS(1)+XIEPS(2))/2.0)

```

```
0031      GO TO 998
0032      3  NDIM=101
0033      5  CALL IQSF(0.1,XIEPS,INTDI,NDIM)
0034      SUM=SUM+INTDI(NDIM)
0035      IF(I.LE.101)GO TO 998
```

```
      C
      C      IF IXO IS IN THE SECOND XI RANGE THE INTEGRAL PART
      C      FROM THE START OF THE SECOND RANGE TO IXO IS FOUND AND ADDED
      C      TO SUM FOR THE TOTAL INTEGRAL. IF IT IS IN THE THIRD RANGE
      C      THE INTEGRAL PART COVERING THE SECOND RANGE IS FOUND AND
      C      ADDED TO SUM
```

```
0037      IF(I.GE.191)GO TO 4
0039      NDIM=I-100
0040      IF(NDIM.GT.2)GO TO 8
0042      SUM=SUM+((XIEPS(101)+XIEPS(102))/2.0)
0043      GO TO 998
0044      4  NDIM=91
0045      8  IJ=101
0046      DO 9 J=1,181
0047      XIEPS(J)=XIEPS(IJ)
0048      9  IJ=IJ+1
0049      CALL IQSF(1.0,XIEPS,INTDI,NDIM)
0050      SUM=SUM+INTDI(NDIM)
0051      IF(I.LE.191)GO TO 998
```

```
      C
      C      FOR IXO IN THE THIRD XI RANGE THE REMAINDER OF THE INTEGRAL
      C      (FROM THE BEGINNING OF THE THIRD RANGE TO IXO) IS FOUND
      C      AND ADDED TO SUM FOR THE TOTAL INTEGRAL
```

```
0053      NDIM=I-190
0054      IF(NDIM.GT.2)GO TO 12
0056      SUM=SUM+(10.0*(XIEPS(91)+XIEPS(92))/2.0)
0057      GO TO 998
0058      12 IJ=91
0059      DO 13 J=1,91
0060      XIEPS(J)=XIEPS(IJ)
0061      13 IJ=IJ+1
0062      CALL IQSF(10.0,XIEPS,INTDI,NDIM)
0063      SUM=SUM+INTDI(NDIM)
0064      998 INTDI(1)=SUM
0065      999 RETURN
0066      END
```

```

0001      SUBROUTINE IQSF(H,Y,Z,NDIM);
C
C      THIS SUBROUTINE WAS LIFTED BODILY FROM IBM'S SSP WHERE IT WAS
C      CALLED "QSF", HERE THE INTEGRAL IS FOUND BY SIMPSON'S RULE
C      H      THE INCREMENT OF ARGUMENT VALUES (I.E. A CONSTANT)
C      Y      THE INPUT FUNCTION VALUES, SEPARATED BY H
C      Z      THE RESULTING INTEGRAL VALUES
C      NDIM   THE NUMBER OF VALUES TO BE INTEGRATED OVER
C

```

```

0002      DOUBLE PRECISION Y(1),Z(1),SUM1,SUM2,AUX,AUX1,AUX2
0003      HT=.33333333*H
0004      L1=1
0005      L2=2
0006      L3=3
0007      L4=4
0008      L5=5
0009      L6=6
0010      IF (NDIM=5)7,8,1

```

```

C
C      NDIM IS GREATER THAN 5. PREPARATIONS OF INTEGRATION LOOP
C

```

```

0011      1  SUM1=Y(L2)+Y(L2)
0012      SUM1=SUM1+SUM1
0013      SUM1=HT*(Y(L1)+SUM1+Y(L3))
0014      AUX1=Y(L4)+Y(L4)
0015      AUX1=AUX1+AUX1
0016      AUX1=SUM1+HT*(Y(L3)+AUX1+Y(L5))
0017      AUX2=HT*(Y(L1)+3.875*(Y(L2)+Y(L5))+2.625*(Y(L3)+Y(L4))+Y(L6))
0018      SUM2=Y(L5)+Y(L5)
0019      SUM2=SUM2+SUM2
0020      SUM2=AUX2-HT*(Y(L4)+SUM2+Y(L6))
0021      Z(L1)=0.
0022      AUX=Y(L3)+Y(L3)
0023      AUX=AUX+AUX
0024      Z(L2)=SUM2-HT*(Y(L2)+AUX+Y(L4))
0025      Z(L3)=SUM1
0026      Z(L4)=SUM2
0027      IF (NDIM=6)5,5,2

```

```

C
C      INTEGRATION LOOP
C

```

```

0028      2  DO 4 I=7,NDIM,2
0029      SUM1=AUX1
0030      SUM2=AUX2
0031      AUX1=Y(I-1)+Y(I-1)
0032      AUX1=AUX1+AUX1
0033      AUX1=SUM1+HT*(Y(I-2)+AUX1+Y(I))
0034      Z(I-2)=SUM1
0035      IF (I-NDIM)3,6,6
0036      3  AUX2=Y(I)+Y(I)
0037      AUX2=AUX2+AUX2
0038      AUX2=SUM2+HT*(Y(I-1)+AUX2+Y(I+1))
0039      Z(I-1)=SUM2
0040      5  Z(NDIM-1)=AUX1

```

```

0041 Z(NDIM)=AUX2
0042 RETURN
0043 Z(NDIM-1)=SUM2
0044 Z(NDIM)=AUX1
0045 RETURN
C
C      END OF INTEGRATION LOOP
0046 C
0047 C      IF (NDIM-3)12,11,8
0048 C
C      NDIM IS EQUAL TO 4 OR 5
0049 C
0050 C      SUM2=1.125*HT*(Y(L1)+Y(L2)+Y(L2)+Y(L2)+Y(L3)+Y(L3)+Y(L3)+Y(L4))
0051 C      SUM1=SUM1+SUM2
0052 C      SUM1=HT*(Y(L1)+SUM1+Y(L3))
0053 C      Z(L1)=0.
0054 C      AUX1=Y(L3)+Y(L3)
0055 C      AUX1=AUX1+AUX1
0056 C      Z(L1)=SUM2-HT*(Y(L2)+AUX1+Y(L4))
0057 C      IF (NDIM=5)10,9,9
0058 C      AUX1=Y(L4)+Y(L4)
0059 C      AUX1=AUX1+AUX1
0060 C      Z(L5)=SUM1+HT*(Y(L3)+AUX1+Y(L5))
0061 C      Z(L3)=SUM1
0062 C      Z(L4)=SUM2
0063 C      RETURN
C
C      NDIM IS EQUAL TO 3
0064 C
0065 C      SUM1=HT*(1.25*Y(L1)+Y(L2)+Y(L2)+Y(L2)+.25*Y(L3))
0066 C      SUM2=Y(L2)+Y(L2)
0067 C      SUM2=SUM2+SUM2
0068 C      Z(L3)=HT*(Y(L1)+SUM2+Y(L3))
0069 C      Z(L1)=0.
0070 C      Z(L2)=SUM1
0071 C      RETURN
0072 C      END

```

## Appendix B

## Auxiliary listings

A listing is provided of the BASIC program that produces values of  $\xi$ ,  $e^{-\psi}$ ,  $\psi'$ , and  $e^{-\psi}\psi'$  (see equation 4, page 7). The last set of values are those entered as isothermal gas sphere data for the appropriate  $\xi$  values as specified on page 36.

To obtain values used in this thesis for the first range of  $\xi$  (0.0 to 9.9 in increments of 0.1), the step size to enter is 0.001 and the number of steps is 100; for the second range of  $\xi$  (10 to 99 in increments of 1) the step size is 0.01 and the number of steps is 100; and for the third  $\xi$  range (100 to 1000 in increments of 10) the step size is 0.1 and the number of steps is 100.

As can be seen for the portion of an output run included in Appendix J, the values of  $\xi$  are not exact, but the small difference is not considered significant and so is ignored. Also, when the program is run for the second  $\xi$  range, values for  $e^{-\psi}$ ,  $\psi'$ , and  $e^{-\psi}\psi'$  are calculated for  $\xi=1, 2, 3, \dots, 9$ . These  $e^{-\psi}\psi'$  values were not used since values corresponding to the first nine  $\xi$  values were provided by calculations for the first  $\xi$  range. Similarly, the first nine sets of numbers produced in third range calculations were ignored since second range calculations had included them.

The BASIC program does not give a value of  $e^{-\psi}$  for  $\xi=0$ , a necessary value, but since for this  $\xi$  the product  $e^{-\psi}\psi'=0$  this is not a problem.

Also included in this Appendix are the modifications performed on YAHOO to get the programs BGIN and TAFCHEC. BGIN is the variant that reads the counted background density as a constant and only makes best fit determinations for  $x_0$ ,  $\alpha$ , and  $\sigma_C$ . The first page of a typical output of BGIN is also provided in Appendix J.

TAFCHEC was used for the program testing in Chapter III, section (ii). The only difference between TAFCHEC and YAHOO is that the former also calculates the  $\chi^2$  found for each  $x_0$  when comparing the data to the model made using the current  $x_0$  and Taff's values of  $\alpha$ ,  $\sigma_C$ , and  $\sigma_{bg}$ . This provides the bracketed numbers of Tables 3 and 5 (pages 23 and 27 respectively).

Detailed explanations of the modifications done to YAHOO to obtain BGIN and TAFCHEC are given in Appendix C.

```

10 DIM Y(2),Z(2),F(2),A(2),B(2),C(2),D(2)
20 X=0
30 Y(1)=0
40 Y(2)=0
50 PRINT 'ENTER STEP SIZE, NUMBER OF STEPS'
60 INPUT H,N
70 PRINT H,N
71 PRINT
72 PRINT 'X', 'EXP(-PSI)', 'PSI', 'EXP(-PSI)*PSI'
73 PRINT
75 FOR K=1 TO 100
80 GOSUB 110
85 X3=EXP(-Y(1))
86 X4=X3*Y(2)
90 PRINT X,X3,Y(2),X4
95 NEXT K
100 STOP
110 FOR J=1 TO N
120 Z(1)=Y(1)
130 Z(2)=Y(2)
140 GOSUB 360
150 A(1)=F(1)
160 A(2)=F(2)
170 Z(1)=Y(1)+H*A(1)/2
180 Z(2)=Y(2)+H*A(2)/2
190 X=X+H/2
200 GOSUB 360
210 B(1)=F(1)
220 B(2)=F(2)
230 Z(1)=Y(1)+H*B(1)/2
240 Z(2)=Y(2)+H*B(2)/2
250 GOSUB 360
260 C(1)=F(1)
270 C(2)=F(2)
280 Z(1)=Y(1)+H*C(1)
290 Z(2)=Y(2)+H*C(2)
300 X=X+H/2
310 GOSUB 360
312 D(1)=F(1)
315 D(2)=F(2)
320 Y(1)=Y(1)+(A(1)+2*B(1)+2*C(1)+D(1))*H/6
330 Y(2)=Y(2)+(A(2)+2*B(2)+2*C(2)+D(2))*H/6
340 NEXT J
350 RETURN
360 F(1)=Z(2)
370 IF X>0 THEN 400
380 F(2)=1/3
390 RETURN
400 F(2)=EXP(-Z(1))-2*Z(2)/X
410 RETURN
420 END

```

Ready

## Modifications to YAHOO to get BGIN

The line numbers referred to are those of YAHOO as it is found in Appendix A. All changes are in the MAIN program; the subroutines SIGI, DIVIN, and IQSF are left unchanged.

Change line 4 to:

```
DOUBLE PRECISION INTDI(281), XIEPS(281), CHISQ, DIVN,  
SIGC, SC(20), XX1, XX2, SUM1, SUM2, Z1, Z2, EI, UI
```

Change line 19 to:

```
READ(1,230) SC1, SBG
```

Delete line 21.

Change line 22 to:

```
WRITE(6,880) SC1, SBG
```

Change line 23 to:

```
880 FORMAT(/,5X,'INITIAL CENT DENS=',1PE11.2,/,14X,  
'BG DENS=',1PE11.2)
```

Delete line 61.

Change line 69 to:

```
25 FORMAT(4(4X,'ALPHA    CENT DENS  CHI-SQ  '))
```

Replace lines 111 through 115 inclusive by:

```
SUM1=0.0
```

```
SUM2=0.0
```

Change line 117 to:

```
Z1=SC(IP)*SIGISO(L)+SBG
```

Replace lines 123 through 132 inclusive by:

```
EI=Z2/Z1
```

```
UI=(1./Z1)+((2.*Z2/Z1)/Z1)+(((Z2/Z1)*Z2/Z1)/Z1)
```

```
SUM1=SUM1+BI(L)*SIGISO(L)*(2.*EI+EI*EI)
```

```
203 SUM2=SUM2+BI(L)*SIGISO(L)*SIGISO(L)*UI
```

```
IF(ABS(SUM2)-GT.1.0E-12)GO TO 204
```

Delete line 135.

Change line 142 to:

```
SC(IP+1)=SC(IP)+SUM1/(2.*SUM2)
```

Delete line 143.

Change line 148 to:

```
IF(XX2.LE.XX1)GO TO 207
```

Delete lines 152 through 157 inclusive.

Delete line 160.

Change line 161 to:

IF(XX1.LE.0.0001)GO TO 209

Delete line 169.

Delete line 172.

Change line 176 to:

GO TO 703

Delete lines 178 through 182 inclusive.

Change line 184 to:

310 SC(IR)=0.0

Delete line 185.

Change line 188 to:

NCALC(I)=3.141593\*BI(I)\*(SIGC\*SIGISO(I)+SBG)

Delete line 207.

Replace lines 211 through 214 inclusive by:

```
AXXA(IZ+2)=CHISQ
IZ=IZ+3
IF(IZ.LE.11)GO TO 29
```

Replace lines 227 through 232 inclusive by:

```
IF(IAM.EQ.1)WRITE(6,805)SC(IP), SIGISO(L), IP, L
805 FORMAT(10X,'SC(IP)=' ,1PE11.3,4X,'SIGISO(L)=' ,1PE11.3,
      IP=' ,I3,' L=' ,I3,/,10X,'PROBLEMS IN THE
      203 LOOP')
IF(IAM.EQ.2)WRITE(6,806)DNOM, SC(IP)
806 FORMAT(10X,'DNOM=' ,1PE11.3,' AND NON-ITERATION
      OCCURRED TOO OFTEN SC=' ,1PE11.3)
```

Delete lines 236 and 238.

Change lines 250 and 251 to:

```
318 WRITE(6,322)A2, S2, C2
322 FORMAT(13X,'MIN FROM PROGRAM: ',3(1PE11.3))
```

Delete line 258.

Delete line 269.

Insert between lines 277 and 278:

```
X1=ALPHA
```

X2=SIGC

X3=CHISQ

Change lines 280 and 281 to:

342 WRITE(6,343)A2, S2, C2

343 FORMAT(14X,'MINIMUM METHOD: ',3(1PE11.3))

Modifications to YAHOO to get TAFCHC

Again line numbers refer to those of YAHOO as it appears in Appendix A and all subroutines are unchanged.

Insert between lines 24 and 25:

READ(1,235)TAL, TSC, TSBG

235 FORMAT(E5.2,2(2X,E5.2))

WRITE(6,236)TAL, TSC, TSBG

236 FORMAT(/,' TAFF'S VALUES: ALPHA=',1PE11.2,/,18X,

'SIGC=',1PE11.2,/,17X,'SIGBG=',1PE11.2)

Insert between lines 56 and 57:

ITAFF=5

Insert between lines 102 and 103:

IF(ITAFF.GT.100)GO TO 820

Insert between lines 107 and 108:

```
IF (ITAFF.GT.100)GO TO 820
```

Insert between lines 281 and 282:

```
ITAFF=500
```

```
ALPHA=TAL
```

```
GO TO 10
```

```
820 CHISQ=0.0
```

```
DO 821 I=1,J
```

```
NCALC(I)=3.141593*BI(I)*(TSC*SIGISO(I)+TSBG)
```

```
821 CHISQ=CHISQ+((NOBS(I)-NCALC(I))**2)/NCALC(I)
```

```
WRITE(6,882)ALPHA, CHISQ
```

```
882 FORMAT(/,26X,'TAFF'S VALUES : ',1PE11.3,22X,  
1PE11.3)
```

## Appendix C

## Detailed program explanations

A detailed explanation of the program YAHOO is provided. Also given are explanations of the modifications of YAHOO needed to obtain BGIN and TAFCHC.

In all cases in this Appendix, line numbers refer to the line numbers of YAHOO as they occur in Appendix A. The insertions, deletions, changes, and replacements referred to in explanations of the modifications for BGIN and TAFCHC are those listed in Appendix B.

\*YAHOO

## MAIN Program

Lines	Function and/or relation to theory
1-5	Declaration statements
6-9	Read in and rewrite a message at the beginning of the data deck. This checks to make sure that the proper type of data is being used and to make sure the printer is on the 132 line width mode (item 1 on page 36).
10-11	Isothermal gas sphere density data is entered (data is from the BASIC program; item 2 on page 36).

- 12-19 J, NOBS, ROUT, and initial estimates for  $\sigma_c$  (SC1) and  $\sigma_{bg}$  (SBG1) are read in (items 4 to 7 on page 36). The command to skip a line in line 13 allows the program to jump over the line describing the format of items 4 to 6 (item 3 on page 36).
- 20-21 Values two times those of the initial estimates for  $\sigma_c$  and  $\sigma_{bg}$  are put aside for future use (lines 173 and 178).
- 22-23 The initial estimates for  $\sigma_c$  and  $\sigma_{bg}$  are printed out.
- 24 Format for line 20.
- 25-29 If there are more rings than the necessary array sizes permit, a proper notice is printed and the program stops.
- 30 IJK, an error marker needed later on, is set to zero.
- 31-31 The number of rings being used is printed out.
- 33-44 The series XI ( $\xi$  in equation 4, page 7), the unitless radius of the isothermal gas sphere, is calculated for the corresponding densities entered in line 10.
- 45-46 Table titles are printed.
- 47  $ROUT(1) = r_1 = 0$ , see explanation of equation (1), page 6.
- 48-55 A series of values is calculated and printed.  
 $BI(I) = \beta_i = (r_{i+1}^2 - r_i^2)$ , see equation (1), page 6,

and series of equations defining the Newton-Raphson terms, pages 10 and 11. NOBS and ROUT are reprinted to ensure proper entry; SIGOB and RAV are printed to enable the drawing of a radial density diagram for the cluster.

56 Start of the XO loop.  $XO = x_0$  in equation (4), page 7, and is the upper limit to integration of the isothermal gas sphere. As can be seen from XI, data are sufficient to allow a maximum XO of 1000 (lines 33-44).

57 IND is a marker used to determine whether the program is calculating values by (I) increasing  $\alpha$  or by (II) averaging the  $\alpha$  values producing the two smallest  $\chi^2$ .

IND=5 → (I)

IND=70 → (II)

For case (II) storage spaces are needed for the smallest  $\chi^2$  values and their associated  $\alpha$  values, they are C1, C2, A1, and A2. Intermediate values are stored in C3 and A3. For the current minimum  $\chi^2$  in case (II), the associated values obtained for  $\sigma_C$  and  $\sigma_{bg}$  are stored in S2 and SB2 respectively.

58-59 C2 and A2 are set abnormally high so as to allow the first value for  $\chi^2$  obtained to become the current minimum. It is necessary to set them high because finding minimum values works by comparison.

(An alternate method would be to assign C1 and C2 (and A1 and A2) the first two  $\chi^2$  (and  $\alpha$ ) values calculated in the loop starting at line 79, but counters, etc. would have to be added making this method more cumbersome.)

60-61 Since  $\sigma_c$  and  $\sigma_{bg}$  are solved iteratively, the iterated solutions are stored in arrays for later testing. These arrays, SC(I) and SBG(I) respectively, start with the estimated values that were entered as data.

62 An initial  $\alpha$  is calculated.

63  $\log(\alpha)$  is stored. Since  $\alpha$  is incremented in steps of  $\log(\alpha)+0.08$  this value is necessary.

64  $\text{LOGAL} = \log(\alpha_{\text{initial}}) + 4$ . When (or if)  $\alpha$  reaches this value, the program moves to case (II).

65 IZ is a counter needed for storing a triple row of results before printing; see lines 209-219.

66-67 The current value of X0 is printed.

68-69 Headings for the results are printed.

70-71 The values  $\xi e^{-\psi} \psi'$  are calculated (see equation 4, page 7) as XIEPS(I).

72 The integral

$$\int_0^{x_0} \xi e^{-\psi} \psi' d\xi$$

is calculated in subroutine DIVIN.

73-77 If there is an error somewhere in the subroutine,

IJK=111: This causes the printing of the message  
and the choosing of the next XO.

78 The integral is returned to the MAIN program as  
INTDI(1). Since the array INTDI is needed later,  
the integral is stored as DIVN.

79 An important loop is started. This one calculates  
the density of an isothermal gas sphere at the  
distances at which observed densities are found.

80  $X = x_i$  in equation (4). It is the unitless distance  
of the observed density.

81 If X is greater than the upper limit of integration  
this loop is exited. Go to line 104; calculation  
is impossible under these conditions.

83  $X^2$  is calculated for later usage.

84-85 The array XI is searched to find the position of  
the value  $> X$ .

87-89 If no value of XI suits, a message is printed and  
the program stops.

90-92 The values  $e^{-\psi} \psi' \sqrt{\xi^2 - x^2}$  are calculated as XIEPS (see  
equation 4, page 7).

93 The position of the first XI  $> X$  is decreased by one  
and

94-95 all XIEPS values up to the first XI  $> X$  are set to  
zero.

96 The integral

$$\int_x^{x_0} \sqrt{\xi^2 - x^2} e^{-\psi \xi} d\xi$$

is calculated in the subroutine SIGI; the result is stored in INTDI(1).

- 97-101 Check for errors in the subroutine, if there is one the message is printed and the next X0 is chosen. If there are no errors, continue.
- 102 End of the isothermal density loop. The isothermal gas sphere density value for this value of RAV is calculated. The operations return to line 80 to calculate the  $\sigma_{iso}$  for the next RAV.
- 103 After  $\sigma_{iso}$  is calculated for each RAV the program goes to line 108.
- 104 Operations go here if conditions in line 81 are met. If I=1 (i.e. the initial X > X0) then the operations are sent to line 220 to increase  $\alpha$  and so decrease X.
- 106-107 If I > 1, then the values for  $\sigma_{iso}$  not yet calculated, and so unable to be calculated, are set to zero.
- 108-109 After  $\sigma_{iso}$  is calculated two counters are set. The loop to follow runs 20 times, but can go to 40, 60, 80, or 100. The counter II indicates how many groups of 20 times the loop has run. The counter IXY will be explained later.
- 110 Start of the iteration loop for the Newton-Raphson

method. The iteration runs 20 times, which has been found through tests to be sufficient to get convergence to within  $10^{-3}$ . Tests are done later to check for  $10^{-4}$  interior convergence and the 20 step iterative procedure can be repeated up to four times if necessary.

111-115 Summation terms to be used in the iteration are set to zero initially.

116 An interior loop which is used to perform the necessary summations is started.

117  $Z1 = \sigma_c \sigma_{i80}(x_i) + \sigma_{bg}$ . This is the density of an isothermal gas sphere model at the distance  $x_i$  using the current density values of  $\sigma_c$  and  $\sigma_{bg}$ .

118-121  $Z1$  is tested to see if it equals zero. If so, IAM, a printing command, is set accordingly and the operations move to line 225.

122-125 If  $Z1 \neq 0$ , continue setting up sub-components of the summations. Referring to the equations of pages

10 and 11,  $E1 = 2\epsilon_i - \epsilon_i^2$ ,

and  $E2 = u_i$

126-130  $F = f$ ;  $FC = f_x$ ;  $GBG = g_y$ ;  
 $G = g$ ;  $FBG = f_y g_x$ ; see pages 10 and 11

Line 130 is the end of the summation loop.

131 The denominator term from the equations of page 12 (i.e.  $f_x g_y - f_y^2$ ) is calculated.

132 The size of DNOM is checked. If it is too small,

the size of the calculated value using DNOM would probably exceed the computer's capacity, and so no iteration is performed. If DNOM is not too small operations proceed to line 141.

- 134-135 Instead of iterating, the next values of  $\sigma_c$  and  $\sigma_{bg}$  are set to the previous values.
- 136 Also, counter IXY is increased by 1.
- 137 If this has happened less than 6 times in a row (i.e.  $IXY \leq 5$ ) and the loop is at less than the 19<sup>th</sup> iterative step (i.e.  $IP < 19$ ), then operations return to the beginning of the iteration loop, line 110, for the next iterative step.
- 139-140 If this has happened 6 or more times and  $IP=19$ , then an error message counter is set and the operations go to line 225.
- 141 If the value of DNOM is sufficiently large iteration can be performed and the value of IXY is reset to zero.
- 142-143 The iterative steps are performed (see the equations on page 12).
- 144 After the steps are performed, return to the start of the Newton-Raphson loop, line 110.
- 145-147 After 20 iterations a loop is started to check the last 6  $\sigma_c$  and  $\sigma_{bg}$  values, in groups of 3 consecutive values, for convergence, with some leeway for slight nonconvergence. This is done by

comparing the size differences between the L and L-1 terms and the L and L+1 terms. If the difference between L and L-1 is greater than the difference between L and L+1, then the series is converging. Leeway is built in by adding 0.005 of the L term to the L-(L-1) difference. XX1 is the L-(L-1) difference with the leeway term, and XX2 is the (L+1)-L difference.

- 148 If convergence occurs for  $\sigma_c$ , the same test is used for  $\sigma_{bg}$ .
- 150-151 If  $\sigma_c$  convergence does not occur, the error message counter is set and operations go to line 225.
- 152-158 Convergence for  $\sigma_{bg}$  is tested. If it is found, operations return to the loop's start, line 145, and if convergence is not found the error message counter is set and operations move to line 225.
- 159-161 After convergence for the last 6 iterations of  $\sigma_c$  and  $\sigma_{bg}$  has been confirmed, the degree of convergence is tested. If the difference between the last and second last iterated values for both  $\sigma_c$  and  $\sigma_{bg}$  is less than or equal to  $10^{-4}$  of the last iterated value, the values are satisfactory and operations proceed to line 171. In this check XX1 refers to  $\sigma_c$  and XX2 to  $\sigma_{bg}$ .
- 163 If the degree of convergence is not sufficient and

the iterative loop has been run less than 5 times, operations proceed to line 167.

- 165-166 If the degree of convergence is insufficient and the loop has run 5 times an error message counter is set and operations move to line 225.
- 167 From line 163. The counter which keeps track of the number of times the iteration loop is run is incremented by 1.
- 168-169 The last iterated value for  $\sigma_c$  and  $\sigma_{bg}$  from the last run through the iteration loop is moved to a lower place in the SC and SBG arrays and will be the initial value for the next run through of the iteration loop.
- 170 The program is sent to the start of the Newton-Raphson iteration loop, line 110.
- 171-172 From line 161. If convergence standards are met, the final values obtained from the iteration loop are accepted as the best  $\sigma_c$  and  $\sigma_{bg}$  for the  $x_0$ - $\alpha$  combination used.
- 173-182 This section checks to see if the accepted values are greater than twice the initial estimates which were fed in. If they are, the initial estimates are used as the first values in the Newton-Raphson iteration loop for the next  $\alpha$  value. If the accepted values are less than twice the initial estimates then the accepted values will be used.

This is done because tests have found that if initial values in the iteration loop are too large by several times, the loop usually converges to the wrong root of the set of equations. However, if the initial estimates are too small, but still positive, this will not occur.

- 183-185 After the initial values for the next run of the iteration loop have been set, the rest of the  $\sigma_c$  and  $\sigma_{bg}$  arrays are set to zero as a safety measure.
- 186 Since the  $\chi^2$  test involves a summation, the space used to store the  $\chi^2$  value is initially set to 0.
- 187 The loop to calculate  $\chi^2$  is started and runs once for each ring.
- 188 The theoretical number of galaxies for the specific ring is calculated from the ring area and the density in galaxies/arcmin<sup>2</sup>. This density is calculated from the  $\sigma_c$  and  $\sigma_{bg}$  values (obtained from the iteration loop) and from the isothermal gas sphere densities previously obtained for these rings.
- 189 The  $\chi^2$  is calculated.
- 190 If IND=5 (see line 57) the program is still operating in method (I). If IND=70 the program is operating by method (II). If the program is in method (II) operations proceed to line 262.
- 192 The value of  $\chi^2$  is checked. If  $\chi^2 < 0$ , then at

least one of the values found for  $\sigma_C$  and  $\sigma_{bg}$  is large and negative and so physically unreasonable. In this case the present  $\chi^2$  is not to be compared to the current minimum  $\chi^2$  and operations go to line 209.

- 194-208 This section preserves the minimum  $\chi^2$  and associated  $\alpha$ ,  $\sigma_C$ , and  $\sigma_{bg}$  as C2, A2, S2, and SB2. The  $\chi^2$  and  $\alpha$  values preceding and following the minimum  $\chi^2$  are saved, respectively as C1, A1 and C3, A3. This is done so the minimum  $\chi^2$  and associated values are isolated from the rest of the results found for a given X0 and may be printed separately and also so that the three smallest  $\chi^2$  and associated  $\alpha$  values are available for method (II).
- 209-212 The current  $\chi^2$  and associated values are stored in part of an array, AXXA, in groups of 4.
- 213 The array index, IZ, is incremented by 4 to allow the next group of 4 values to be stored the next time operations reach line 209. This means that consecutive groups of results, with 4 numbers per group, are stored linearly in larger collections of 3 groups. This is due to the results being printed in the same manner in which they are stored and paper width only allows the printing of 12 numbers. The output, to be read sequentially,

must be read as 3 groups of 4 numbers from left to right across the page before proceeding to the next line.

214 Since AXXA has only 12 spaces, when they are filled a line of results must be printed before more can be stored. If it is filled by now IZ=13, so this line checks to see if AXXA is filled. If it is not, proceed to line 220.

216-219 Because AXXA is filled, its contents are printed and IZ is reset to allow values to be stored in the array again.

220-221 From lines 214 or 104.  $\alpha$  is increased by incrementing  $\log(\alpha)$ .

222  $\log(\alpha)$  is checked to see if it is too large (see lines 62-64). If it is not too large a best  $\sigma_c$  and  $\sigma_{bg}$  will be found for the new  $x_0$ - $\alpha$  combination starting at line 79.

224 Since  $\alpha$  is now too large, go to line 245.

225 From lines 121, 140, 151, 157, or 166. If the program is in method (I) it proceeds to line 245.

227-243 Since the program is in method (II) the proper message is printed to explain why the program cannot operate properly as indicated by the error message counter IAM.

244 The program goes to line 282 to choose a new  $x_0$ , and reverts to method (I).

- 245-249 From line 225. Since the program cannot operate any further in method (I), the last of the results stored in AXXA are printed and IZ is reset for the next run of method (I).
- 250-251 The minimum  $\chi^2$  and associated values as found from method (I) for the current XO are printed.
- 252-258 The program is about to commence operating in method (II). In this method the smallest  $\chi^2$  is still called C2, but the second smallest  $\chi^2$  is called C3. These lines check the  $\chi^2$  preceding and following C2 as found in method (I) to see which is smaller. If C3 is already smaller than C1 the program proceeds to line 256. If C1 is smaller, C3 is assigned its value and A3 is assigned the value of A1.
- 256 IND is reset to indicate the usage of method (II).
- 257-258 The initial  $\sigma_C$  and  $\sigma_{bg}$  to be used in the Newton-Raphson iteration loop are set to be the values producing the minimum  $\chi^2$ .
- 259 A new  $\alpha$  is found by averaging the  $\alpha$  values producing the two smallest  $\chi^2$  values.
- 260 A counter to indicate how often method (II) has run for this XO is set.
- 261 With the new  $\alpha$ , new values of  $\sigma_C$ ,  $\sigma_{bg}$ , and  $\chi^2$  are to be found. Proceed to line 79.
- 262 From line 190. The  $\chi^2$  found from the new  $\alpha$  as

- obtained by method (II) is compared to the previous minimum  $\chi^2$ . If it is not smaller, go to line 271.
- 264-270 Since the new  $\chi^2$  is smaller than C2, values are reassigned accordingly, with the new  $\chi^2$  becoming C2 and the old C2 becoming C3, the  $\alpha$  values being reassigned similarly, and the  $\sigma_c$  and  $\sigma_{bg}$  producing this new minimum  $\chi^2$  being stored.
- 271 From line 262. Even though the new  $\chi^2$  is greater than C2, it is checked to see if it smaller than the second smallest  $\chi^2$ . If not, operations go to line 275.
- 273-274 Since the new  $\chi^2$  is smaller than the previous second smallest  $\chi^2$ , C3 and A3 are reassigned accordingly.
- 275 From lines 270, 271, or 274. IDD is checked to see if method (II) has averaged  $\alpha$  values the required number of times. If it has, go to line 280.
- 277 A new  $\alpha$  is obtained from those associated with the two smallest  $\chi^2$  values.
- 278 The method (II) frequency counter is incremented.
- 279 With the new  $\alpha$ , proceed to line 79.
- 280-282 From line 275. Since method (II) has been run the appropriate number of times the results obtained are printed. Then the program chooses a new X0 and returns to begin method (I) again.

283-286 From lines 29, 89, or 282. Either a fatal error has occurred or the program has operated over the required range of X0 values. Several lines are skipped on the output and the program ends.

### Subroutine SIGI

This subroutine is called from line 96 in the MAIN program and is used to calculate the integral

$$\int_x^{x_0} \sqrt{\xi^2 - x^2} e^{-\psi} \psi' d\xi$$

The factors transferred to this subroutine from the MAIN program are the values  $x$  and  $x_0$ , the series of values of  $\xi$  from 0 to 1000, and the series of values for  $\sqrt{\xi^2 - x^2} e^{-\psi} \psi'$  corresponding to the  $\xi$  values. These factors are represented in this subroutine as X, IX0, XI, and EPSI respectively, with the last two being arrays. The values of EPSI from XI=0 (i.e. XI(1)) to the value of XI nearest but still smaller than X are all equal to zero (see MAIN, lines 84-95).

The major facet complicating this subroutine is that while XI increases in three ranges with different incremental step sizes in each range (i.e. in the first

range XI increases in steps of 0.1 from 0 to 9.9; in the second XI range the increment size is 1 from 10 to 99; and in the third range XI increases in steps of 10 from 100 to 1000) and X and IXO can be in any of these ranges, the integration subroutine IQSF can only integrate over an interval using identical incremental steps. Therefore, unless X and IXO occur in the same range, the different ranges must be integrated separately and the results summed.

Lines	Function and/or relation to theory
1	Subroutine declaration statement and transfer of necessary data. INTDI is an array needed by the secondary integration subroutine IQSF to store results as the integration proceeds and IJK is the error marker mentioned in the MAIN program (see MAIN lines 73-77 and 97-101) and is also used to indicate whether or not X equals a specific value of XI.
2-3	Declaration of arrays and double precision. SUM is the space in which results of separate integrations are added.
4	The error marker is set to zero.
5	A marker used to indicate whether or not IXO is equal to a specific value of XI is set to zero.
6	X is checked again to see if it has a negative value. If so operations proceed to line 17.

- 8 X is compared to IXO, if  $X < IXO$  the integration can be performed and so operations proceed to line 13.
- 10-12 Since  $X > IXO$ , an error message is printed and the program is sent to line 176.
- 13 Initial value of SUM is set.
- 14-16 A loop is used to determine the position (I) of the value of XI equal to or immediately greater than X. If a value of XI equals X the program is sent to line 21, and if a value is not equal but larger than X, operations go to line 20.
- 17-19 From line 6 or if X is larger than all values of XI. In this case an error message is printed and the program is sent to line 176.
- 20 From the loop in lines 14-16. The marker is set to 25 to indicate that no value of XI equals X.
- 21-23 From line 20 or the loop in lines 14-16. A loop is used to determine the position (K) of the value of XI equal to or greater than IXO. If a value of XI equals IXO the program is sent to line 43, and if a value is not equal but larger than IXO the program is sent to line 27.
- 24-26 If all values of XI are smaller than IXO the error message is printed and operations are sent to line 176.
- 27 From the loop in lines 21-23. The marker is set to 30 to indicate that no value of XI equals IXO.

28 Proceed to line 43.

29 From line 55. If operations reach this line then IXO is between two adjacent values of XI, namely XI(K-1) and XI(K). Since IQSF can only integrate up to XI(K-1) or XI(K) and not between them, the area under the EPSI curve between XI(K-1) and IXO must be calculated another way. Accordingly, the average position between XI(K-1) and XI(K) is found: if IXO is greater or equal to this average, the area between IXO and XI(K) is found and subtracted from the SUM and the curve is integrated out to XI(K); if IXO is less than the average, the area between XI(K-1) and IXO is found and added to the SUM and the curve is integrated out to XI(K-1). To obtain the area between IXO and the required XI value (to be called XI(R)), the values of EPSI at XI(K-1) and XI(K) were first interpolated linearly to obtain an EPSI value at IXO. Then with EPSI for IXO and XI(R) and with the difference between IXO and XI(R) the area was calculated as a trapezoid. In line 29 the average position between XI(K-1) and XI(K) is found.

30 If XAV<IXO the program is sent to line 38.

32-35 The area under the EPSI curve between XI(K-1) and IXO is calculated and added to the SUM.

36 Since the integration is to proceed to the (K-1)<sup>th</sup>

position, but is told to integrate to position "K", the value of K is decreased by 1.

37 Go to line 43.

38-41 From line 30. The area under the curve of EPSI between IXO and XI(K) is calculated and subtracted from the SUM.

42 Go to line 57.

43 From the loop in lines 21-23 or lines 27 or 28. NDIM is the effective dimension of the variable being integrated; to use IQSF NDIM must be larger than 2.

44 If the value of  $NDIM < 1$  go to line 45, if  $NDIM = 1$  go to line 48, and if  $NDIM > 1$  go to line 53. To get  $NDIM = 0$  both X and IXO must be between XI(I-1) and the midpoint between XI(I-1) and XI(I); initially  $I = K$ . For  $NDIM = 1$  either: X and IXO are between XI(I-1) and XI(I) with IXO greater than the average of XI(I-1) and XI(I) - producing a  $SUM < 0$  (see lines 38-41); or X is between XI(I-1) and XI(I) and IXO is between XI(I) and the midpoint between XI(I) and XI(I+1) - producing a  $SUM > 0$  (see lines 32-35).

45-46 From 44. Since  $EPSI = 0$  at X, linear extrapolation with the EPSI value at XI(I) will give an EPSI at IXO. With this and the values for X and IXO the area, and so the total area, has been found.

47 Go to line 170.

- 48-50 From line 44. If the first case for  $NDIM=1$  occurs the total area (i.e. integral) is found in line 48 in the same manner as for  $NDIM=0$ . For the second case the area found for the interval from  $XI(I)$  to  $IXO$  (see lines 32-35) is added to the area bounded by the right triangle with corners  $X$ ,  $XI(I)$ , and  $EPSI(I)$ , with the right angle at  $XI(I)$ .
- 52 In both cases the total integral has been found, so the program proceeds to line 170.
- 53 From line 44.  $IJK=0$  means  $X$  is between  $XI(I-1)$  and  $XI(I)$ , and because the integration only starts at  $XI(I)$  the area between  $X$  and  $XI(I)$  is calculated and becomes the total integral until further integration can be carried out.
- 55 If  $IXO$  is not equal to any value of  $XI$  go back to line 29, if it is equal to one, continue.
- 57 From lines 42 or 55. Under the conditions specified, both  $X$  and  $IXO$  occur in the first range of  $XI$  values. If this is the case proceed to line 70.
- 59 If only  $X$  is in the first range of  $XI$  values go to line 81.
- 61 If  $X$  and  $IXO$  are in the second range of  $XI$  values go to line 125.
- 63 If only  $X$  is in the second range of  $XI$  values go to line 136.

- 65 If X (and so IXO) is in the third range of XI values go to line 160.
- 67-69 All possible combinations of values of X and IXO have been covered. However, if somehow the program does reach these lines an error message to locate the problem is printed and the program is sent to line 174.
- 70 From line 57. If  $NDIM > 2$  IQSF can be used, and so proceed to line 74.
- 72  $NDIM=2$ , so the rest of the integration can be performed in this line.
- 73 Integration is complete so proceed to line 170.
- 74-77 Because IQSF works from an array, starting at the first space and proceeding as far as is specified, the values of the array EPSI must be shifted so that  $EPSI(I)$  becomes  $EPSI(1)$ ,  $EPSI(I+1)$  becomes  $EPSI(2)$ , etc.
- 78 The subroutine to perform the integration is called. The parameters sent to this subroutine are, respectively, the integration step size, the values of the function being integrated, a storage space for integration results, and the effective dimension of the array to be integrated (i.e. the number of values from I to K inclusive for I and K in the same XI range). The result from IQSF is returned in  $INTDI(NDIM)$ .

- 79 The result of this integration is added to results found previously, if any.
- 80 Integration is complete; proceed to line 170.
- 81 From line 59. The 0.1 incremental steps go from (originally) EPSI(1) to EPSI(101). If I=100 IQSF cannot be used. If I<100 IQSF can be used so operations proceed to line 86.
- 83 Since IQSF cannot be used, the integrations to the end of the first XI range are completed in this line.
- 84 When EPSI is shifted for further integration the original EPSI(101) must become EPSI(1), etc. NDIM is set to 101 so the term EPSI(NDIM) can be used initially.
- 85 Go to line 93.
- 86-90 From line 81. NDIM is set to the proper value and EPSI is shifted accordingly.
- 91-92 IQSF is used and the results are added to the previous SUM.
- 93 From lines 85 or 92. If IXO is in the third XI range go to line 107.
- 95 If K > 102 IQSF can be used so proceed to line 99.
- 97 If K=102 the integration between the spaces initially called EPSI(101) and EPSI(102) must be done in this manner. NDIM is used instead of 101 because the array may have been shifted. This

- step completes integration.
- 98 Go to line 170.
- 99-106 From line 95. The array EPSI is shifted the proper number of spaces, NDIM is reset, the integration is performed with the results added to previous answers, and with all integration completed operations proceed to line 170.
- 107-113 From line 93. EPSI is shifted, NDIM is reset, IQSF is used, and the results added to SUM.
- 114 If  $K=191$  the integrations are complete and operations proceed to line 170; if  $K=192$  integrations cannot be completed with IQSF so operations proceed to line 115; if  $K > 192$  IQSF can be used and operations proceed to line 117.
- 115-116 From line 114. These complete the integration and sends operations to line 170.
- 117-124 From line 114. In a fashion similar to lines 99-106 these lines complete the integration and send operations to line 170.
- 125-128 From line 61. If NDIM is of insufficient size for use of IQSF the integrations are completed here and operations are sent to line 170. If NDIM is large enough to use IQSF go to line 129.
- 129-135 EPSI is shifted, integrations are completed, and operations are sent to line 170.
- 136 From line 63. If  $I < 190$  IQSF can be used, and so

- proceed to line 141.
- 138 If I=190 integrations for the second XI range are completed in this line.
- 139-140 NDIM is reset appropriately and operations proceed to line 148.
- 141-147 From line 136. Integration procedures for the second XI range are completed.
- 148 From lines 140 or 147. If  $K > 192$  IQSF can be used and so operations proceed to line 152.
- 150-151 With  $K=192$ , final integration is performed and operations proceed to line 170.
- 152-159 From line 148. Final integration for the third XI range is performed, the result is added to previous results and operations proceed to line 170.
- 160 From line 65. If  $NDIM > 2$  IQSF can be used so operations move to line 164.
- 162-163 Since  $NDIM=2$ , final integration is performed in this manner and operations go to line 170.
- 164-169 From line 160. Integration procedures are performed for the third XI range. This completes integrations for this range.
- 170 From lines 52, 73, 80, 98, 106, 116, 124, 128, 135, 151, 159, 163, or 169. Whenever the integration has been completed the program has been sent here. The final result of the integration, SUM, is placed in INTDI(1) where it can be retrieved by

- the MAIN program.
- 171 The error marker IJK is set to 0 to indicate subroutine SIGI has operated correctly.
- 172 A further safety check is made, if  $SUM > 0$  the program proceeds to line 177.
- 174-175 From lines 69 and 172. Something drastically wrong has happened. An error message is printed with much relevant data.
- 176 From lines 12, 19, 26, and 175. Because some sort of error has occurred the error marker is set to 111.
- 177-178 The program returns to the MAIN section and subroutine SIGI ends.

#### Subroutine DIVIN

This subroutine is called from line 72 in the MAIN program and is used to calculate the integral

$$\int_0^{x_0} \xi e^{-\psi} \psi' d\xi$$

The factors transferred to this subroutine are the series of values  $\xi e^{-\psi} \psi'$  (called XIEPS) corresponding to the  $\xi$  values, the integration cutoff  $x_0$  (called IXO), and the

series of  $\xi$  values (called XI). XI characteristics have been described elsewhere, see for example the introduction to the explanation of the subroutine SIGI in this Appendix.

Lines	Function and/or relation to theory
1	Subroutine declaration statement and transfer of necessary data. INTDI and IJK are as described for SIGI, line 1.
2-3	Déclaration of arrays and double precision.
4	The storage space for integration results is set to 0.
5-7	A loop is set up that searches for a value of XI greater than or equal to IXO. If the XI value is less than IXO the search continues; if an XI value equals IXO the program goes to line 25; and if no XI value equals IXO, the first XI value greater than IXO sends operations to line 12.
8-11	If IXO is larger than all values of XI an error message is printed, the error marker is set to 111, and operations are sent to line 65
12-24	From line 6. Since IXO occurs between 2 values of XI (i.e. $XI(I-1) < IXO < XI(I)$ ), integration cannot be exact and so these lines perform the same sort of computations, and for the same reasons, as lines 29-41 in subroutine SIGI.
25	From lines 19 or 24. If $I > 101$ then the entire

first range of XI values is to be integrated over.  
In this case proceed to line 32.

27 Since less than the entire first range is to be  
integrated over, NDIM is assigned the proper value.

28 If  $NDIM > 2$  IQSF can be used; operations go to line  
33.

30 Since  $NDIM=2$ , the total integration is performed  
by this line.

31 Since all integrations are completed, go to line 64.

32 From line 25. NDIM is set to the appropriate value.

33 From lines 28 or 32. Integrations for the first XI  
range are performed using IQSF.

34 Integration results are added to previous results,  
if any.

35 If  $I \leq 101$  then integrations are complete and the  
program is sent to line 64.

37 If  $I \geq 191$  the entire second range of XI values is  
to be integrated over. In this case proceed to  
line 44.

39 Since less than the entire second range is to be  
integrated, NDIM is set to the appropriate value.

40 If IQSF can be used go to line 45.

42-43 The integration for the second XI range is completed  
and added to previous results and the operations  
are sent to line 64.

44 From line 37. NDIM is set to the appropriate value.

45-48 From lines 40 or 44. The array XIEPS is shifted  
the proper number of places.

49 IQSF is called to integrate over the second XI range.

50 The results of this integration are added to the  
previous SUM.

51 If  $I \leq 191$  all necessary computations have been made  
and operations proceed to line 64.

53 Since IX0 occurs in the third XI range, more  
integration needs to be performed, and so NDIM is  
set appropriately.

54 If IQSF can be used go to line 58.

56-57 Final integration and summation are completed and  
operations proceed to line 64.

58-61 From line 54. XIEPS is shifted the proper number  
of places.

62 Final use of IQSF, on the set of values  
corresponding to the third XI range.

63 Final summation of results.

64 From lines 31, 35, 43, 51, 57, or 63. The final  
result is assigned to INTDI(1) for access by the  
MAIN program upon leaving this subroutine.

65-66 From lines 11 or 64. Operations return to the  
MAIN program and subroutine DIVIN ends.

## Subroutine IQSF

This subroutine is called from lines 78, 91, 104, 112, 122, 133, 146, 157, and 168 in the subroutine SIGI and from lines 33, 49, and 62 in the subroutine DIVIN.

It is part of IBM's Scientific Subroutine Package where it is called "QSF". This subroutine performs integrations numerically following the method of Simpson's rule. Further details and explanations may be found in the SSP manual on page 87.

\*Modifications to YAHOO to get BGIN

The changes in lines 4 to 69 are due to  $\sigma_{bg}$  being used as a constant. Wording changes in the format statements reflect this difference in usage of the value read in for SBG in line 19.

The changes in lines 111 through 132 are performed because of the change in the Newton-Raphson method. With respect to the terms of page 15 (and so pages 10 and 11) the variables in the program are:

SUM1 $\equiv$ f

SUM2 $\equiv$ f<sub>x</sub>

EI $\equiv$  $\epsilon$ <sub>1</sub>

$$UI \equiv \mu_i$$

$$BI(I) \equiv \beta_i$$

$$SIGISO(I) \equiv \sigma_{iso}(x_i)$$

In the last line of the group replacing lines 123 through 132 the size of SUM2 is tested. If it is too small the value of

$$SUM1/(2.*SUM2)$$

(in the new version of line 142) would probably exceed the size limit of the computer.

The new version of line 142 produces a new iterative value of  $\sigma_c$  in the manner described on page 15.

All changes and deletions in the rest of the program are obvious consequences of the use of  $\sigma_{bg}$  as a constant.

The lines inserted between lines 277 and 278 keep track of the latest values of  $\alpha$ ,  $\sigma_c$ , and  $\chi^2$ .

\*Modifications to YAHOO to get TAFCHC

The lines inserted between lines 24 and 25 read in and reprint Taff's values for  $\alpha$ ,  $\sigma_c$ , and  $\sigma_{bg}$ .

The variable inserted between lines 56 and 57 is a marker used to determine whether or not TAFCHC has completed all the functions YAHOO performs for a given  $x_0$ . If it has, then ITAFF's value is changed from 5 to 500,  $\sigma_{iso}$  is calculated for Taff's  $\alpha$  and the current  $x_0$ , a model isothermal gas sphere is created from this  $\sigma_{iso}$  and Taff's values of  $\sigma_c$  and  $\sigma_{bg}$ , and the  $\chi^2$  is found from comparison of the data to this model.

The lines inserted between lines 102 and 103 and again between lines 107 and 108 check to see if TAFCHC has completed the YAHOO functions. If so, the values for  $\sigma_{iso}$  using Taff's value of  $\alpha$  have been calculated (lines 79 to 107 inclusive) and the program can calculate the  $\chi^2$ .

Since line 281 completes the YAHOO functions, ITAFF's value is reassigned,  $\alpha$  is set to Taff's value, and operations return to line 79 to calculate  $\sigma_{iso}$ .

After this has been done operations go to the line flagged 820. Here  $\chi^2$  is set to 0 and a loop calculates the theoretical number of galaxies in each ring from the model produced with Taff's values.  $\chi^2$  is then calculated from these theoretical values of Taff and the actual number of galaxies (the data set NOBS).

Once the  $\chi^2$  has been found both it and the Taff value of  $\alpha$  are printed. The  $\alpha$  value is printed as a safety check since its variable name in the program, ALPHA, is changed continuously during the program's execution. Taff's values of  $\sigma_c$  and  $\sigma_{bg}$  are not reprinted because the spaces they are assigned to (TSC and TSBG respectively) remain unchanged once they are read in.

After printing Taff's  $\alpha$  and the calculated  $\chi^2$ , the program increments  $x_0$  and continues with the YAHOO functions for it.

## Appendix D

## Plate and cluster information

The table on the next page lists information relating to the plates used in this thesis. Also listed are the redshift of each cluster as well as the distance and richness classifications and the 1950 positions; the last three items are from Abell (1958).

All plates used were taken by Dr. G.A. Welch.

Object	plate number	Exposure (minutes)	Emulsion	Filter	z	D	R	Centre R.A.	(1950) Dec.
A2052	PS5736	20	103a-D	Wr.12	.0351	3	0	15 <sup>h</sup> 14 <sup>m</sup> .0	+07°12'
	PS6868	120	IIIa-J	Wr.4					
A2593	PS7154	20	103a-D	Wr.12	.044	3	0	23 22.0	+14 22
	PS7173	120	IIIa-J	Wr.4					
A2626	PS6875	20	103a-D	Wr.12	.055	3	0	23 34.0	+20 53
	PS7142	120	IIIa-J	Wr.4					
A154	PS7145	20	103a-D	Wr.12	.056	3	1	01 08.3	+17 24
	PS7156	120	IIIa-J	Wr.4					

Appendix E  
Strip counts

Tabulated in this appendix are the results of the strip counts. Since the strips were centred on the major galaxy in three of the clusters, this central galaxy was counted twice for each orientation, once for each strip which contained half of it (strips 6 and 7). For the fourth cluster the centre held a binary galaxy. This cluster had the strips centred between the members of the binary and each member of the binary was treated like all other galaxies in the cluster; each was only counted once for each orientation.

After the three sets of strip counts for each cluster (one set of counts for each magnitude limit) are two items: a list of four cluster centres, the three from the different magnitude limits and the Abell (1958) centre; and a diagram of the centre area of the cluster, at twice the print scale, locating the four centres. The diagrams are centred on the locations of the centres of strip counting and the boxes for the Abell centres come from the one digit difference in accuracy stated in the tables of cluster centres. The squares of the diagram correspond to the 1.5 cm width of the grid used to make the strip counts.

A2052

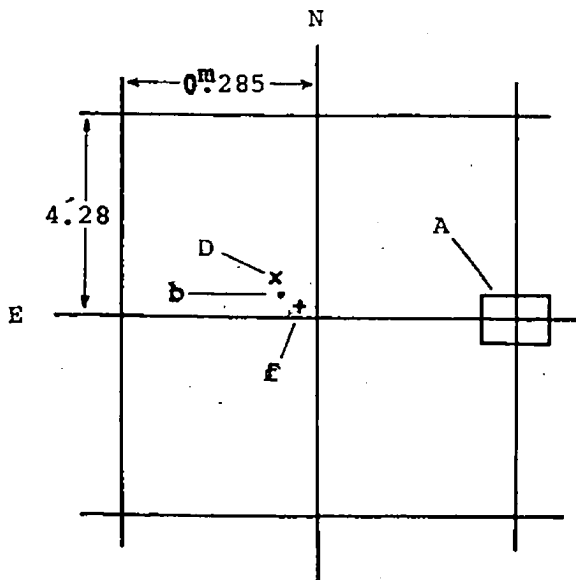
135

Mag. limit	Strip No.	Orientation			
		E+W	N+S	NE+SW	SE+NW
b	1	1	2	4	2
	2	3	1	2	0
	3	4	5	4	1
	4	3	2	5	4
	5	8	6	4	9
	6	6	9	7	8
	7	9	8	9	10
	8	4	5	1	5
	9	5	1	3	3
	10	1	3	5	3
	11	0	2	1	1
	12	2	2	0	0
		total	46	46	45
D	1	9	12	7	12
	2	14	12	14	9
	3	11	10	14	7
	4	21	21	25	15
	5	27	21	24	26
	6	27	31	18	29
	7	22	20	23	30
	8	18	18	12	22
	9	15	10	12	11
	10	9	22	12	16
	11	9	4	16	6
	12	11	11	11	4
		total	193	192	188
f	1	26	28	23	26
	2	40	28	36	25
	3	33	21	42	19
	4	34	41	42	33
	5	43	52	40	54
	6	54	66	30	61
	7	50	46	58	58
	8	42	42	37	49
	9	37	30	32	33
	10	22	35	29	30
	11	28	24	27	18
	12	26	21	27	13
		total	435	434	423

A2052

Cluster centre (1950)

Source	R.A.	Dec.
Abell	$15^{\text{h}}14^{\text{m}}0$	$+07^{\circ}12'$
b	$15^{\text{h}}14.33$	$+07^{\circ}12.3'$
D	$15^{\text{h}}14.36$	$+07^{\circ}12.7'$
f	$15^{\text{h}}14.31$	$+07^{\circ}12.0'$



A2593

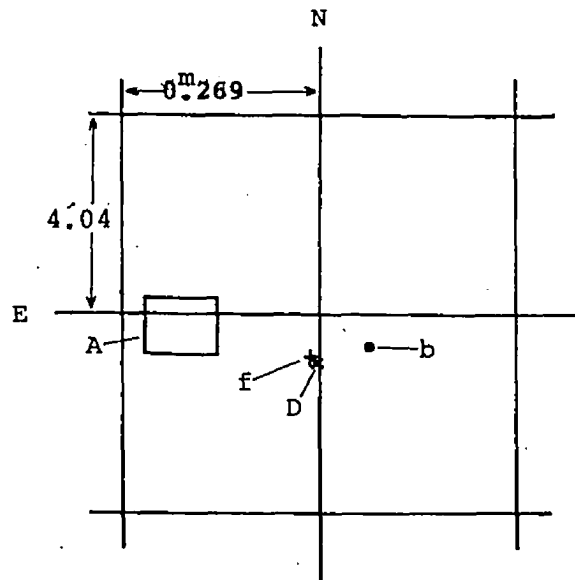
137

Mag. limit	Strip No.	Orientation			
		E+W	N+S	NE+SW	SE+NW
b	1	0	2	2	2
	2	1	3	2	2
	3	4	3	3	0
	4	1	5	1	1
	5	7	3	5	9
	6	7	5	9	9
	7	6	8	8	7
	8	5	6	3	6
	9	6	4	7	4
	10	5	3	2	1
	11	3	4	0	2
	12	1	2	4	2
		total	46	48	46
D	1	8	20	12	16
	2	15	19	20	23
	3	22	26	23	25
	4	31	39	21	50
	5	41	30	37	54
	6	64	57	80	49
	7	71	49	50	39
	8	44	32	31	42
	9	36	32	47	35
	10	29	37	34	32
	11	23	39	28	17
	12	16	18	22	23
		total	400	398	405
f	1	11	26	22	29
	2	38	33	22	32
	3	31	36	33	33
	4	38	46	35	63
	5	52	41	47	58
	6	73	56	79	54
	7	71	45	56	50
	8	54	45	39	43
	9	38	41	58	39
	10	32	46	45	38
	11	30	50	35	23
	12	25	31	23	27
		total	493	496	494

A2593

Cluster centre (1950)

Source	R.A.	Dec.
Abell	$23^{\text{h}}22^{\text{m}}0$	$+14^{\circ}22'$
b	23 21.76	+14 21.7
D	23 21.80	+14 21.1
f	23 21.82	+14 21.4

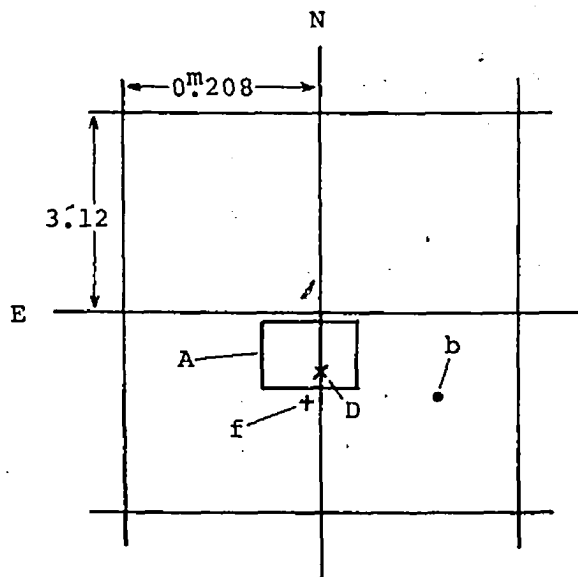


Mag. limit	Strip No.	A2626 Orientation 139			
		E-W	N-S	NE-SW	SE-NW
b	1	0	1	3	3
	2	1	1	1	2
	3	2	3	3	1
	4	4	5	6	5
	5	5	4	1	5
	6	5	9	3	9
	7	13	7	6	11
	8	5	5	7	4
	9	4	2	7	0
	10	6	6	8	4
	11	1	4	5	1
	12	6	4	2	3
	total	52	51	52	48
D	1	18	16	17	23
	2	34	14	19	32
	3	20	18	37	26
	4	26	27	31	31
	5	22	33	30	37
	6	36	38	30	36
	7	58	43	24	46
	8	25	32	33	32
	9	26	28	33	20
	10	30	29	32	23
	11	22	31	23	23
	12	17	27	27	11
	total	334	336	336	340
f	1	60	39	39	33
	2	71	39	43	35
	3	62	39	63	50
	4	48	50	57	47
	5	41	63	57	57
	6	77	69	68	78
	7	97	92	67	87
	8	76	75	67	85
	9	50	71	72	56
	10	69	82	59	61
	11	44	53	52	64
	12	37	59	54	41
	total	732	731	698	694

A2626

Cluster centre (1950)

Source	R.A.	Dec.
Abell	$23^{\text{h}}34^{\text{m}}0$	$+20^{\circ}53'$
b	23 33.86	+20 51.1
D	23 33.99	+20 51.2
f	23 34.01	+20 51.1

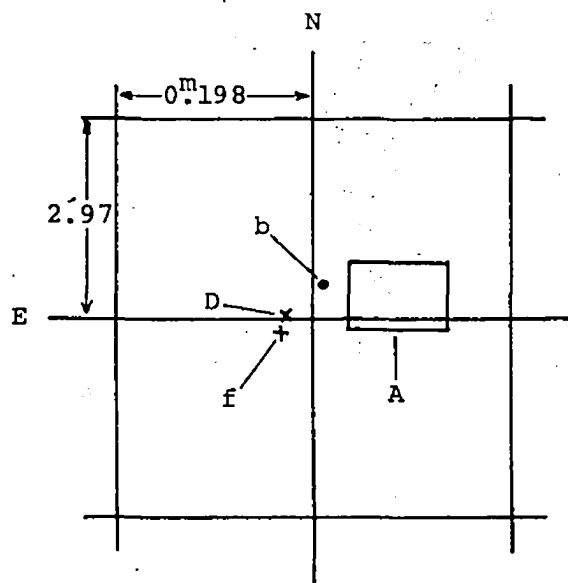


Mag. limit	Strip No.	A154 Orientation 141			
		E-W	N-S	NE-SW	SE-NW
b	1	1	5	6	1
	2	1	4	5	4
	3	7	6	5	2
	4	4	3	2	3
	5	3	0	3	5
	6	13	10	6	8
	7	3	7	14	6
	8	10	4	5	6
	9	3	4	3	5
	10	3	2	1	5
	11	3	4	4	4
	12	1	3	1	3
	total	52	52	55	52
D	1	15	13	24	17
	2	15	14	18	23
	3	25	14	18	14
	4	26	24	20	28
	5	18	21	23	17
	6	40	38	40	32
	7	34	33	46	41
	8	34	24	20	23
	9	14	23	22	19
	10	18	16	10	20
	11	8	20	18	14
	12	12	17	7	17
	total	259	257	266	265
f	1	15	20	29	26
	2	28	27	20	21
	3	27	23	23	22
	4	32	30	25	28
	5	38	23	29	26
	6	49	42	47	48
	7	42	35	59	50
	8	35	31	25	30
	9	18	37	32	26
	10	24	24	8	26
	11	23	32	23	13
	12	17	24	11	17
	total	348	348	331	333

A154

Cluster centre (1950)

Source	R.A. °	Dec.
Abell	01 <sup>h</sup> 08 <sup>m</sup> .3	+17°24'
b	01 08.38	+17 24.0
D	01 08.41	+17 23.8
f	01 08.42	+17 23.5



## Appendix F

## Ring counts

The ring count results are tabulated by quadrant and ring in this appendix for all three magnitude limits of each cluster. The tables contain the ring number, the outer radius in arcminutes of that ring, the number of galaxies in each quadrant, and the number of galaxies for the ring. At the bottom of the tables are the total numbers of galaxies both per quadrant and in the total area counted.

## A2052

Ring	ROUT	b					D					f				
		NE	NW	SE	SW	Σ	NE	NW	SE	SW	Σ	NE	NW	SE	SW	Σ
1	22.24	0	2	1	1	4	1	1	0	4	6	4	3	3	3	13
2	4.48	0	2	0	1	3	2	6	0	0	8	0	6	2	8	16
3	6.72	1	1	3	0	5	6	1	8	4	19	7	6	9	7	29
4	8.96	2	1	2	0	5	5	5	3	1	14	14	11	7	10	42
5	11.20	1	1	2	2	6	6	3	4	5	18	9	9	6	9	33
6	13.44	2	1	0	1	4	11	2	2	3	18	16	8	1	11	36
7	15.68	2	0	0	2	4	3	4	0	9	16	17	4	5	9	35
8	17.92	2	1	0	1	4	4	2	3	3	12	9	5	5	10	29
9	20.16	1	0	0	1	2	7	2	4	4	17	20	6	6	9	41
10	22.40	2	1	0	0	3	2	4	2	4	12	16	10	9	6	41
11	24.64	1	0	0	1	2	6	2	4	5	17	11	4	11	16	42
12	26.88	0	1	3	0	4	7	3	6	8	24	11	8	11	11	41
13	29.12	1	0	0	0	1	5	2	3	2	12	14	9	10	8	41
14	31.36	1	1	1	1	4	0	2	4	6	12	9	7	21	17	54
15	33.60	0	1	0	0	1	7	7	1	5	20	10	13	8	5	36
16	35.84	0	0	1	0	1	2	1	6	3	12	9	14	23	5	51
17	38.08	0	1	0	1	2	7	4	1	3	15	13	17	14	12	56
18	40.32	0	0	0	1	1	3	8	5	6	22	18	25	10	22	75
19	42.56	0	0	0	0	0	13	8	4	4	29	18	12	21	13	64
20	44.80	0	1	0	1	2	14	7	13	4	38	14	15	28	16	73
Σ		16	15	13	14	58	111	74	73	83	341	239	192	210	207	48

A2593

Ring	ROUT	b					D					f				
		NE	NW	SE	SW	Σ	NE	NW	SE	SW	Σ	NE	NW	SE	SW	Σ
1	2.12	1	1	0	1	3	3	7	0	3	13	5	2	0	2	9
2	4.24	0	2	1	0	3	9	5	7	23	7	9	5	3	24	
3	6.36	1	5	1	1	8	15	6	10	33	9	11	8	4	32	
4	8.48	1	0	1	0	2	3	11	7	8	29	7	6	7	4	24
5	10.60	0	0	1	2	3	4	9	12	3	28	11	9	13	8	41
6	12.72	2	0	0	3	5	3	15	12	17	47	14	3	15	18	50
7	14.84	1	0	0	3	4	13	10	9	13	45	6	17	13	16	52
8	16.96	1	2	0	0	3	9	11	3	9	32	12	14	6	8	40
9	19.08	0	1	1	0	2	7	7	7	15	36	9	10	9	14	42
10	21.20	0	0	2	1	3	6	4	7	9	26	9	6	19	11	45
11	23.32	3	2	1	3	9	8	16	7	5	36	18	9	13	12	52
12	25.44	0	0	0	1	1	6	12	7	10	35	15	11	17	10	53
13	27.56	1	0	0	0	1	6	9	8	11	34	15	11	16	13	55
14	29.68	1	1	0	0	2	11	7	11	13	42	13	14	8	15	50
15	31.80	1	0	0	0	1	2	15	14	9	40	15	6	14	12	47
16	33.92	1	1	0	1	3	5	4	5	13	27	10	12	10	19	51
17	36.04	4	2	1	0	7	8	16	6	8	38	17	12	17	18	64
18	38.16	0	1	0	0	1	11	12	6	7	36	10	13	10	15	48
19	40.28	2	2	6	1	11	10	6	11	8	35	6	17	13	11	47
20	42.40	0	3	1	2	6	11	9	12	11	43	13	12	18	13	56
Σ		20	23	16	19	78	150	191	161	176	678	221	204	231	226	882

145

## A2626

Ring	ROUT	b					D					f				
		NE	NW	SE	SW	E	NE	NW	SE	SW	E	NE	NW	SE	SW	E
1	1.63	1	0	0	1	2	0	3	0	1	4	2	4	2	3	11
2	3.27	1	1	1	1	4	4	5	2	6	17	7	5	10	9	31
3	4.90	1	1	1	2	5	4	3	2	4	13	6	8	7	14	35
4	6.53	1	0	0	2	3	7	5	2	5	19	12	8	7	14	41
5	8.16	0	2	0	1	3	4	4	3	10	21	7	15	8	19	49
6	9.80	2	1	0	2	5	11	4	1	8	24	10	9	6	19	44
7	11.43	3	1	1	2	7	7	7	6	7	27	14	14	13	13	54
8	13.06	2	0	1	2	6	7	10	4	14	35	12	14	16	25	67
9	14.70	2	0	2	0	4	11	7	15	6	39	27	16	30	22	95
10	16.33	0	0	2	0	2	9	4	8	8	29	19	8	27	17	71
11	17.96	1	1	0	2	4	10	11	12	10	43	26	21	21	17	85
12	19.59	0	1	2	3	6	6	6	6	14	32	16	14	22	34	86
13	21.23	1	0	3	0	4	9	12	15	13	49	17	24	19	23	83
14	22.86	1	1	1	2	5	10	3	8	8	29	21	9	21	19	70
15	24.49	2	0	1	0	3	8	3	14	14	39	20	14	36	23	93
16	26.12	1	2	3	1	7	13	8	12	10	43	31	21	38	22	112
17	27.76	2	1	3	0	6	17	16	16	10	59	32	27	40	26	125
18	29.39	5	0	0	1	6	11	17	14	15	57	27	27	33	40	127
19	31.02	0	1	4	0	5	17	7	12	17	53	28	12	31	31	102
20	32.66	0	0	4	1	5	15	12	17	21	65	37	29	38	43	147
Σ		26	13	29	23	91	180	147	169	201	697	371	299	425	433	1528

A154

Ring	ROUT	b					D					f				
		NE	NW	SE	SW	Σ	NE	NW	SE	SW	Σ	NE	NW	SE	SW	Σ
1	1.55	0	1	2	0	3	0	5	4	4	13	2	8	4	4	18
2	3.11	1	0	1	1	3	4	5	2	7	18	5	6	2	6	19
3	4.66	1	1	1	2	5	5	4	4	4	17	8	5	2	6	21
4	6.22	1	3	1	0	5	2	9	4	2	17	2	6	9	4	21
5	7.77	0	0	2	1	3	7	5	7	3	22	6	6	11	5	28
6	9.33	1	2	0	0	3	4	4	6	8	22	7	2	5	12	26
7	10.88	1	0	0	2	3	4	5	2	1	12	6	8	1	3	18
8	12.43	1	1	1	0	3	4	8	4	2	18	8	9	8	1	26
9	13.99	3	1	1	1	6	3	5	10	7	25	9	5	8	8	30
10	15.54	0	1	2	3	6	5	5	8	5	23	4	7	8	6	25
11	17.10	3	1	0	0	4	8	4	8	6	26	14	7	12	10	43
12	18.65	4	1	1	0	6	14	7	10	3	34	13	8	19	7	47
13	20.21	1	1	1	1	4	4	6	6	8	24	7	4	4	12	27
14	21.76	0	2	0	1	3	8	4	3	9	24	9	11	13	9	42
15	23.31	1	0	2	1	4	3	5	17	2	27	7	10	11	6	34
16	24.87	0	3	4	0	7	6	10	13	6	35	11	12	14	5	42
17	26.42	1	0	8	1	10	8	10	16	8	42	16	8	13	6	43
18	27.98	1	0	4	1	6	6	3	13	9	31	6	7	12	16	41
19	29.53	1	3	1	2	7	6	13	10	13	42	4	16	14	7	41
20	31.09	0	1	2	1	4	5	6	11	4	26	11	8	15	8	42
Σ		21	22	34	18	95	106	123	158	111	498	155	153	185	141	634

## Appendix G

## Background counts

Below are tabulated the background counts for each cluster's three magnitude limits. These counts were taken in 9 cm by 9 cm squares in each corner of each print (8.75 cm squares for A2052). Besides the number counts (N) and the background densities in galaxies/arcmin<sup>2</sup> ( $\sigma$ ), the total counting area in arcmin<sup>2</sup> are presented for each cluster. The densities of the  $\Sigma$  column are those used as the initial estimates for the program YAHOO and also as the fixed values of  $\sigma_{bg}$  in the program BGIN.

The background counts were also used to calculate  $\Delta M$  in Table 12.

## A2052

Total area counted over = 2480.0 arcmin<sup>2</sup>

Mag. limit	Corner				$\Sigma$	
	NE	NW	SE	SW		
b	N	6	2	2	1	11
	$\sigma$	9.68(-3)	3.23(-3)	3.23(-3)	1.61(-3)	4.44(-3)
D	N	33	12	50	8	103
	$\sigma$	5.32(-2)	1.94(-2)	8.06(-2)	1.29(-2)	4.15(-2)
f	N	87	48	105	38	278
	$\sigma$	1.40(-1)	7.74(-2)	1.69(-1)	6.13(-2)	1.12(-1)

A2593

Total area counted over = 2348.0 arcmin<sup>2</sup>

Mag. limit	Corner				Σ	
	NE	NW	SE	SW		
b	N	4	4	3	4	15
	σ	6.81(-3)	6.81(-3)	5.11(-3)	6.81(-3)	6.39(-3)
D	N	27	60	53	42	182
	σ	4.60(-2)	1.02(-1)	9.03(-2)	7.16(-2)	7.75(-2)
f	N	39	95	71	60	265
	σ	6.64(-2)	1.62(-1)	1.21(-1)	1.02(-1)	1.13(-1)

A2626

Total area counted over = 1401.8 arcmin<sup>2</sup>

Mag. limit	Corner				Σ	
	NE	NW	SE	SW		
b	N	11	5	7	3	26
	σ	3.14(-2)	1.43(-2)	2.00(-2)	8.56(-3)	1.85(-2)
D	N	92	66	68	74	300
	σ	2.63(-1)	1.88(-1)	1.94(-1)	2.11(-1)	2.14(-1)
f	N	202	146	123	151	622
	σ	5.76(-1)	4.17(-1)	3.51(-1)	4.31(-1)	4.44(-1)

A154

Total area counted over = 1270.2 arcmin<sup>2</sup>

Mag. limit.	Corner				Σ	
	NE	NW	SE	SW		
b	N	5	0	8	8	21
	σ	1.57(-2)	0.00(-0)	2.52(-2)	2.52(-2)	1.65(-2)
D	N	32	26	40	37	135
	σ	1.01(-1)	8.19(-2)	1.26(-1)	1.17(-1)	1.06(-1)
f	N	36	29	62	47	174
	σ	1.13(-1)	9.13(-2)	1.95(-1)	1.48(-1)	1.37(-1)

Appendix H  
Complete results

The data for each magnitude limit of a given cluster were used in the programs YAHOO and BGIN for two cases each; using data for all 20 rings and just using data for the inner 10 rings. Each cluster has therefore 12 sets of results. Table 12 displays parts of these results but this appendix lists the complete results.

The tables display, in columns from left to right: ML - the magnitude limit for this set of rows;  $\Delta M$  - the difference in magnitude between the b limit and the D and f magnitude limits; Prog - the program used; NR - the number of rings used; NG - the number of galaxies used;  $\alpha$  - the best fit scale factor;  $\sigma_c$  - the best fit central density;  $\sigma_{bg}$  - for YAHOO the best fit background density, for BGIN the counted background as obtained from the counts in Appendix G (in BGIN this value is necessarily the same for both 10 and 20 ring cases for a given cluster and magnitude limit);  $x_0$  - the best fit integration cutoff to the isothermal gas sphere model;  $\chi^2$  - the calculated  $\chi^2$  obtained from comparing the best fit model to the data; and Prob - the probability that any  $\chi^2$  would be smaller than the one actually found. For the last column the number of degrees of freedom used is  $(NR-\kappa)$ , where  $\kappa=5$  for YAHOO and  $\kappa=4$  for BGIN.

In these tables the units used are:

$\Delta M$  - magnitudes

$\alpha$  - arcmin

$\sigma_c$  - galaxies/arcmin<sup>2</sup>

$\sigma_{bg}$  - galaxies/arcmin<sup>2</sup>

## A2052

ML	$\Delta M$	Prog	NR	NG	$\alpha$	$\sigma_c$	$\sigma_{bg}$	$x_0$	$\chi^2$	Prob		
b	-	YAHOO	10	40	1.311(-1)	3.567(-0)	8.516(-3)	200	2.063	.1596		
			20	58	2.179(-1)	2.069(-0)	2.419(-3)	200	8.480	.0969		
		BGIN	10	40	1.717(-1)	2.689(-0)	4.44(-3)	200	2.207	.1003		
			20	58	1.824(-1)	2.464(-0)	4.44(-3)	200	10.22	.1451		
		D	1.6	YAHOO	10	140	2.899(-0)	2.841(-1)	8.203(-3)	30	4.446	.5129
					20	341	2.876(-0)	2.386(-1)	4.314(-2)	10	24.61	.9446
BGIN	10			140	2.662(-0)	2.693(-1)	4.15(-2)	10	4.605	.4046		
	20			341	2.952(-0)	2.361(-1)	4.15(-2)	10	24.88	.9280		
f	2.3			YAHOO	10	315	2.404(-0)	4.968(-1)	1.277(-1)	10	8.056	.8468
					20	848	2.714(-0)	4.670(-1)	1.134(-1)	10	17.52	.7113
		BGIN	10	315	2.714(-0)	4.710(-1)	1.12(-1)	10	8.368	.7876		
			20	848	2.773(-0)	4.583(-1)	1.12(-1)	10	17.59	.6516		

## A2593

ML	AM	Prog	NR	NG	$\alpha$	$\sigma_c$	$\sigma_{bg}$	$x_0$	$\chi^2$	Prob
b	-	YAHOO	10	36	1.468(-0)	1.963(-1)	3.146(-3)	30	5.122	.5988
			20	78	1.431(-0)	1.789(-1)	1.187(-2)	20	30.80	.9907
		BGIN	10	36	1.503(-0)	1.897(-1)	6.39(-3)	20	5.120	.4715
			20	78	1.192(-0)	2.043(-1)	6.39(-3)	200	32.30	.9909
D	1.8	YAHOO	10	312	3.095(-0)	6.347(-1)	5.737(-3)	70	12.66	.9732
			20	678	2.615(-0)	6.390(-1)	4.519(-2)	60	18.00	.7373
		BGIN	10	312	3.173(-0)	5.519(-1)	7.75(-2)	10	12.90	.9553
			20	678	2.271(-0)	6.981(-1)	7.75(-2)	20	19.71	.7664
f	2.1	YAHOO	10	359	3.747(-0)	4.975(-1)	4.548(-2)	160	8.775	.8816
			20	882	3.911(-0)	4.571(-1)	6.340(-2)	80	15.08	.5543
		BGIN	10	359	3.680(-0)	4.336(-1)	1.13(-1)	10	8.820	.8160
			20	882	3.995(-0)	4.051(-1)	1.13(-1)	10	17.27	.6317

## A2626

ML	$\Delta M$	Prog	NR	NG	$\alpha$	$\sigma_c$	$\sigma_{bg}$	$x_0$	$x^2$	Prob		
b	-	YAHOO	10	40	1.407(-0)	2.095(-1)	9.671(-3)	160	4.298	.4926		
			20	91	1.294(-0)	2.215(-1)	1.185(-2)	140	6.662	.0336		
		BGIN	10	40	1.287(-0)	2.137(-1)	1.85 (-2)	30	4.322	.3668		
			20	91	1.271(-0)	2.162(-1)	1.85 (-2)	30	6.787	.0228		
		D	1.8	YAHOO	10	228	1.035(-0)	5.499(-1)	2.022(-1)	160	5.511	.6433
					20	697	1.574(-0)	4.659(-1)	1.668(-1)	140	19.01	.7867
BGIN	10			228	9.660(-1)	5.696(-1)	2.14 (-1)	50	5.520	.5210		
	20			697	1.152(-0)	5.186(-1)	2.14 (-1)	20	26.14	.9479		
f	2.3			YAHOO	10	498	1.080(-0)	1.128(-0)	5.364(-1)	10	8.811	.8832
					20	1528	1.454(-0)	1.204(-0)	3.786(-1)	80	29.80	.9873
		BGIN	10	498	9.637(-1)	1.238(-0)	4.44 (-1)	200	9.861	.8694		
			20	1528	1.208(-0)	1.118(-0)	4.44 (-1)	20	34.50	.9954		

A154

ML	ΔM	Prog	NR	NG	α	σ <sub>c</sub>	σ <sub>bg</sub>	x <sub>0</sub>	χ <sup>2</sup>	Prob		
b	-	YAHOO	10	40	5.214(-2)	1.083(+1)	3.769(-2)	200	1.947	.1436		
			20	95	6.333(-1)	4.577(-1)	1.790(-2)	180	9.057	.1255		
		BGIN	10	40	6.748(-1)	4.455(-1)	1.65 (-2)	200	2.981	.1888		
			20	95	6.748(-1)	4.450(-1)	1.65 (-2)	200	9.120	.0916		
		D	1.3	YAHOO	10	187	6.174(-2)	3.638(+1)	1.704(-1)	200	4.745	.5522
					20	498	5.064(-1)	2.549(-0)	1.049(-1)	180	17.00	.6811
BGIN	10			187	5.549(-1)	2.313(-0)	1.06 (-1)	120	5.323	.4969		
	20			498	5.453(-1)	2.342(-0)	1.06 (-1)	160	17.02	.6157		
f	1.5			YAHOO	10	232	1.006(-1)	2.421(+1)	1.709(-1)	190	3.819	.4242
					20	634	1.917(-1)	1.058(+1)	1.505(-1)	200	17.63	.7174
		BGIN	10	232	1.444(-1)	1.569(+1)	1.37 (-1)	200	3.939	.3151		
			20	634	2.639(-1)	7.364(-0)	1.37 (-1)	200	18.13	.6779		

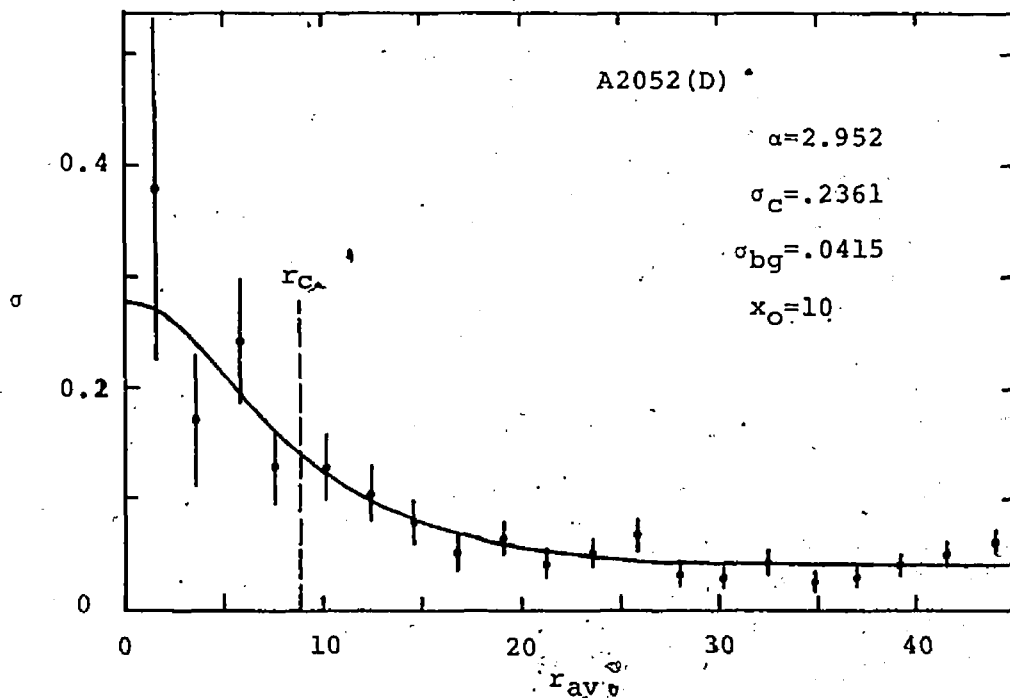
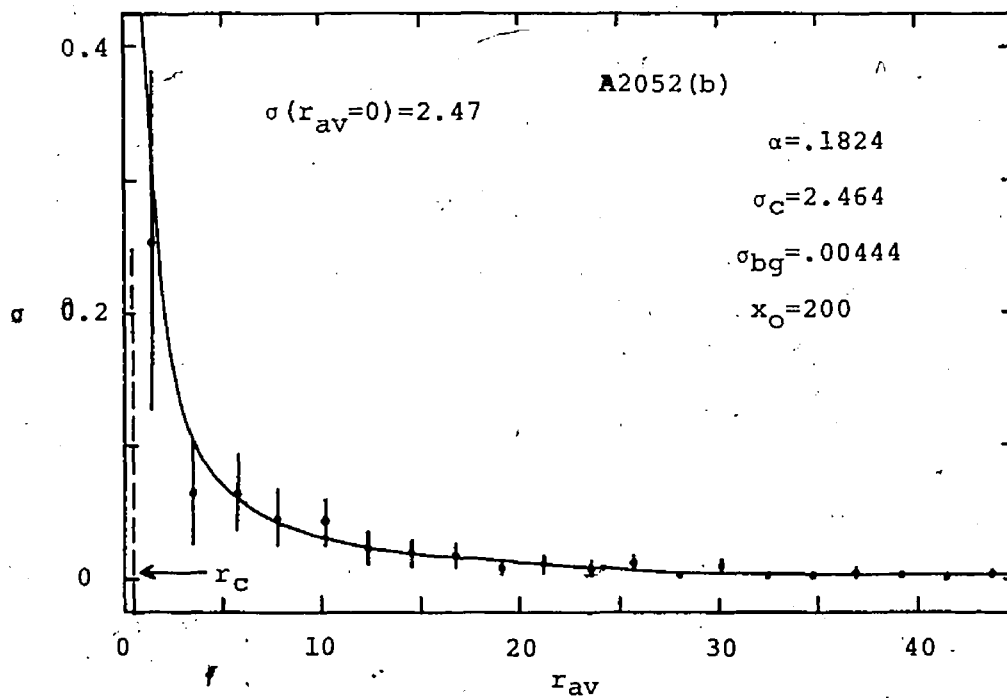
Appendix I  
Density profiles

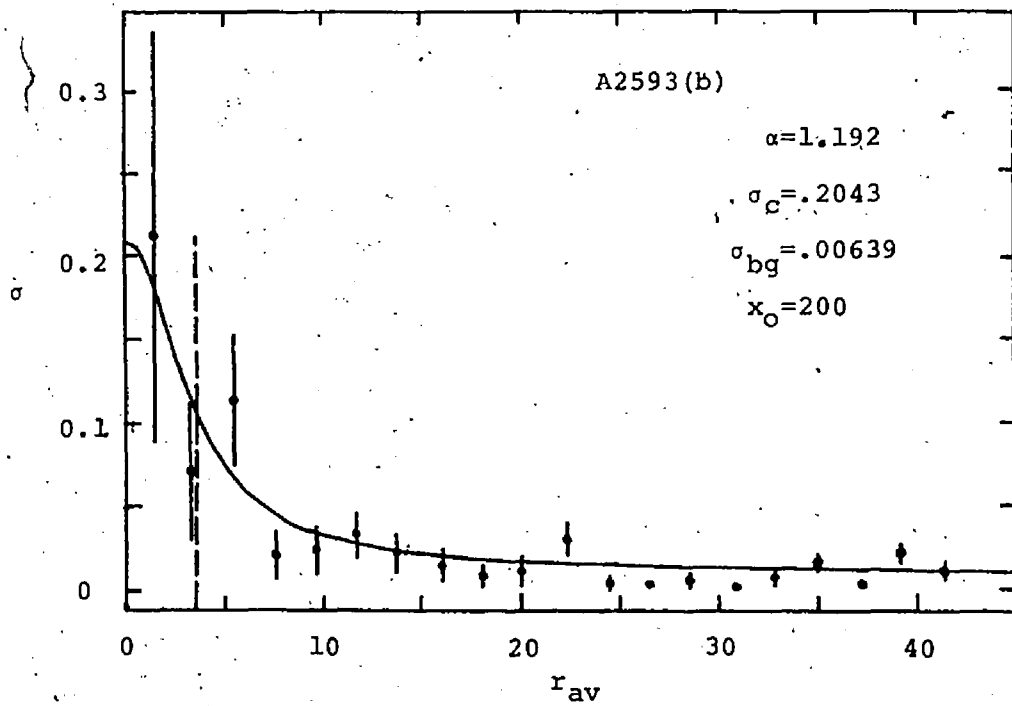
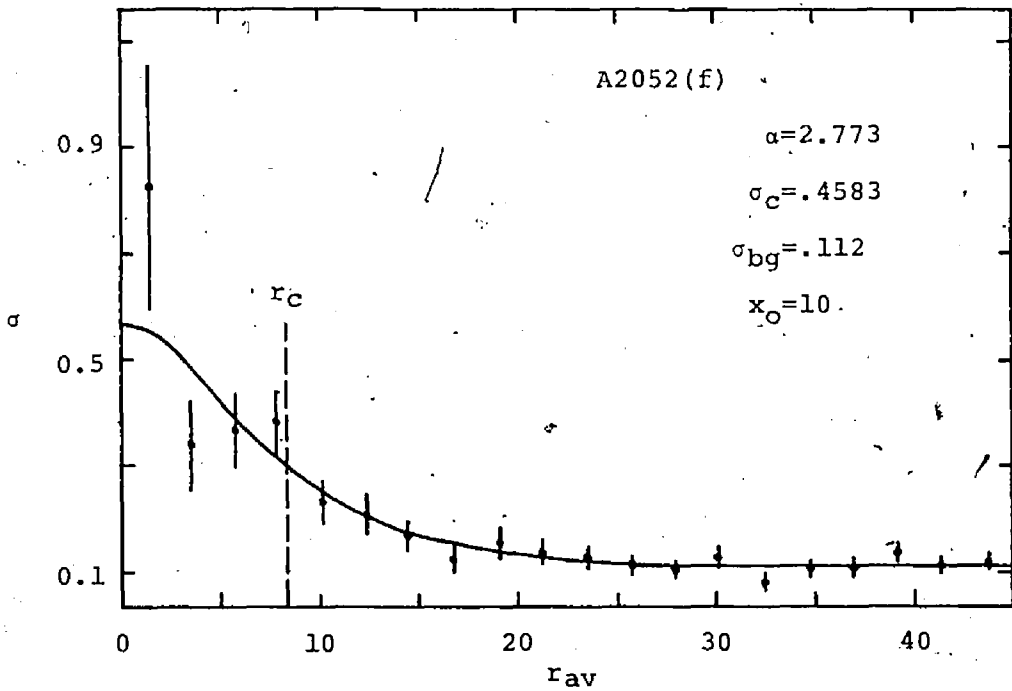
In Table 16 the accepted core radii are presented, having been calculated from the parameters produced by the program version BGIN when all 20 rings are used. In this appendix the counted density profiles are presented for all three magnitude limits for each cluster. These were produced from the ring count data of Appendix F.

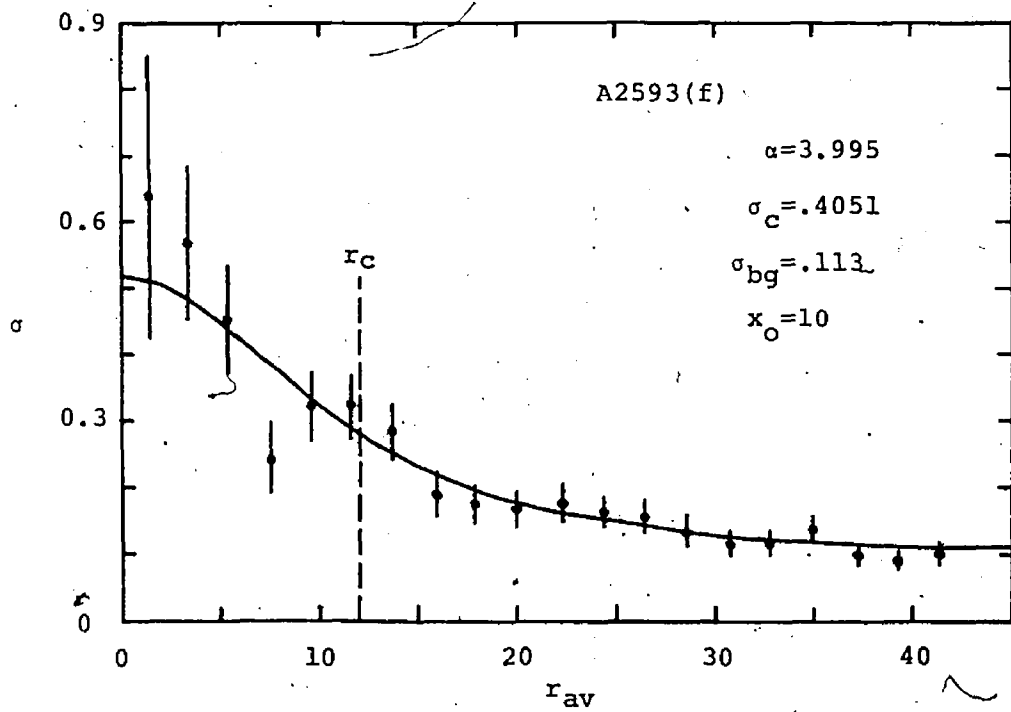
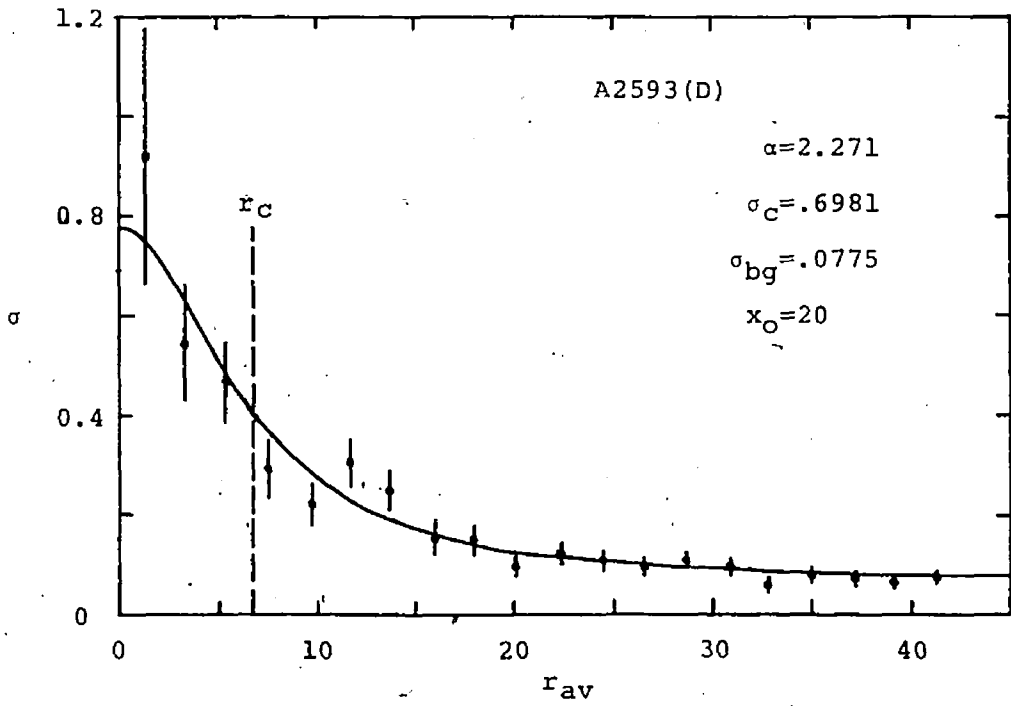
Superimposed on these profiles are the best fitting models created from the BGIN(20) parameters specified on the individual graphs (these parameters are included in Appendix H). The model profiles also indicate the core radii  $r_c$  (in arcmin) which are transformed to the radii of Table 16.

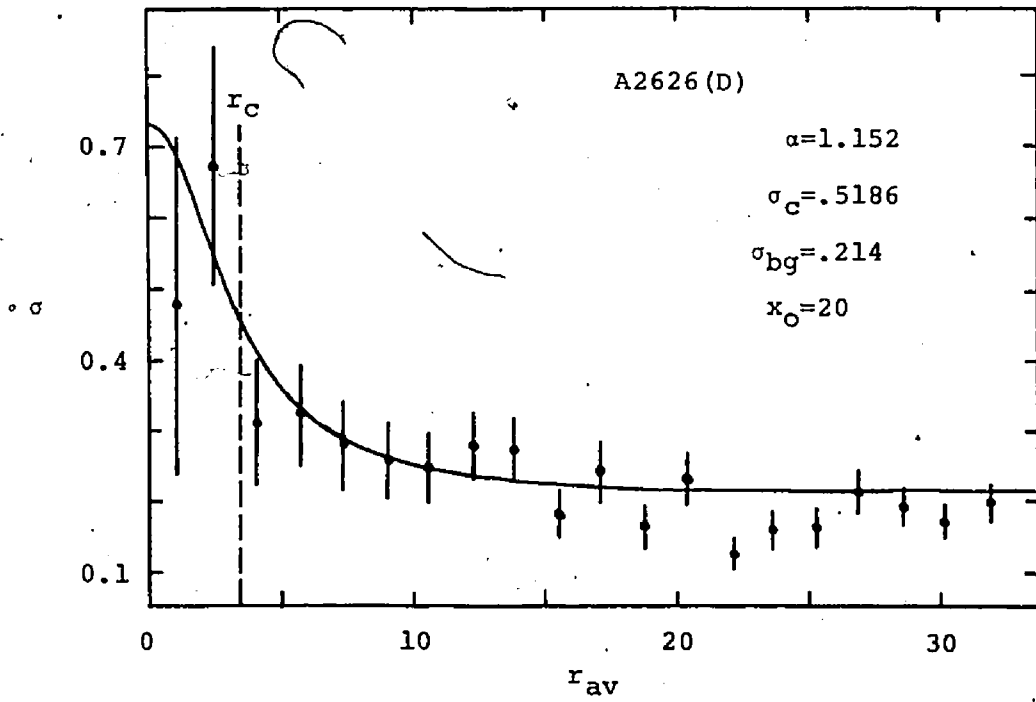
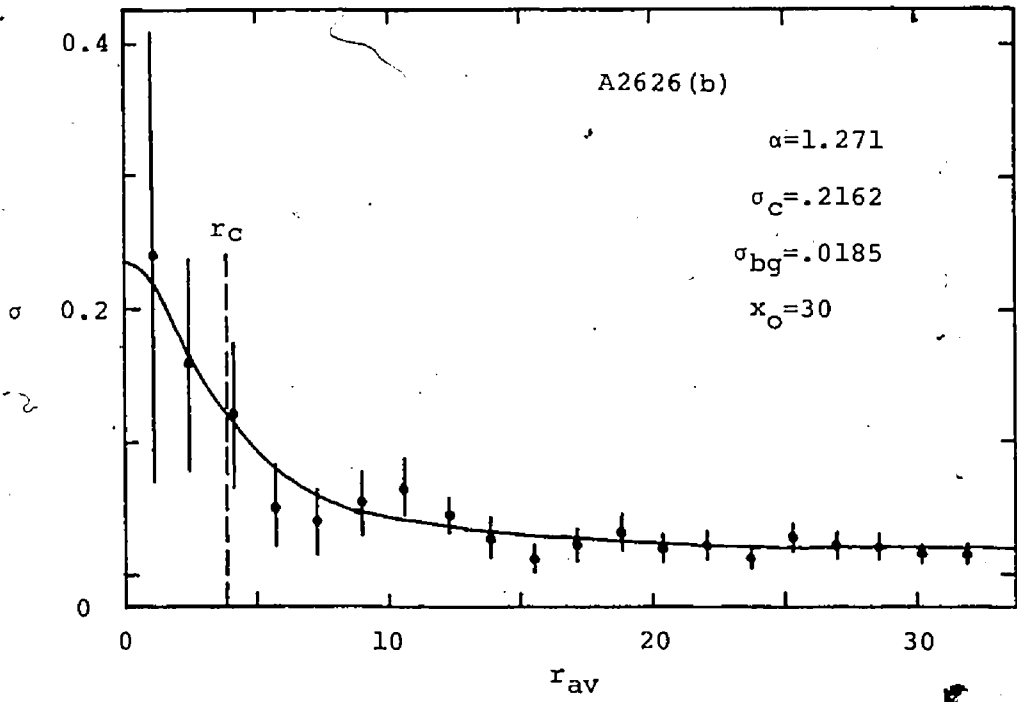
The error bars on these graphs are set to be equal to the square root of the number of galaxies occurring in a particular ring. Despite the fact that the outer rings have more galaxies than the inner rings, the densities enclosed by the error bars decrease as  $r_{av}$  increases because of the increased area, and so smaller densities, covered by these outer rings.

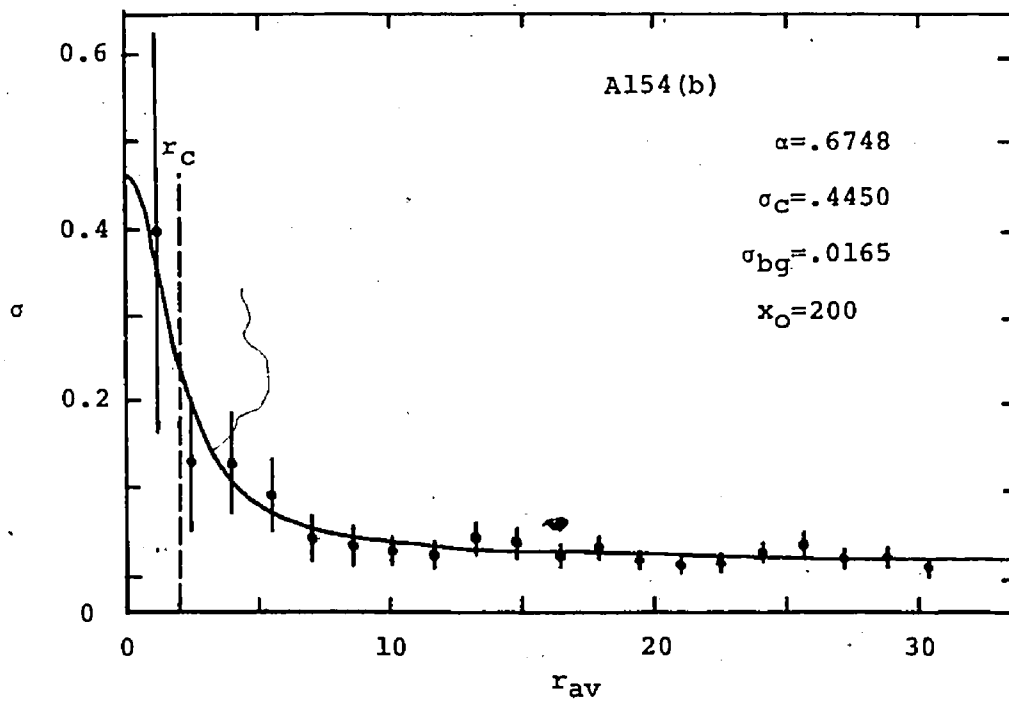
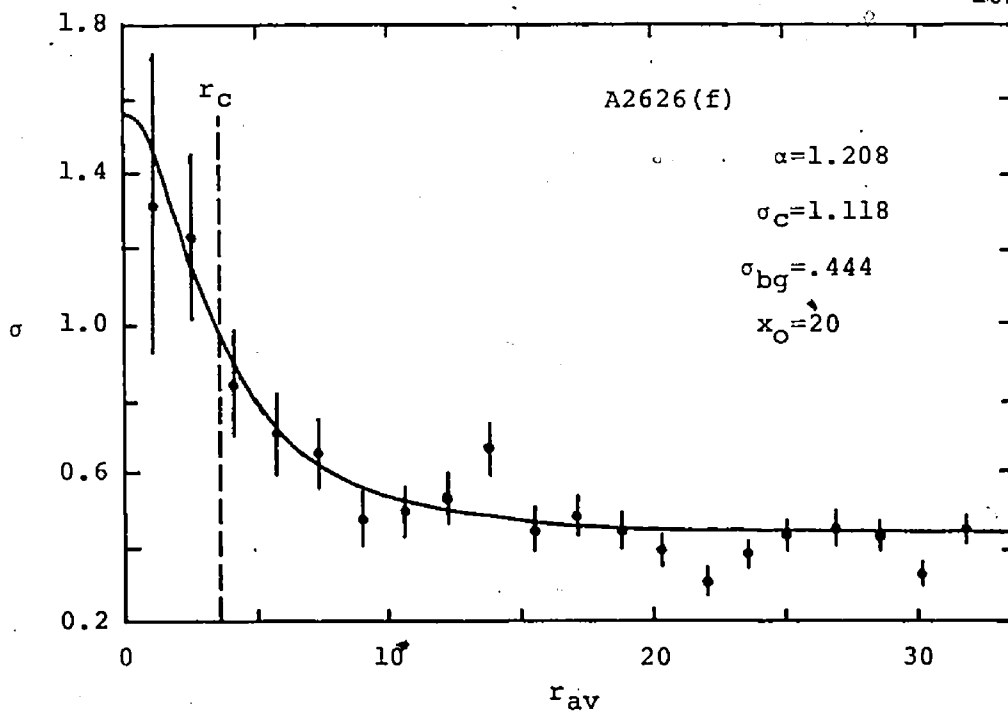
The units on all profiles are:  $r_{av}$  and  $\alpha$  - arcmin;  $n$ ,  $\sigma_c$ , and  $\sigma_{bg}$  - galaxies/arcmin<sup>2</sup>.

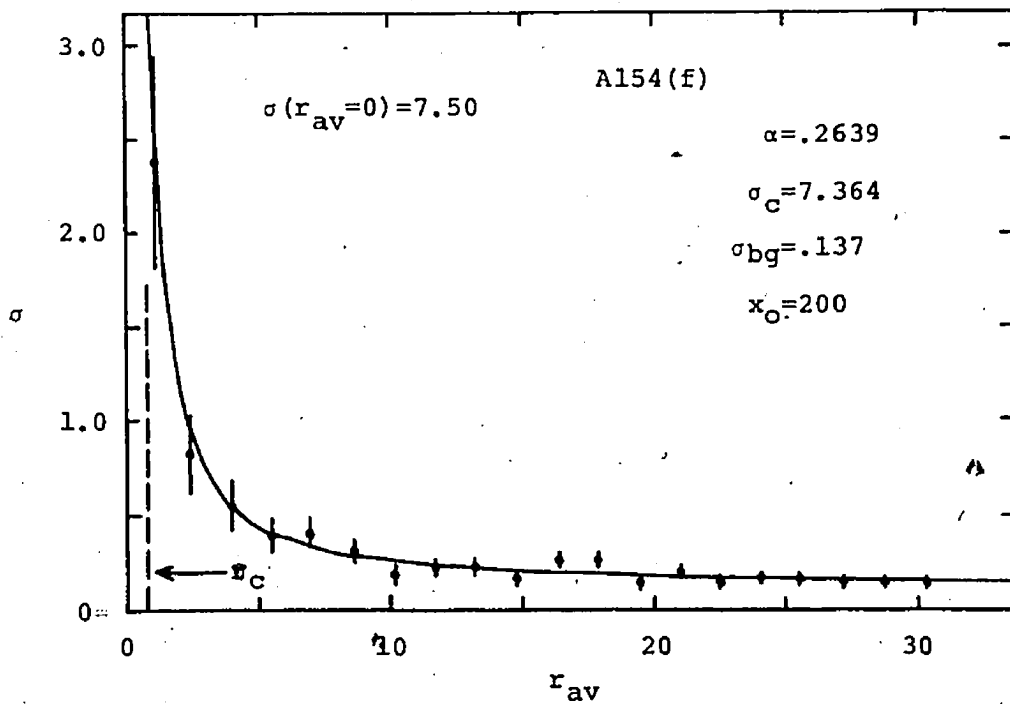
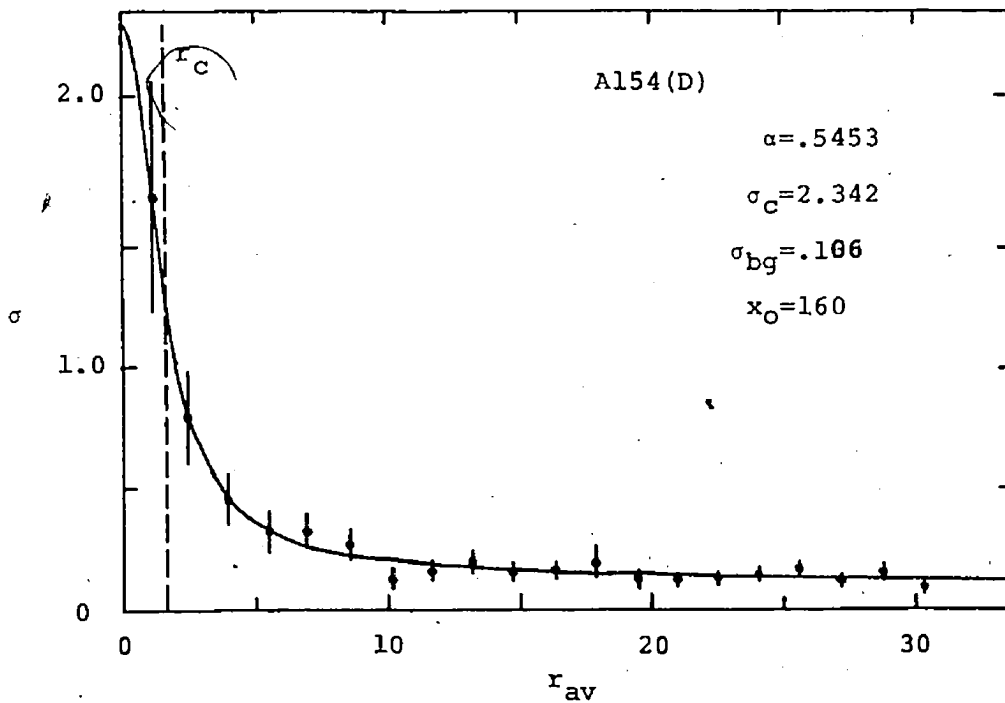












Appendix J  
Sample output

This appendix contains sample output from the programs YAHOO, BGIN, and the BASIC program used to produce the series of values  $e^{-\psi}$ .

Both YAHOO and BGIN begin by reprinting the line used to check terminal speed and width, followed by the initial estimate for  $\sigma_c$ . The next number is either called the estimate for  $\sigma_{bg}$  (if YAHOO is being used) or the actual value of  $\sigma_{bg}$  (if BGIN is being used). The number of rings used is then printed. If this is less than the total available in the data file (i.e. less than 20) the remainder of the ring data will be ignored for all computations.

The table that follows reprints the number of galaxies in each ring and that ring's inner and outer radii as a safety check. (Obviously the outer radius of one ring is the inner radius of the next ring outwards.) Also tabulated are the calculated observed densities of these rings and their average radii. These last two columns are used to draw observed density profiles of the type in Appendix I.

Then the main part of the output begins with the printing of the  $x_0$  value for the subsequent series of  $\alpha$

values. The table of numbers following  $x_0$  lists the  $\alpha$  values found by incrementing  $\log(\alpha)$ , and, for YAHOO, the  $\sigma_C$  and  $\sigma_{bg}$  values arising from this particular  $x_0$ - $\alpha$  combination and the resultant  $\chi^2$ . There are three sets of these four values in each row; groups are to be read across, and not down, the page. For BGIN's output  $\sigma_{bg}$  has already been set, so printed across the page are four sets of three values:  $\alpha$ , the  $\sigma_C$  found by the Newton-Raphson method, and the resulting  $\chi^2$ .

After the possible range of  $\alpha$  values has been printed, the minimum  $\chi^2$  in the table and its causative parameters are printed. Then the  $\chi^2$  and associated parameters obtained from the  $\alpha$  averaging technique are listed.

The program then proceeds to the next  $x_0$  value and continues.

A sample output from the BASIC program is included to show that the  $\xi$  values are not as exact for the  $e^{-\psi\psi'}$  values, as YAHOO and BGIN make them. Remarks on how this program was used for this thesis are included in Appendix B.

RUN YAHOD

THIS DATA IS THESIS MATERIAL. DO NOT EDIT OR DELETE. (COLIN MIGHT CRY IF YOU DO.)

INITIAL CENT DENS= 3.00E-01

INITIAL BG DENS= 4.15E-02

THERE ARE 20 RINGS

NDBS	RQUT	SIGOB	RAV
6.0000	0.0000	0.3804	1.5839
8.0000	2.2400	0.1692	3.5418
19.0000	4.4800	0.2411	5.7109
14.0000	6.7200	0.1269	7.9196
18.0000	8.9600	0.1269	10.1420
18.0000	11.2000	0.1038	12.3708
16.0000	13.4400	0.0781	14.6030
12.0000	15.6800	0.0508	16.8373
17.0000	17.9200	0.0634	19.0729
12.0000	20.1600	0.0401	21.3093
17.0000	22.4000	0.0514	23.5467
24.0000	24.6400	0.0662	25.7843
12.0000	26.8800	0.0305	28.0224
12.0000	29.1200	0.0282	30.2607
20.0000	31.3600	0.0438	32.4993
12.0000	33.6000	0.0246	34.7381
15.0000	35.8400	0.0288	36.9770
22.0000	38.0800	0.0399	39.2160
29.0000	40.3200	0.0497	41.4551
38.0000	42.5600	0.0618	43.6944
	44.8000		

XD IS EQUAL TO 10

ALPHA	CENT DENS	BG DENS	CHI-SQ	ALPHA	CENT DENS	BG DENS	CHI-SQ	ALPHA	CENT DENS	BG DENS	CHI-SQ
1.902E-01	1.757E+01	6.269E-02	1.185E+02	2.287E-01	5.755E+00	6.269E-02	1.185E+02	2.750E-01	2.906E+00	6.269E-02	1.185E+02
3.306E-01	1.762E+00	6.269E-02	1.185E+02	3.975E-01	1.591E+00	6.208E-02	1.156E+02	4.779E-01	1.228E+00	6.146E-02	1.118E+02
5.745E-01	8.475E-01	6.128E-02	1.104E+02	6.907E-01	1.325E+00	5.780E-02	9.389E+01	8.304E-01	1.068E+00	5.596E-02	7.982E+01
9.984E-01	8.421E-01	5.427E-02	6.795E+01	1.200E+00	6.899E-01	5.225E-02	5.607E+01	1.443E+00	5.684E-01	5.002E-02	4.419E+01
1.735E+00	4.595E-01	4.786E-02	3.397E+01	2.086E+00	3.607E-01	4.610E-02	2.774E+01	2.508E+00	2.823E-01	4.451E-02	2.513E+01
3.015E+00	2.257E-01	4.264E-02	2.474E+01	3.625E+00	1.805E-01	4.078E-02	2.809E+01	4.358E+00	1.441E-01	3.899E-02	3.596E+01
5.240E+00	1.223E-01	3.573E-02	4.370E+01	6.299E+00	1.092E-01	3.138E-02	5.121E+01	7.574E+00	1.015E-01	2.601E-02	5.876E+01
9.105E+00	9.826E-02	1.926E-02	6.617E+01	1.095E+01	9.950E-02	1.040E-02	7.307E+01	1.316E+01	1.057E-01	-1.531E-03	7.917E+01
1.582E+01	1.181E-01	1.824E-02	8.429E+01	1.902E+01	1.386E-01	-4.191E-02	8.839E+01	2.287E+01	1.895E-01	-7.516E-02	9.167E+01
2.750E+01	2.166E-01	-1.239E-01	9.403E+01	3.306E+01	2.844E-01	-1.929E-01	9.593E+01	3.975E+01	3.847E-01	-2.940E-01	9.715E+01
4.779E+01	5.270E-01	-4.370E-01	9.824E+01	5.745E+01	7.387E-01	-6.490E-01	9.870E+01	6.907E+01	1.038E+00	-9.485E-01	9.923E+01

MIN FROM PROGRAM:

MINIMUM METHOD :

3.015E+00	-2.257E-01	4.264E-02	2.474E+01
2.876E+00	2.386E-01	4.314E-02	2.461E+01

XD IS EQUAL TO 20

ALPHA	CENT DENS	BG DENS	CHI-SQ	ALPHA	CENT DENS	BG DENS	CHI-SQ	ALPHA	CENT DENS	BG DENS	CHI-SQ
9.512E-02	5.745E+01	6.269E-02	1.185E+02	1.144E-01	1.863E+01	6.269E-02	1.185E+02	1.375E-01	9.315E+00	6.269E-02	1.185E+02
1.653E-01	5.405E+00	6.269E-02	1.185E+02	1.987E-01	4.517E+00	6.214E-02	1.159E+02	2.389E-01	3.358E+00	6.154E-02	1.124E+02
2.873E-01	2.218E+00	6.137E-02	1.111E+02	3.454E-01	3.070E+00	5.852E-02	9.828E+01	4.152E-01	2.483E+00	5.677E-02	8.654E+01
4.992E-01	1.993E+00	5.492E-02	7.518E+01	6.002E-01	1.584E+00	5.310E-02	6.439E+01	7.216E-01	1.267E+00	5.115E-02	5.365E+01
8.675E-01	1.004E+00	4.914E-02	4.339E+01	1.043E+00	7.734E-01	4.747E-02	3.581E+01	1.254E+00	5.920E-01	4.594E-02	3.051E+01
1.508E+00	4.590E-01	4.430E-02	2.671E+01	1.812E+00	3.568E-01	4.265E-02	2.529E+01	2.179E+00	2.775E-01	4.105E-02	2.690E+01
2.620E+00	2.250E-01	3.869E-02	2.893E+01	3.150E+00	1.877E-01	3.601E-02	3.184E+01	3.787E+00	1.599E-01	3.308E-02	3.592E+01
4.553E+00	1.396E-01	2.979E-02	4.098E+01	5.474E+00	1.246E-01	2.609E-02	4.708E+01	6.581E+00	1.142E-01	2.166E-02	5.392E+01
7.912E+00	1.082E-01	1.611E-02	6.110E+01	9.512E+00	1.064E-01	8.795E-03	6.818E+01	1.144E+01	1.092E-01	-1.037E-03	7.480E+01
1.375E+01	1.178E-01	-1.490E-02	8.054E+01	1.653E+01	1.332E-01	-3.431E-02	8.543E+01	1.987E+01	1.583E-01	-6.228E-02	8.929E+01
2.389E+01	1.957E-01	-1.018E-01	9.242E+01	2.873E+01	2.515E-01	-1.592E-01	9.466E+01	3.454E+01	3.341E-01	-2.428E-01	9.619E+01

RUN BGIN

THIS DATA IS THESIS MATERIAL. DO NOT EDIT OR DELETE. (COLIN MIGHT CRY IF YOU DO.)

INITIAL CENT DENS= 3.00E-01  
 BG DENS= 4.15E-02

THERE ARE 20 RINGS

NOBS	ROUT	SIGOB	RAV
6.0000	0.0000	0.3806	1.5839
8.0000	2.2400	0.1692	3.5418
19.0000	4.4800	0.2411	5.7109
14.0000	6.7200	0.1269	7.9196
18.0000	8.9600	0.1269	10.1420
18.0000	11.2000	0.1038	12.3708
16.0000	13.4400	0.0781	14.6030
12.0000	15.6800	0.0508	16.8373
17.0000	17.9200	0.0634	19.0729
12.0000	20.1600	0.0401	21.3095
17.0000	22.4000	0.0514	23.5467
24.0000	24.6400	0.0662	25.7843
12.0000	26.8800	0.0305	28.0224
12.0000	29.1200	0.0282	30.2607
20.0000	31.3600	0.0438	32.4993
12.0000	33.6000	0.0246	34.7381
15.0000	35.8400	0.0288	36.9770
22.0000	38.0800	0.0399	39.2160
29.0000	40.3200	0.0497	41.4551
38.0000	42.5600	0.0618	43.6944
	44.8000		

X0 IS EQUAL TO 10

ALPHA	CENT DENS	CHI-SQ	ALPHA	CENT DENS	CHI-SQ	ALPHA	CENT DENS	CHI-SQ	ALPHA	CENT DENS	CHI-SQ
1.902E-01	1.874E+01	1.866E+02	2.287E-01	6.139E+00	1.866E+02	2.750E-01	3.100E+00	1.866E+02	3.306E-01	1.879E+00	1.866E+02
3.975E-01	2.259E+00	1.787E+02	4.779E-01	1.506E+00	1.714E+02	5.745E-01	1.193E+00	1.657E+02	6.907E-01	1.865E+00	1.307E+02
8.304E-01	1.292E+00	1.098E+02	9.984E-01	9.804E-01	9.110E+01	1.200E+00	7.958E-01	7.212E+01	1.443E+00	6.394E-01	5.404E+01
1.735E+00	5.013E-01	3.936E+01	2.086E+00	3.837E-01	3.051E+01	2.508E+00	2.941E-01	2.629E+01	3.015E+00	2.296E-01	2.490E+01
3.625E+00	1.784E-01	2.815E+01	4.358E+00	1.378E-01	3.662E+01	5.240E+00	1.086E-01	4.657E+01	6.299E+00	8.686E-02	5.803E+01
7.574E+00	7.043E-02	7.048E+01	9.105E+00	5.808E-02	8.306E+01	1.095E+01	4.884E-02	9.496E+01	1.316E+01	4.198E-02	1.056E+02
1.582E+01	3.690E-02	1.146E+02	1.902E+01	3.318E-02	1.219E+02	2.287E+01	3.050E-02	1.276E+02	2.750E+01	2.855E-02	1.320E+02
3.306E+01	2.717E-02	1.352E+02	3.975E+01	2.619E-02	1.376E+02	4.779E+01	2.551E-02	1.393E+02	5.745E+01	2.503E-02	1.404E+02
6.907E+01	2.470E-02	1.413E+02	8.304E+01	2.446E-02	1.419E+02	9.984E+01	2.430E-02	1.423E+02	1.200E+02	2.419E-02	1.426E+02
1.443E+02	2.411E-02	1.428E+02	1.735E+02	2.406E-02	1.429E+02	2.086E+02	2.402E-02	1.430E+02	2.508E+02	2.400E-02	1.431E+02
3.015E+02	2.398E-02	1.431E+02	3.625E+02	2.396E-02	1.431E+02	4.358E+02	2.396E-02	1.432E+02	5.240E+02	2.395E-02	1.432E+02
6.299E+02	2.395E-02	1.432E+02	7.574E+02	2.394E-02	1.432E+02	9.105E+02	2.394E-02	1.432E+02	1.095E+03	2.394E-02	1.432E+02
1.316E+03	2.394E-02	1.432E+02	1.582E+03	2.394E-02	1.432E+02						
	MIN FROM PROGRAM		3.015E+00	2.296E-01	2.490E+01						
	MINIMUM METHOD		2.952E+00	2.361E-01	2.488E+01						

X0 IS EQUAL TO 20

ALPHA	CENT DENS	CHI-SQ									
9.512E-02	6.149E+01	1.866E+02	1.144E-01	1.987E+01	1.866E+02	1.375E-01	9.936E+00	1.866E+02	1.653E-01	5.765E+00	1.866E+02
1.987E-01	6.419E+00	1.794E+02	2.389E-01	4.223E+00	1.724E+02	2.873E-01	2.866E+00	1.888E+02	3.454E-01	4.701E+00	1.380E+02
4.152E-01	3.228E+00	1.181E+02	4.992E-01	2.424E+00	1.004E+02	6.002E-01	1.894E+00	8.284E+01	7.216E-01	1.477E+00	6.611E+01
8.675E-01	1.135E+00	5.098E+01	1.043E+00	8.499E-01	4.040E+01	1.254E+00	6.352E-01	3.300E+01	1.508E+00	4.808E-01	2.766E+01
1.812E+00	3.638E-01	2.550E+01	2.179E+00	2.753E-01	2.688E+01	2.620E+00	2.127E-01	2.971E+01	3.150E+00	1.688E-01	3.446E+01
3.787E+00	1.324E-01	4.124E+01	4.553E+00	1.066E-01	4.965E+01	5.474E+00	8.693E-02	5.944E+01	6.581E+00	7.178E-02	7.018E+01
7.912E+00	6.006E-02	8.130E+01	9.512E+00	5.098E-02	9.224E+01	1.144E+01	4.396E-02	1.024E+02	1.375E+01	3.861E-02	1.115E+02
1.653E+01	3.457E-02	1.191E+02	1.987E+01	3.157E-02	1.253E+02	2.389E+01	2.936E-02	1.302E+02	2.873E+01	2.777E-02	1.338E+02
3.454E+01	2.663E-02	1.365E+02	4.152E+01	2.582E-02	1.385E+02	4.992E+01	2.525E-02	1.399E+02	6.002E+01	2.485E-02	1.409E+02

167

Ready

RUNNH  
ENTER STEP SIZE, NUMBER OF STEPS

? .1, 100

.1 100

XI EXP(-PSI) PSI EXP(-PSI)\*PSI

10	.238359E-1	.251061	.598429E-2
20	.449904E-2	.113128	.508965E-3
29.9998	.18658E-2	.694362E-1	.129554E-3
39.9997	.104079E-2	.494812E-1	.514997E-4
49.9995	.674007E-3	.383822E-1	.258564E-4
59.9994	.476767E-3	.031363	.149529E-4
69.9997	.357342E-3	.265801E-1	.949818E-5
80.0003	.278964E-3	.231133E-1	.644777E-5
90.0009	.224449E-3	.204869E-1	.459828E-5
100.002	.184835E-3	.184279E-1	.340612E-5
110.002	.155053E-3	.167689E-1	.260007E-5
120.003	.132042E-3	.154024E-1	.203376E-5
130.003	.113862E-3	.014256	.162321E-5
140.004	.992299E-4	.132793E-1	.13177E-5
150.005	.872661E-4	.124364E-1	.108528E-5
160.005	.773514E-4	.117008E-1	.905072E-6
170.006	.69038E-4	.110526E-1	.763049E-6
180.006	.619958E-4	.104766E-1	.649505E-6
190.007	.559762E-4	.996097E-2	.557577E-6
200.008	.507887E-4	.949637E-2	.482308E-6
210.008	.462864E-4	.907531E-2	.420063E-6
220.009	.423532E-4	.869172E-2	.368122E-6
230.009	.388966E-4	.834063E-2	.324422E-6
240.01	.358427E-4	.801792E-2	.287384E-6
250.011	.33131E-4	.772017E-2	.255777E-6
260.01	.307123E-4	.744448E-2	.228637E-6
270.008	.28546E-4	.71884E-2	.2052E-6
280.005	.265981E-4	.694984E-2	.184853E-6
290.003	.248404E-4	.006727	.167101E-6
300	.232488E-4	.651831E-2	.151543E-6
309.998	.218033E-4	.632244E-2	.13785E-6
319.995	.204866E-4	.61382E-2	.125751E-6
329.993	.192837E-4	.596456E-2	.115019E-6
339.991	.181822E-4	.58006E-2	.105468E-6
349.988	.17171E-4	.564551E-2	.96939E-7
359.986	.162405E-4	.549857E-2	.892996E-7
369.983	.153824E-4	.535914E-2	.824367E-7
379.981	.145895E-4	.522665E-2	.762543E-7
389.978	.138554E-4	.510057E-2	.706704E-7
399.976	.131744E-4	.498044E-2	.656141E-7
409.973	.125415E-4	.486585E-2	.610251E-7
419.971	.119525E-4	.47564E-2	.568508E-7
429.969	.114033E-4	.465177E-2	.530454E-7
439.966	.108905E-4	.455162E-2	.495693E-7
449.964	.104109E-4	.445567E-2	.463876E-7
459.961	.996182E-5	.436366E-2	.4347E-7
469.959	.954071E-5	.427535E-2	.407899E-7
479.956	.914532E-5	.419051E-2	.383236E-7
489.954	.877362E-5	.410895E-2	.360503E-7
499.951	.842375E-5	.403047E-2	.339517E-7
509.949	.809406E-5	.39549E-2	.320112E-7
519.947	.778305E-5	.388208E-2	.302144E-7
529.944	.748934E-5	.381186E-2	.285483E-7
539.942	.721167E-5	.37441E-2	.270012E-7